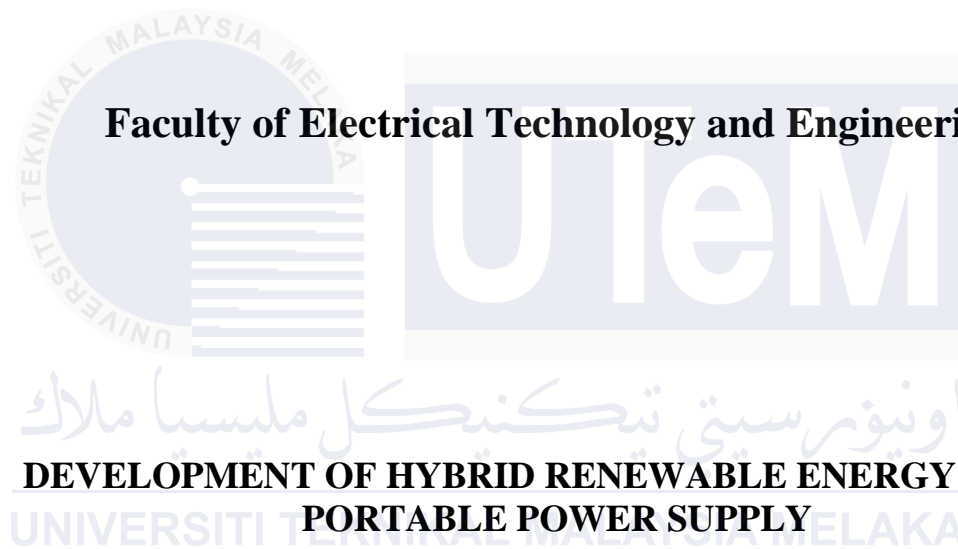




Faculty of Electrical Technology and Engineering



**DEVELOPMENT OF HYBRID RENEWABLE ENERGY BASED
PORTABLE POWER SUPPLY**

ANUTTIK A/L NIKOM

Bachelor of Electrical Engineering Technology with Honours

2023

DEVELOPMENT OF HYBRID RENEWABLE ENERGY BASED PORTABLE POWER SUPPLY

ANUTTIK A/L NIKOM



**A project report submitted
in partial fulfillment of the requirements for the degree of
Bachelor of Electrical Engineering Technology with Honours**



اونيورسيتي تېكنيكل مليسيا ملاك

Faculty of Electrical Technology and Engineering

UNIVERSITI TEKNIKAL MALAYSIA MELAKA

UNIVERSITI TEKNIKAL MALAYSIA MELAKA

2023

BORANG PENGESAHAN STATUS LAPORAN
PROJEK SARJANA MUDA II

Tajuk Projek : Development of Hybrid Renewable Energy based Portable Power Supply.

Sesi Pengajian : 2023/2024

Saya Anuttik A/L Nikom mengaku membenarkan laporan Projek Sarjana

Muda ini disimpan di Perpustakaan dengan syarat-syarat kegunaan seperti berikut:

1. Laporan adalah hakmilik Universiti Teknikal Malaysia Melaka.
2. Perpustakaan dibenarkan membuat salinan untuk tujuan pengajian sahaja.
3. Perpustakaan dibenarkan membuat salinan laporan ini sebagai bahan pertukaran antara institusi pengajian tinggi.
4. Sila tandakan (✓):

☒

SULIT*

(Mengandungi maklumat yang berdarjah keselamatan atau kepentingan Malaysia seperti yang termaktub di dalam AKTA RAHSIA RASMI 1972)

☐

TERHAD*

(Mengandungi maklumat terhad yang telah ditentukan oleh organisasi/badan di mana penyelidikan dijalankan)

☒

TIDAK TERHAD

Disahkan oleh:

(TANDATANGAN PENULIS)

Alamat Tetap:

(COP DAN TANDATANGAN PENYELIA)

AZHAN BIN AB. RAHMAN

Pensyarah

Jabatan Teknologi Kejuruteraan Elektrik
Fakulti Teknologi Kejuruteraan Elektrik & Elektronik
Universiti Teknikal Malaysia Melaka (UTeM)

Tarikh: 12/1/2024

Tarikh: 12/1/2024

*CATATAN: Jika laporan ini SULIT atau TERHAD, sila lampirkan surat daripada pihak berkuasa/organisasi berkenaan dengan menyatakan sekali tempoh laporan ini perlu dikelaskan sebagai SULIT atau TERHAD.

DECLARATION

I declare that this project report entitled “Development of Hybrid Renewable Energy based Portable Power Supply” is the result of my own research except as cited in the references. The project report has not been accepted for any degree and is not concurrently submitted in candidature of any other degree.

Signature :

Student Name :

ANUTTIK A/L NIKOM

Date :

12/1/2024

UNIVERSITI TEKNIKAL MALAYSIA MELAKA

APPROVAL

I hereby declare that I have checked this project report and in my opinion, this project report is adequate in terms of scope and quality for the award of the degree of Bachelor of Electrical Engineering Technology with Honours.

Signature :

Supervisor Name : DR AZHAN BIN AB RAHMAN

Date : 12/1/2024

اوتیورسیتی نیکیکل ملیسیا ملاک
UNIVERSITI TEKNIKAL MALAYSIA MELAKA

DEDICATION

*To my beloved mother, Pannee A/P Epit, and father, Nikom A/L Ainim @ Ah Lee,
Thank you for consistently maintaining faith in me, even when I lacked confidence in my
own abilities.*

The efficacy of your prayers has led me to my current position.



اونيورسيتي تيكنيكل مليسيا ملاك

UNIVERSITI TEKNIKAL MALAYSIA MELAKA

ABSTRACT

Camping activities nowadays involve equipment that relies on electricity supply. Therefore, a portable power supply is one of the best solutions that meet this purpose. However, a portable power supply normally comes with a single source of power supply, and problems might arise if this single power supply is suddenly not functional. Thus, this project aims to rectify this by proposing a hybrid portable power supply that consists of a combination battery, solar panel, and mechanical pedal. PSCAD software indicates a constant capacitor voltage which means that a consistent electricity supply is achievable, and the result also shows positive and negative converter current readings. The preliminary result shows that the battery in a portable power supply is charging and discharging. The simulation will be validated with the development of hardware. By carrying out hardware development, this project obtained analysis results on a variety of cable sizes with the aim of reducing charging time. Based on the results of the solar energy analysis carried out, the 10.0 mm² cable has a very good impact on the battery charging time reduction process in the period taken from 20% to 100% state of charge, which is 7 hours. As for the results of the cable size analysis by the mechanical pedal, the lowest time to reach 100% of the state of charge is 8 hours and 33 minutes for a 10.0 mm² cable. Additionally, this project includes the ability to generate power using solar energy and a mechanical pedal in order to shorten charging times by utilizing various cable sizes. In addition, analysis on a variety of loads is also carried out in order to obtain the results of the efficiency of the hybrid portable power supply. According to various load evaluations, when used with a fan speed of 3, the battery takes at least 47 minutes to reach a state of charge of 20%, resulting in a power consumption of 33.7W. The lowest discharging rate for the load analysis is fan speed position 1, which is 19.5 watts and takes 2 hours to reach 20% of the hybrid portable power supply's state of charge. In conclusion, it is hoped that this project will reduce the cost of outdoor activities and maximize the energy used to power up camper's gear and offers a versatile option for outdoor activities.

ABSTRAK

Sama seperti kandungan abstrak di dalam bahasa Inggeris, di halaman ini adalah abstrak yang telah diterjemah ke dalam bahasa Melayu. Aktiviti perkhemahan pada masa kini melibatkan peralatan yang bergantung kepada bekalan elektrik. Oleh itu, bekalan kuasa mudah alih adalah salah satu cara untuk mengatasi masalah ini. Walau bagaimanapun, bekalan kuasa mudah alih biasanya disertakan dengan satu sumber bekalan kuasa, dan masalah bekalan terputus akan berlaku jika sumber bekalan kuasa kehabisan atau tidak berfungsi. Oleh itu, projek ini bertujuan untuk membetulkannya dengan mencadangkan bekalan kuasa mudah alih hibrid yang terdiri daripada gabungan bateri, panel solar, dan pedal mekanikal. Perisian PSCAD menunjukkan voltan kapasitor malar yang bermaksud bekalan elektrik yang konsisten boleh dicapai, dan hasilnya juga menunjukkan bacaan arus penukar positif dan negatif. Keputusan awal menunjukkan bahawa bateri dalam bekalan kuasa mudah alih sedang mengecas dan menyahcas. Simulasi akan disahkan dengan pembangunan perkakasan. Dengan menjalankan pembangunan perkakasan, projek ini memperolehi keputusan analisis terhadap kepelbagaian saiz kabel, dengan bertujuan pengurangan masa mengecas. Berdasarkan keputusan analisis tenaga suria yang dijalankan, kabel bersaiz 10.0 mm² memberi impak yang sangat bagus untuk proses pengurangan masa mengecas bateri dalam tempoh diambil dari 20% hingga 100% keadaan cas ialah 7 jam. Bagi keputusan analisis saiz kabel oleh pedal mekanikal pula, masa yang terendah untuk mencapai 100% daripada keadaan cas ialah 8 jam 33 minit bagi kabel 10.0 mm². Lalu projek ini berserta dengan daya kebolehan menjana kuasa melalui tenaga suria dan pedal mekanikal agar dapat mengurangkan masa mengecas dengan menggunakan saiz kabel yang berbeza. Di samping itu, ujian terhadap kepelbagaian beban juga dijalankan supaya memperolehi keputusan kecekapan keupayaan hibrid bekalan kuasa mudah alih ini. Berdasarkan penilaian beban, apabila digunakan dengan kelajuan kipas 3, bateri mengambil masa sekurang-kurangnya 47 minit untuk mencapai keadaan pengecasan sebanyak 20%, menghasilkan penggunaan kuasa sebanyak 33.7W. Kadar nyahcas paling rendah untuk analisis beban ialah kedudukan kelajuan kipas 1, iaitu 19.5 watt dan mengambil masa 2 jam untuk mencapai 20% keadaan cas. Kesimpulannya, projek ini diharapkan dapat mengurangkan kos aktiviti luar dan memaksimumkan tenaga yang digunakan untuk menghidupkan peralatan perkhemahan dan menawarkan pilihan serba boleh untuk aktiviti luar.

ACKNOWLEDGEMENTS

First and foremost, I would like to express my gratitude to my supervisor, Dr Azhan Bin Ab Rahman for their precious guidance, words of wisdom and patient throughout this project.

I am also indebted to Universiti Teknikal Malaysia Melaka (UTeM) and my parent for the financial support which enables me to accomplish the project. Not forgetting my fellow colleague, Chan Pui Kit for the willingness of sharing his thoughts and ideas regarding the project.

I would like to acknowledge Encik Adli for providing me with the necessary AC wire as well as for offering motivation and understanding, which greatly contributed to the successful completion of my project.

Finally, I would like to thank all the staffs at the Faculty of Electrical Engineering and Technology, fellow colleagues and classmates, the faculty members, as well as other individuals who are not listed here for being co-operative and helpful.

TABLE OF CONTENTS

	PAGE
DECLARATION	
APPROVAL	
DEDICATIONS	
ABSTRACT	i
ABSTRAK	ii
ACKNOWLEDGEMENTS	iii
TABLE OF CONTENTS	iv
LIST OF TABLES	vi
LIST OF FIGURES	viii
LIST OF SYMBOLS	xii
LIST OF ABBREVIATIONS	xiii
CHAPTER 1 INTRODUCTION	1
1.1 Background	1
1.2 Problem Statement	4
1.3 Project Objective	5
1.4 Scope of Project	6
CHAPTER 2 LITERATURE REVIEW	7
2.1 Introduction	7
2.2 Background Study	7
2.2.1 History of Hybrid Renewable Energy.	8
2.2.2 Concept of Hybrid Renewable Energy.	9
2.2.3 Components of hybrid renewable energy	16
2.2.4 Application of hybrid renewable energy	18
2.3 Research Literature	20
2.3.1 Nonvolatile Portable Power Supply, Performance Capabilities and Organization Principles in Continental Areas.	20
2.3.2 Portable Concentrated Sunlight Power Supply Using 40% Efficient Solar Cells.	22
2.3.3 Design and Performance Analysis of a Portable Solar PV Power Supply.	23
2.3.4 Building of A Portable Solar AC and DC Power Supply.	26
2.3.5 Development of Portable Solar Power Plant Equipped with IoT Connectability.	29
2.3.6 Magnet Dynamo	31

2.3.7	A Novel Design and Fabrication of Energy Generating Oscillatory Swing – A Play way Technique for Public Parks.	32
2.3.8	A hybrid kinetic energy harvester for applications in electric driverless buses.	34
2.3.9	Analysis of magnetic Rayleigh-Taylor instability in a direct energy conversion system which convert inertial fusion plasma kinetic energy into pulsed electrical energy.	36
2.3.10	Photovoltaics battery module power supply system with CIGS film applied in portable device.	38
2.4	Research Summary.	41
2.5	Summary	43
CHAPTER 3	METHODOLOGY	45
3.1	Introduction	45
3.2	Methodology	45
3.3	Project Architecture	48
	3.3.1 Parameters	49
	3.3.2 Project Equipment	49
3.4	Table of project equipment.	63
3.5	Project Quotation	66
3.6	Project Design	67
3.7	Project Simulation	68
	3.7.1 Solar Photovoltaic Circuit	68
	3.7.2 Dynamo Circuit	69
	3.7.3 Battery Circuit	70
	3.7.4 Switching Control Circuit	71
	3.7.5 Full Circuit Design	71
3.8	Project Hardware	73
3.9	Gantt Chart	76
3.10	Summary	77
CHAPTER 4	PRELIMINARY RESULTS AND DISCUSSIONS	78
4.1	Introduction	78
4.2	Simulation Results and Analysis	78
4.3	Hardware Result and Analysis	84
4.4	Summary	135
CHAPTER 5	CONCLUSION AND RECOMMENDATIONS	136
5.1	Conclusion	136
5.2	Recommendation	139
5.3	Future Works	140
5.4	Potential of Commercialize the Project	141
REFERENCES		143

LIST OF TABLES

TABLE	TITLE	PAGE
Table 2.1	Three major types of solar PV panels.[11]	10
Table 2.2	The comparison between PWM and MPPT solar charge controller.[14]	12
Table 2.3	Types of batteries.[16]	14
Table 2.4	The comparison between three types of solar inverters.[18]	15
Table 2.5	PV System Data[27]	24
Table 2.6	The characteristic of solar PV charge controller and batteries[27]	24
Table 2.7	Annual Energy Production Cost for Different Tilt Angle Optimization for Summer, Winter, and all seasonal[27]	24
Table 2.8	The effect of shading versus cleaning panel.[27]	25
Table 2.9	The Power Consumption for selected hardware are devices.[29]	29
Table 2.10	Specification and dimension of material.[37]	33
Table 2.11	The result of the experiment of oscillatory swinging.[37]	34
Table 2.12	Summary of the research article.	41
Table 3.1	List of project equipment.	63
Table 3.2	List of equipment of this project.	66
Table 4.1	Solar PV charging with a cable diameter of 0.8 mm ² .	85
Table 4.2	Solar PV charging with a cable diameter of 1.5 mm ² .	90
Table 4.3	Solar PV charging with cable diameter of 4.0 mm ² .	95
Table 4.4	Solar PV with cable diameter of 10.0 mm ² .	100
Table 4.5	Table of Summary: Solar PV various cable size charging.	105
Table 4.6	Mechanical Charging with cable diameter at 1.0 mm ² .	106
Table 4.7	Mechanical Charging with cable diameter at 1.5 mm ² .	110

Table 4.8 Mechanical Charging with cable diameter at 4.0 mm ² .	114
Table 4.9 Mechanical Charging with cable diameter at 10.0 mm ²	118
Table 4.10 Table of Summary: Mechanical Pedal various cable size charging.	122
Table 4.11 Various load discharge of a fan speed at position 1.	123
Table 4.12 Various load discharge of a fan speed at position 2.	126
Table 4.13 Various load discharge of a fan speed at position 3.	129



LIST OF FIGURES

FIGURE	TITLE	PAGE
Figure 1.1	Types of portal power supply.[2]	2
Figure 1.2	Percentage of renewable energy in total literature. [6]	3
Figure 2.1	Early hybrid power from gasoline/kerosine engine drives the dynamo which charges the storage battery. [7]	8
Figure 2.2	PV-Wind hybrid energy system.[8]	9
Figure 2.3	Hybrid renewable energy generation.[9]	10
Figure 2.4	Two major types of wind turbines.[12]	11
Figure 2.5	Three-phase full wave bridge rectifier.[15]	13
Figure 2.6	Schematic diagram of a stand-alone hybrid energy system.[20]	16
Figure 2.7	Schematic wiring diagram of PV-Wind off-grid system.[21]	17
Figure 2.8	Complete Off-grid power system for any application.[22]	18
Figure 2.9	Renewable Energy Source (RES) in multichannel system functional diagram.[23]	21
Figure 2.10	Deployed foldable 50-W CPV generator. [24]	22
Figure 2.11	The Spectrolab C1MJ cell efficiency versus the sunlight concertation and temperature.[28]	23
Figure 2.12	Photogeneration of electron-hole pair in a semiconductor.[29]	26
Figure 2.13	Conversion of sunlight to generate electricity.[29]	27
Figure 2.14	The system integrated for a portable power supply.[29]	28
Figure 2.15	The block diagram of portable power supply to the battery storage system.[32]	30
Figure 2.16	Block diagram of IoT system that use communicate with portable power supply.[32]	31
Figure 2.17	The schematic diagram of a dynamo.[35]	32

Figure 2.18 The hybrid flowchart to categorize the different energy conversions.[38]	35
Figure 2.19 An electric driverless bus with equipment needed.[38]	36
Figure 2.20 Magnetic flux compression during expansion phase. [39]	37
Figure 2.21 Data of initial plasma.[39]	38
Figure 2.22 Block diagram of the photovoltaic battery module power supply system with CIGS film applied in the portable devices. [40]	39
Figure 2.23 Multiplexer on chip. [40]	40
Figure 3.1 The project progress flowchart.	47
Figure 3.2 Block diagram of project.	48
Figure 3.3 PSCAD V5 software.	50
Figure 3.4 Solar panel.	51
Figure 3.5 12V 30W DC Motor.	52
Figure 3.6 Seal Lead Acid battery.	53
Figure 3.7 Charge controller.	54
Figure 3.8 Solar inverter	55
Figure 3.9 Earth Leakage Circuit Breaker.	56
Figure 3.10 Miniature Circuit Breaker.	56
Figure 3.11 Arduino Uno Rev3.	57
Figure 3.12 Liquid Crystal Display I2C.	58
Figure 3.13 Switch socket outlet	58
Figure 3.14 AC cable for off-grid PV system.	59
Figure 3.15 PV DC cable.	60
Figure 3.16 Grounding cable.	61
Figure 3.17 Electrical panel box.	62
Figure 3.18 Project layout	67
Figure 3.19 Solar Photovoltaic circuit.	68

Figure 3.20 Mechanical dynamo circuit.	69
Figure 3.21 Battery circuit.	70
Figure 3.22 Switching control circuit.	71
Figure 3.23 Full circuit layout.	72
Figure 3.24 Top view.	74
Figure 3.25 Front view.	74
Figure 3.26 Side view.	75
Figure 4.1 Simulation result of solar voltage.	79
Figure 4.2 Mechanical dynamo waveform result.	80
Figure 4.3 Battery voltage of circuit design.	81
Figure 4.4 Result of capacitor voltage in circuit design.	82
Figure 4.5 The converter current in simulation circuit.	83
Figure 4.6 Solar charging time with wire diameter at 0.8 mm^2 .	86
Figure 4.7 The relationship between temperature and current for wire diameter at 0.8 mm^2 .	87
Figure 4.8 The solar power, respectively, is proportional to the current and time for the wire diameter at 0.8 mm^2 .	89
Figure 4.9 Solar charging time with wire diameter at 1.5 mm^2 .	91
Figure 4.10 The relationship of panel temperature and current generated with cable diameter at 1.5 mm^2 .	93
Figure 4.11 Solar PV generated power with cable diameter at 1.5 mm^2 .	94
Figure 4.12 Solar PV charging time with cable diameter at 4.0 mm^2 .	97
Figure 4.13 The panel temperature and current versus time with cable diameter at 4.0 mm^2 .	98
Figure 4.14 The solar PV generated power and current versus time with cable diameter at 4.0 mm^2 .	99
Figure 4.15 The solar PV system charging time over time with a cable diameter at 10.0 mm^2 .	101

Figure 4.16 The solar PV generated current and panel temperature versus time with cable diameter at 10.0 mm ² .	103
Figure 4.17 The solar PV generated power and current versus time with cable diameter at 10.0 mm ² .	104
Figure 4.18 The mechanical charging using cable diameter at 1.0 mm ² .	107
Figure 4.19 The power and current generated from mechanical pedal using cable diameter at 1.0 mm ² .	109
Figure 4.20 The mechanical pedal charging using cable diameter at 1.5 mm ² .	111
Figure 4.21 The power and current generated from mechanical pedal using cable diameter at 1.5 mm ² .	113
Figure 4.22 The mechanical charging process of cable diameter of 4.0 mm ² .	115
Figure 4.23 The output power and current over time of a cable with a diameter of 4.0 mm ² .	117
Figure 4.24 The graph of generator and battery voltage over time by using the cable diameter of 10.0 mm ² .	119
Figure 4.25 The output power and current from the generator over time in minutes by using mechanical pedal with a cable diameter of 10.0 mm ² .	121
Figure 4.26 The battery and load voltage over duration of discharging.	124
Figure 4.27 The power consumption of load current over the time of discharging.	125
Figure 4.28 The battery and load voltage over time of fan speed position 2.	127
Figure 4.29 The load current and power consumption of fan speed position 2 over time.	128
Figure 4.30 The discharging load and battery voltage over time of fan speed at position 3.	131
Figure 4.31 The discharging load current and power consumption for the fan speed position 3 over time.	132
Figure 4.32 Arduino UNO signal indicator of voltage and current for the hybrid portable power supply.	133
Figure 4.32 Arduino UNO signal indicator of power for the hybrid portable power supply.	134

LIST OF SYMBOLS

\$	-	US Dollar
%	-	Percentage
RM	-	Ringgit Malaysia
%/C	-	Temperature Coefficient
V _{AC}	-	Voltage Alternating Current
V _{DC}	-	Voltage Direct Current
A	-	Amperes
Hz	-	Hertz
Ah	-	Amp-hours
kWh	-	kilo-watts hours
W	-	Watts
mm	-	millimeter
MW	-	Megawatts
SAR/kWh	-	Saudi Arabia riyal per kilo-watts hours

اونیورسیتی تکنیکل ملیسیا ملاک

UNIVERSITI TEKNIKAL MALAYSIA MELAKA

LIST OF ABBREVIATIONS

V	-	Voltage
I	-	Current
P	-	Power
BESS	-	Battery Energy Storage System
PWM	-	Pulse Width Modulation
MPPT	-	Maximum Power Point Tracking
AC	-	Alternate Current
DC	-	Direct Current
PV	-	Photovoltaic
RES	-	Renewable Energy Sources
CPV	-	Concentrating Photovoltaic
V_{mp}	-	Voltage at maximum power
I_{mp}	-	Current at maximum power
V_{oc}	-	Voltage at open circuit
I_{sc}	-	Current at short circuit
W/m^2	-	Watt per meter square
V_{AC}	-	Volts Alternating Current
V_{DC}	-	Volts Direct Current
IoT	-	Internet of Things
KEH	-	Kinetic Energy Harvest
MRT	-	Magnetic Rayleigh-Taylor
MFC	-	Magnetic Field Correlation
MHD	-	Magnetohydrodynamic
CIGS	-	Copper Indium Gallium Selenide
PSCAD	-	Power Systems Computer Aided Design
FACTS	-	Flexible Alternating Current Transmission System
ELCB	-	Earth Leakage Circuit Breaker
MCB	-	Miniature Circuit Breaker
USB	-	Universal Serial Bus
UPS	-	Uninterruptible Power Supply
PVC	-	Polyvinyl Chloride
GI	-	Galvanized Iron
UV	-	Ultraviolet
LCD I2C	-	Liquid Crystal Display with Inter-Integrated Circuit
SDA	-	Serial Data
SCL	-	Serial Clock
IGBT	-	Insulated Gate Bipolar Transistor
ESS	-	Energy Storage System
MATLAB	-	Matrix Laboratory
SLA	-	Seal Lead Acid
IP address	-	Internet Protocol address
CAES	-	Compress Air Energy Storage

CHAPTER 1

INTRODUCTION

1.1 Background

A power supply is a device that supplies a source with electrical energy. The primary function is to convert the electric current source into the appropriate voltage, current, and frequency for energizing the load. Consequently, power supplies are also known as electric power converters. There are a few ways to categorize power supplies, including by their features and functions. A regulated power supply is used to maintain a constant output voltage or current, whereas the output voltage or current of an unregulated power supply can fluctuate significantly when the input voltage or load current changes.[1]

A portable power supply, also referred to as a portable power station, is comprised of a few optimal and transportable components that enable users to continue using electrical appliances in and around the home or during outdoor activities. There are specific requirements that must be met when dealing with portable power supplies, such as USB ports and the ability to charge a power station in a variety of ways. The design of a power supply depends on the battery capacity, which can range from 200 watt-hours to 25 kilowatt-hours, and the shape and dimensions of the power supply.

**Togo Power 346Wh**

Best small portable power station

**Bluetti 50S**

Best value portable power station

**Anker PowerHouse 767**

Best overall portable power station

**Anker 757 PowerHouse**

Best portable power station for backup

**EcoFlow Delta Mini**

Best portable power station for camping

Figure 1.1 Types of portal power supply.[2]

In addition, larger power stations can accommodate larger battery capacities, the integrated UPS function is increasingly used as a portable home battery during off-grid situations and power disruptions. [3]A portable power supply is the best choice for recharging common personal electronics and small appliances when away from household AC outlets for extended periods of time, and for having emergency backup power readily available. To establish a power supply, this initiative relies on renewable energy sources, such as solar energy, which is one of the most prevalent off-grid sources of electricity.[3] In addition, using solar panels to provide energy and a storage bank to retain the energy is the best option for lengthy journeys when multiple rechargeable devices are required.

Therefore, portable power can be useful for camping and provide a number of benefits, but there are a number of drawbacks to consider, including limited capacity, weight and size, inconsistency, weather impact, and a higher cost than a generator. In comparison to gasoline-

powered generators, that produces gas pollution which means a generator is not an environment friendly compared to portable power supply. [4] In the context of portable power supplies that used lithium-ion battery packs, the term inconsistent referred to the efficiency of certain differences in parameters such as voltage, capacity, temperature influence, and self-discharge rate after single cells of the same specification and model are combined to form battery packs.[5]

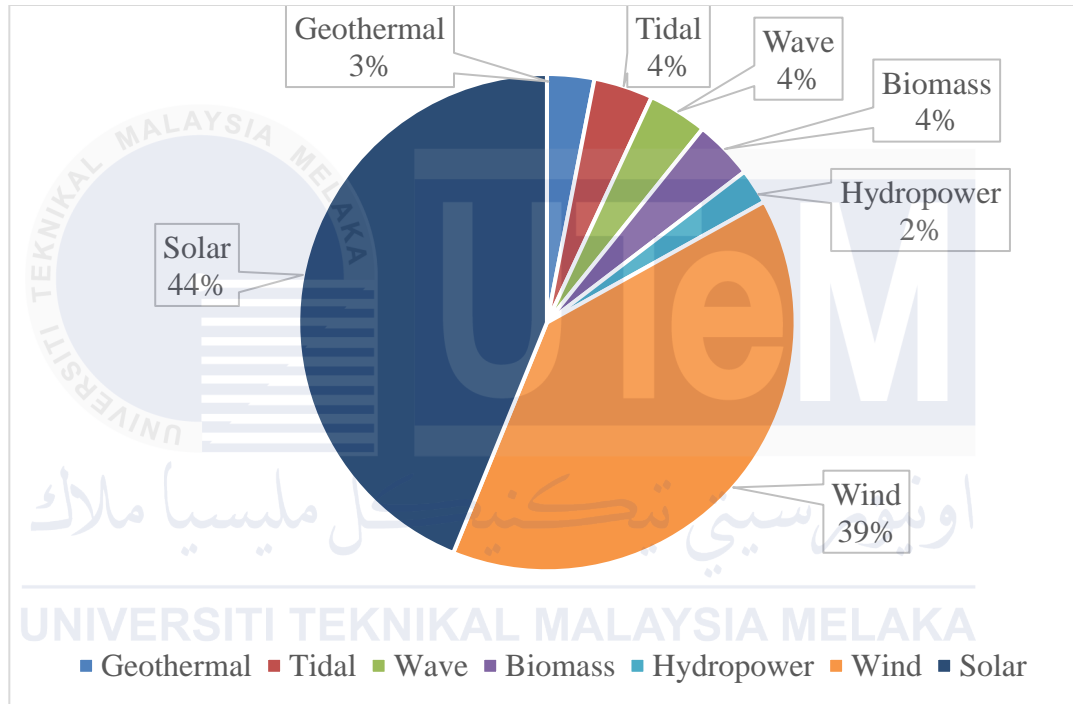


Figure 1.2 Percentage of renewable energy in total literature. [6]

The percentage of renewable energy currently available is depicted in figure 1.2 as a pie chart. Next, solar and wind energy are the most efficient methods to develop a portable power supply base to reduce greenhouse gas emissions and store energy in a battery bank. However, renewable energy is still incompatible with climatic conditions and has high initial costs.

This project applies the hybrid system to the process of enhancing portable power supplies because portable power supplies in the market only offered a single input source, except for rechargeable AC sources. In this thesis, will describe the process of combining solar, dynamo, and battery. To develop this system, it is necessary to implement and investigate the history of solar-

powered portable power supplies from earlier versions. Nevertheless, the effectiveness of the generated energy increased due to the device independence from a single type of input voltage. This means that when there is no solar energy, the user can still generate energy from a mechanical dynamo. So, these are a few techniques for enhancing the performance of this project. Moreover, when considering the lifespan of the system, types of batteries must also be considered, as their capacity can impact the size and weight of portable power sources. The number of batteries plays a crucial role in achieving a lightweight design.

1.2 Problem Statement

When it comes to energizing their devices and equipment during expeditions, campers and outdoor explorers frequently face a significant obstacle. While the wilderness offers a retreat from the modern world, the need for electricity persists for charging smartphones, operating portable refrigeration, and operating illumination systems. It is difficult for campers to maintain a sufficient power source for the duration of their travels with the current solutions for portable power supplies, which require a larger capacity, high costs, and inefficient energy consumption. Consequently, the issue at hand is to develop a portable power supply solution that satisfies campers energy needs while optimizing energy consumption. Existing portable power supply options on the market are typically cumbersome, weighty, and inefficient, resulting in decreased portability and increased reliance on multiple power sources. These solutions are frequently prohibitively expensive, rendering them inaccessible to many outdoor enthusiasts. The need for portable power supplies to be cost-effective hinders the ability to enjoy a comfortable camping experience. The extensive use of non-rechargeable batteries or inefficient energy sources poses environmental concerns. A portable power supply system that strikes a balance between power

capacity, efficiency, and cost must be developed. This solution should emphasize the incorporation of renewable energy sources such as solar panels, mechanical dynamos, and battery enabling campers to harness the energy of nature and reducing their reliance on conventional power infrastructure or non-rechargeable batteries. In a few ways, this issue can be resolved, such as by using a hybrid renewable energy system with an energy storage device. In the meantime, the issue of portable power supplies can be considered in order to avoid excessive weight and bulkiness. In addition, the system should implement intelligent energy management techniques, allowing for the efficient allocation of power to various devices and averting waste.

1.3 Project Objective

This project's primary objective is to create a systematic and effective method for estimating the hybrid renewable energy-based portable power supply system. The following are the specific objectives:

- i) To simulate the hybrid renewable energy system with PSCAD software.
- ii) To develop a hybrid renewable energy-based hardware-based portable power supply for outdoor activities.
- iii) To analyze the design of a portable power supply, it is important to consider several factors, including the battery bank capacity, types of charging, different load discharging, various cable diameter charging, safety features, and system efficiency.

1.4 Scope of Project

The scope of the project will be demonstrated considering a specific limitation specification. This project has the restrictions outlined in this subtopic to safeguard the system hardware and guarantee its proper operation:

- a. A hybrid renewable energy-based portable power supply comprising two distinct energy sources, such as solar PV and mechanical pedal, with a lead-acid battery.
- b. PSCAD software was used in this project to design a hybrid renewable energy simulation circuit based on a portable power supply.
- c. Solar PV has a maximum output power of 10 watts and measures 435 mm × 200 mm.
- d. The battery type is Seal Lead Acid (SLA), with a capacity of 12 V and 7.2 Ah.
- e. To monitor the system status, this project system is designed to communicate with the Arduino UNO in order to display the real-time battery and current status on an LCD I2C.
- f. For the implementation of this project, an emphasis is placed on outdoor activities, particularly camping and adventure, that utilize burdens such as phone charging, a fan, and several lights.
- g. This portable power supply offers a specific number of input and output ports, including two gang switch-socket outlet and four DC ports.

CHAPTER 2

LITERATURE REVIEW

2.1 Introduction

The chapter discusses the concept of hybrid renewable energy systems, which combine two or more renewable energy sources to generate electricity. Integrating multiple sources provides a more stable and reliable power supply, reduces the impact of greenhouse gas pollution, and offers flexibility in meeting specific energy needs. Hybrid systems offer a sustainable and versatile alternative to traditional energy sources and have the potential to play a significant role in the transition towards a more environmentally friendly energy future. The essential advantage of hybrid renewable energy systems is their ability to reduce reliance on traditional fossil fuel-based energy sources. With climate change becoming increasingly urgent, hybrid systems offer a promising solution toward a more sustainable future. These systems provide a reliable and clean energy source that can reduce carbon emissions and mitigate climate change's impact.

2.2 Background Study

In the background study, the essential components will be discussed in terms of hybrid renewable energy. The history of hybrid renewable energy, the concept of hybrid renewable energy, a component of hybrid renewable energy, and applications of hybrid renewable energy are all covered in this subtopic.

2.2.1 History of Hybrid Renewable Energy.

To create energy from renewable sources, hybrid power combines many sources. A hybrid power and energy storage system are referred to as such in power engineering. In 1917, the first hybrid power system operated the dynamo that housed the battery bank using one of two technologies, gasoline or kerosine. [7], [8]The gasoline engine powers the dynamo through a belt that links the engine to the alternator. The pulley attached to the dynamo shaft will turn while the engine operates. The storage battery will then be charged using the electrical energy produced by the alternator.

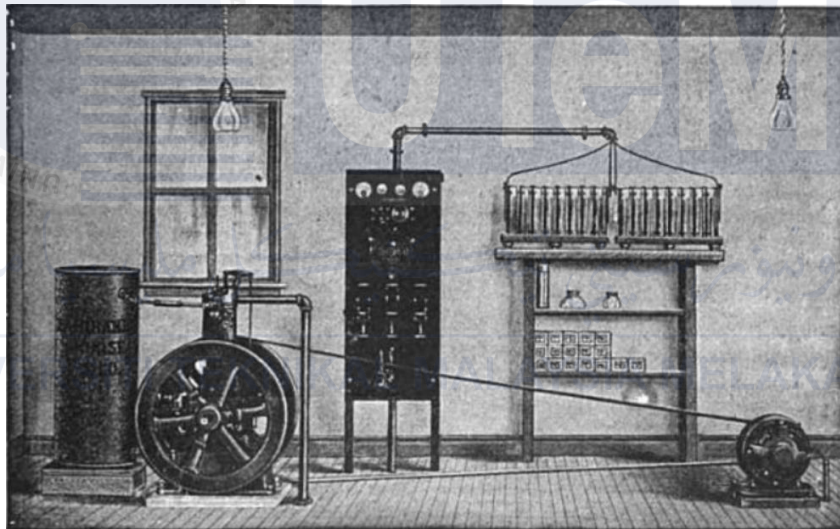


Figure 2.1 Early hybrid power from gasoline/kerosine engine drives the dynamo which charges the storage battery. [7]

Renewable energy sources that include solar photovoltaic (PV), wind turbines, hydropower, and fuel cells, are often used in hybrid systems. [8]The amount of energy generated when two separate sources are joined is likewise more than it would be with a single production. A significant energy storage capacity is required to achieve the highest level of supply dependability, safety, and security. Therefore, standalone hybrid renewable energy systems are

gaining popularity. Due to improvements in renewable energy technology and the relatively cheap cost of petroleum extraction, it is mainly utilized in rural regions.

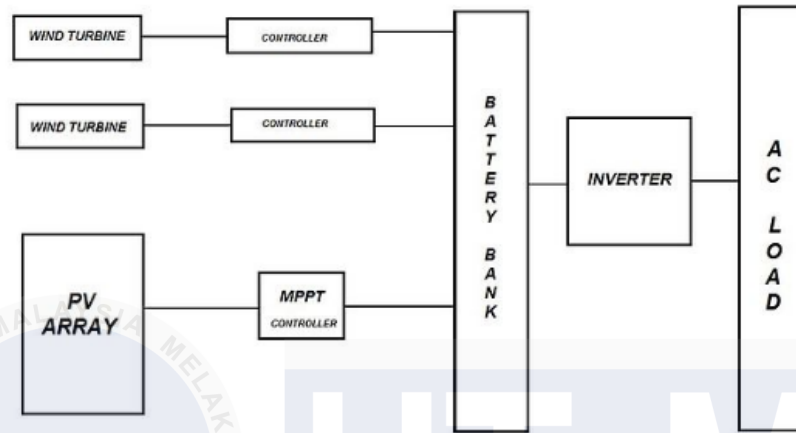


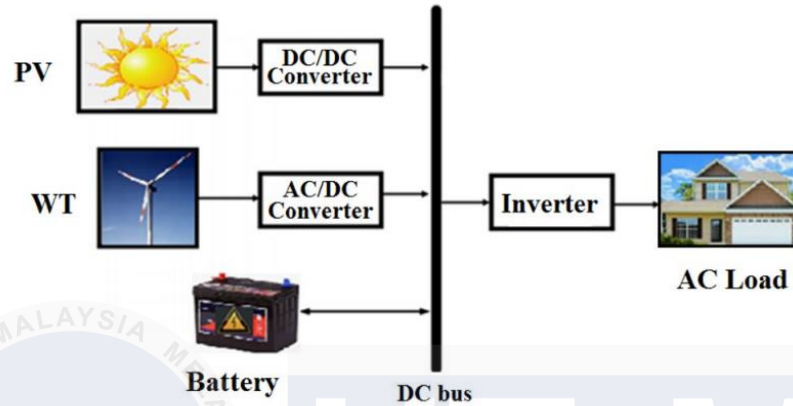
Figure 2.2 PV-Wind hybrid energy system.[8]

A hybrid renewable energy system is a kind that combines a wind turbine with a solar array. The power output of the power system will rise due to this example and is independent of either output power. How the weather affects, for example, when it rains or is cold outside, the output production of PV arrays will decrease or stop working. In contrast, wind turbines may continue running, producing, and storing energy. This thesis shows that hybrid systems provide benefits that are independent of one kind of power production. For example, a \$5 million hybrid system was installed in Western Minnesota in 2019 and is currently operating at 500 kW of solar PV via a 2 MW wind turbine, enhancing the capacity factor, and reducing annual costs by \$150,000.[8]

2.2.2 Concept of Hybrid Renewable Energy.

A system that combines multiple forms of renewable energy to produce electricity is referred to as a "**hybrid renewable energy system**." This strategy may provide a more dependable

and constant supply of electricity while addressing some of the drawbacks of individual energy generated from renewable sources.



• Figure 2.3 Hybrid renewable energy generation.[9]

According to the figure 2.3, the system consists of two combinations of renewable energy sources, including solar, wind, and a battery storage system.[10] The primary component of hybrid renewable energy is the combination of various renewable energy sources to increase the flexibility of generation from multiple sources.

Table 2.1 Three major types of solar PV panels.[11]

Solar Panel Type	Advantages	Disadvantages
Monocrystalline	High efficiency and performance	Higher costs
Polycrystalline	Lower costs	Lower efficiency and performance
Thin-film	Portable and flexible	Lower efficiency and performance

Solar photovoltaic (PV) is the first choice for renewable energy nowadays that is used to generate the electricity which on-grid and off-grid system. A PV cell is a single device designed to connect to other cells to create bigger units known as modules or panels. In this design, PV technologies may advance and become more dependable and effective. In 1839, Alexandre-

Edmond Becquerel made the first recorded observation of the photovoltaic effect. In more significant information about photovoltaics, photons, or bundles of radiant energy, make up the sunshine so that photons may be absorbed and passed through. Only the absorbed photons will produce electricity. The energy of the photons is converted to electrons in the atoms of the solar cell upon photon absorption. To make the system more efficient and assure more dependable generation, solar PV requires two kinds of connections is string and array. Solar PV panels come in three main varieties. For example, monocrystalline, polycrystalline, and thin film.[11]

Wind turbine is the secondary source of figure 2.3, a hybrid system may offer a more reliable power supply, even when nightfall draws near. By combining solar and wind energy, it can take advantage of the strengths of several sources and charge the batteries when the sun is not shining. In essence, wind is the movement of air in reaction to atmospheric pressure variations.

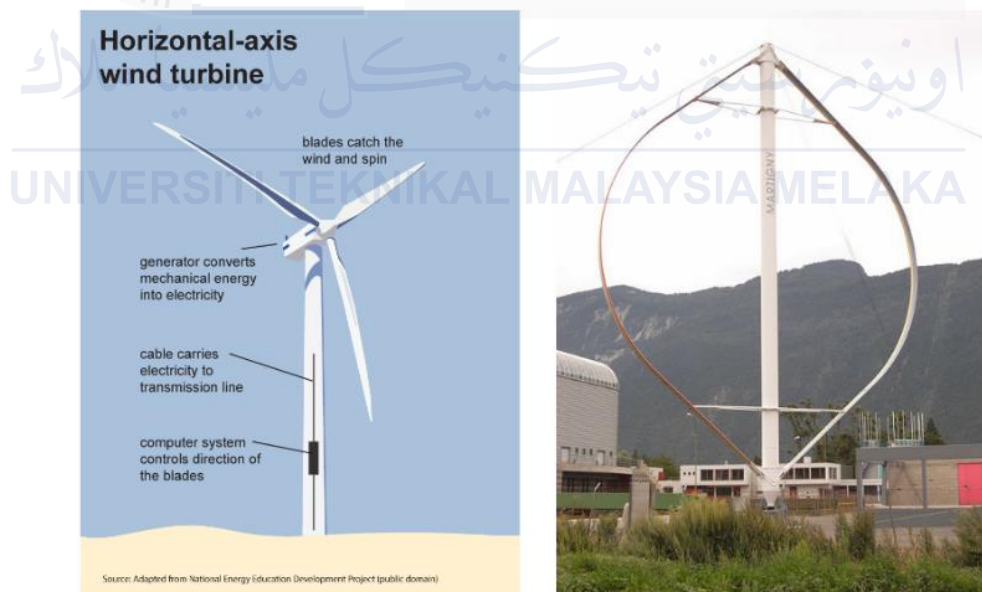


Figure 2.4 Two major types of wind turbines.[12]

Horizontal-axis turbines and vertical-axis turbines are the two main kinds of wind turbines. The amount of power a wind turbine can produce depends on the size of its blades. American scientist Charles F. Brush created the first wind turbine in 1887, which was both onshore

and offshore.[13] It transforms wind energy into usable energy, such as producing electricity using wind turbines. Consequently, wind turbines are machinery that transforms wind kinetic energy into electrical energy. The rotor blades began to rotate as the wind passed them, turning the shaft and generating power.

Charge controller manages the electricity coming into the battery bank from solar energy. This device safeguards the deep cycle batteries against daytime overcharging and from solar panels that could draw power from the battery bank overnight due to reverse power. Charge controllers are available in various configurations, including PWM (pulse width modulation) and MPPT (maximum power point tracking). PWM charge controllers are less expensive but less efficient compared to MPPT controllers. MPPT charge controllers use sophisticated algorithms to optimize the power output of solar panels, resulting in increased charging capacity and greater efficiency.

Table 2.2 The comparison between PWM and MPPT solar charge controller.[14]

PWM Controller	MPPT Controller
Array voltage is “pulled down” to battery voltage.	Convert excess input voltage into amperage.
Generally operate below V_{mp} .	Operate at V_{mp} .
Suitable for small module configurations.	Suitable for large module configurations that have a lower cost per watt.
Often chosen for very hot climates which will not yield as much MPPT boost.	Provide more boost than PWM, especially during cold days and/or when the battery voltage is low.

An MPPT charge controller is more costly than a PWM charge controller. Hence, the two main technologies available for solar charge controllers, PWM and MPPT, may cause the system

to function significantly differently. A PWM solar charge controller will work by connecting the battery storage directly to the solar panels. The PV array output voltage is pulled down to the battery voltage during bulk charging when there is a constant connection from the PV array to the battery bank. If not, an MPPT solar charge controller will gauge the maximum voltage (V_{mp}) from the panel and down-convert it to the battery voltage. The current is increased when the voltage is decreased to meet the battery capacity. Thus, it will draw more power from the PV array. The power of the charge controller is equivalent to the power out of the charge controller.

The **rectifier** transforms alternating current (AC) into direct current (DC). As alternating current (AC) is produced by the wind turbine, it is often utilized to charge the batteries for wind energy.

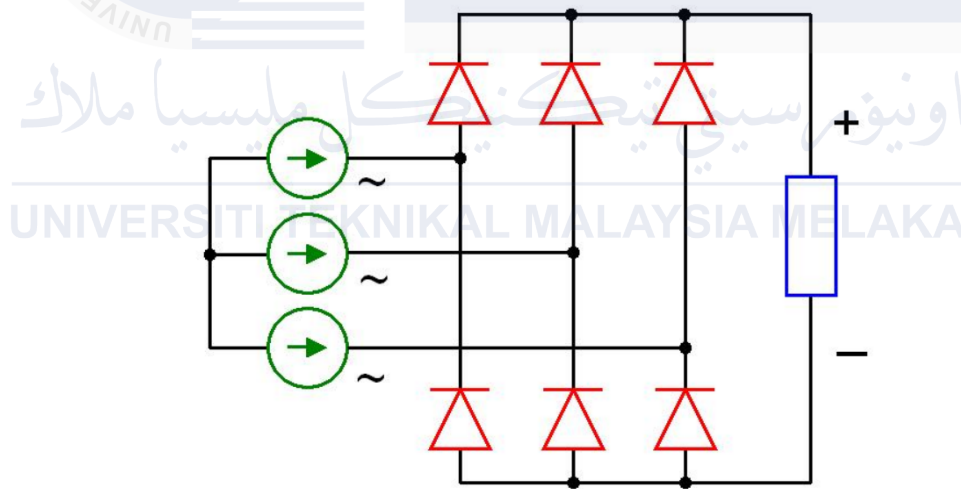


Figure 2.5 Three-phase full wave bridge rectifier.[15]

Rectifiers are utilized in a variety of applications, including power supplies for electronic devices, battery converters, motor drives, and numerous other systems that require a DC voltage. The desired output voltage, required current, efficiency, and cost are a few factors that affect the choice of rectifier type (bridge, half-wave, or others). It operates automatically and continually

assesses the condition and temperature of the batteries and other system parameters to guarantee minimum ripple and steady-state voltage.

Table 2.3 Types of batteries.[16]

Lithium-Ion Battery	Lead Acid Batteries	Flow Batteries	Compressed Air Energy Storage	Flywheel Storage
Consists of a single, enclosed battery that is both charged and discharged using a combination of conductors and electrolytes.	Energy is stored through the chemical processes between sulfuric acid, water, and lead.	Composed of electrochemical cells and two tanks connected by a membrane. Between these tanks, a fluid, usually iron or vanadium, is transferred, and the cells produce electricity.	A system that utilizes heat energy stored in compressed air as power. Systems for compressed air energy storage (CAES) store energy similarly to batteries. However, this energy is produced using the surrounding air or other gases.	A large wheel is attached to a revolving shaft in this energy storage device. The more energy used, the quicker this wheel spins.

Battery Storage is also called a battery energy storage system (BESS) that is used to store energy from renewable sources. When there is no sunshine, and the wind has stopped blowing, battery storage technology is essential for ensuring that homes and businesses can be powered by green energy. As a result, battery energy storage systems are far more sophisticated since they may be powered by electricity produced from renewable sources.[17]

Solar inverter is the most critical component of renewable sources. A solar inverter transforms photovoltaic (PV) panels output energy into usable electricity that may be used to power alternating current (AC) loads. This operating inverter will convert the battery bank direct current into alternating current outputs ranging from 120 to 240 volts.

Table 2.4 The comparison between three types of solar inverters.[18]

Characteristics	On-Grid	Off-Grid	Hybrid
Compatible with	On-Grid Solar Power Systems.	Off-Grid Solar power Systems.	Both On-Grid & Off-Grid Solar Power System
Energy Storage	No solar energy is stored.	Solar energy is stored in batteries.	Solar energy can be stored in batteries.
Power Transfer to Grid	Excess power gets transferred to the utility grid.	Power is not transferred because it is not connected to a grid.	Excess power gets transferred to the utility grid.
Anti Islanding Feature	Present	Absent	Present
Price Range	A 3kW On-Grid Inverter cost about RM 1,700 – RM 2,300	A 3kW Off-Grid Inverter costs about RM1,700 – RM 2,300	A 3kW Hybrid Grid Inverter costs about RM 4,000 – RM 4600

Solar inverters come in various forms, including battery inverters, central inverters, hybrid inverters, and string inverters. They must consider the various inverter brands, types, and sizes while developing a solar PV system.

Watts, a measurement of power in (2.1), is used to describe **loads**. The amount of power used at any moment represents the load of a particular piece of electrical appliance. Like hybrid generating, the facility must provide considerable power or energy to be stored in the battery bank.

$$P = V \times I \quad (2.1)$$

Watt-hours, a unit of energy or the total amount of energy utilized in (2.2) that used in a certain period, are used to quantify energy consumption. The load is multiplied by the number of operating hours when calculating consumption. Therefore, the discharge rate will rise if the load exceeds the energy stored in the battery bank.

$$Energy = Watt \times Hours \quad (2.2)$$

2.2.3 Components of hybrid renewable energy

Technology has progressed to include several renewable energy sources, including solar, wind, and Micro/Pico hydro. Renewable energy components were developed to supply reliable power. Its capability to provide a reliable supply of power. By incorporating several energy sources, the system can account for variations in the individual energy sources and provide a more stable power supply. This is crucial in areas with unpredictable climate conditions or regular energy supply.[19]

In contrast to intermittent energy sources like solar and wind, which depend on weather conditions and cannot be controlled similarly, **dispatchable energy sources** can balance energy supply and demand and provide a stable energy source. These energy sources can be turned on or off as needed, dispatched, or controlled to meet changes in energy demand.

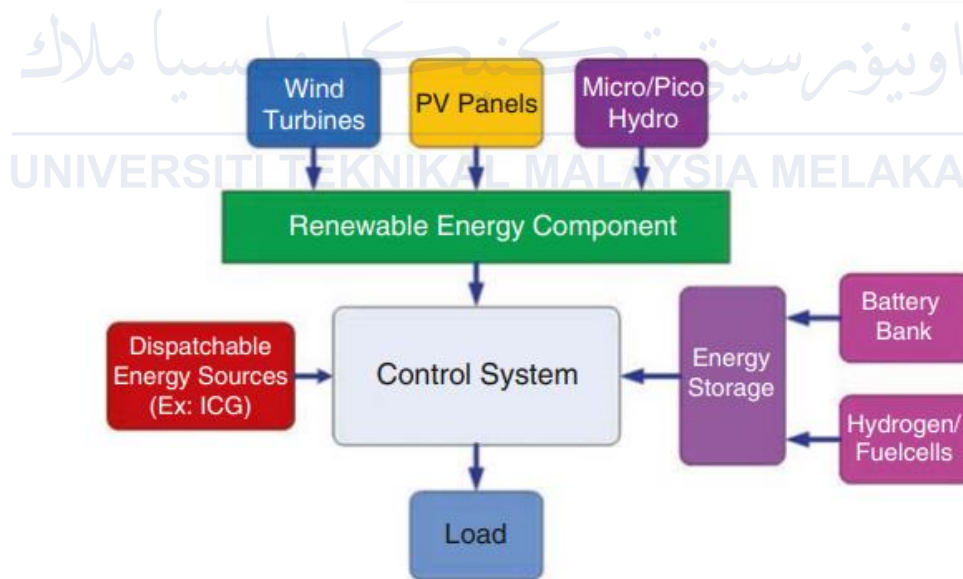


Figure 2.6 Schematic diagram of a stand-alone hybrid energy system.[20]

Control systems monitor and control the hybrid renewable energy system's multiple elements, guaranteeing proper and effective operation. These are made to ensure that produced energy is kept in a secure, effective, and reliable storage bank and that the system can adapt to

variations in energy demand and supply. The practice of storing energy in a form that may be utilized later is called energy storage. Systems for storing extra energy are used to prevent it from being created while energy demand is low and then releasing it when demand is high.

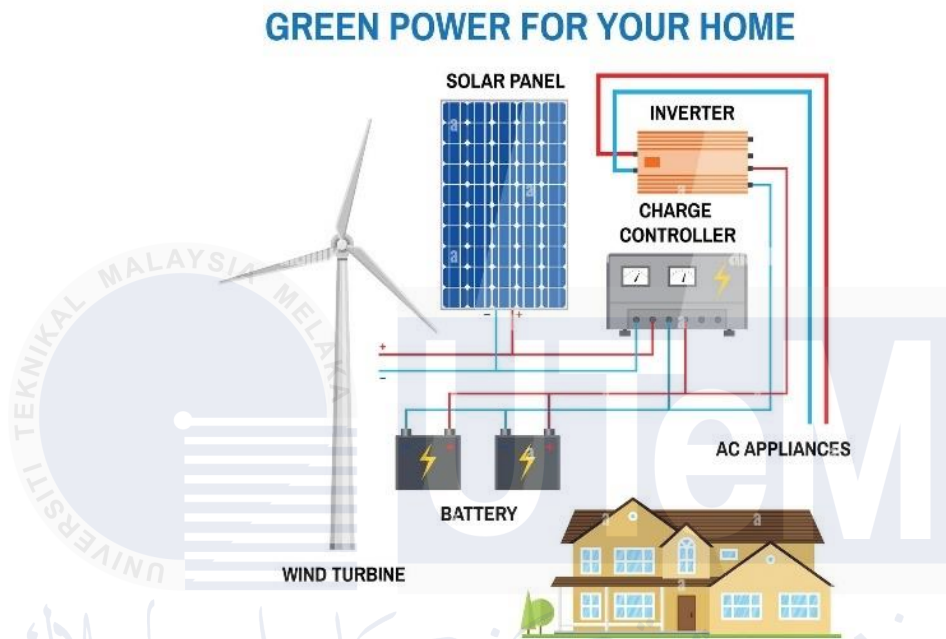


Figure 2.7 Schematic wiring diagram of PV-Wind off-grid system.[21]

Off-grid hybrid renewable energy systems must be protected to operate safely and effectively. Following the rules will help safeguard the devices of the whole system, considering the wire design and system operation. Protection mechanisms, such as overvoltage, overcurrent, lightning, grounding, environmental, and battery protection, are required in hybrid renewable energy systems.

For off-grid hybrid renewable energy depends on the battery capacity. Proper management and protection are required to maintain the safe and effective functioning of batteries. Thermal runaway, overcharging, and over-discharging of batteries may all be avoided by installing **battery safety devices** such as battery management systems. In addition, when the temperature of battery is increased, probability that battery may damage also increased.

2.2.4 Application of hybrid renewable energy

By using hybrid renewable energy comprise several parts that cooperate to produce power. The parts that go into a hybrid system will depend on the kind of renewable energy utilized. The following are some of the essential elements required to produce hybrid energy. Generally, a hybrid system will use two or more renewable energy sources, such as wind, solar, hydro, and biomass. Each source will need a unique combination of components to collect and transform energy into electricity.

Parts of a hybrid system are designed based on a number of variables, including the energy needs of the location, the available resources, and the available funds. A well-designed hybrid renewable energy system could contribute to a cleaner and more secure future by reducing reliance on fossil fuels and providing a reliable and sustainable power source.



Figure 2.8 Complete Off-grid power system for any application.[22]

Rural areas, communications infrastructure, industrial and commercial settings, residential settings, agricultural use, and emergency backup power may all use an off-grid hybrid power system. It may be customized to match the unique requirements of various locations and

industries as a sustainable, affordable, and dependable energy source. Off-grid places are distant from established infrastructure, including roads, electricity lines, and communication networks, are called **remote off-grid areas** since these regions are often remote and challenging to reach, offering power, fresh water, and sanitary facilities.

It may be challenging for facilities, and physical parts of the **telecommunications infrastructure** are crucial for delivering telecommunications services. Towers, fiber-optic cables, satellite networks, and data centers are just a few examples of the many technologies that make up this infrastructure. When implemented, the hybrid power system may provide energy backup for communications services and stability for power sources.[22]

Hybrid power systems that may balance electricity costs, lower carbon emissions, and enhance energy security are directly tied to **industrial and commercial** environments. These devices may benefit environments with high power consumption and high energy prices. A hybrid power system is a precise design for a **residential** environment that might vary based on the size of the house, household energy requirements, and the accessibility of renewable energy sources nearby. For example, a small solar panel array, a wind turbine, and battery storage may make up a hybrid power system for a small residence. The surplus energy would be stored for the night or during wind or solar activity.

Hybrid power systems may be used in **agriculture** to power irrigation systems, farm buildings, and energy and equipment. These systems may be powered by renewable energy sources like solar, wind, and hydro. When renewable energy sources are unavailable, energy storage systems like batteries or pumped hydro storage can be utilized as a fallback power source. However, hospitals, data centers, and emergency response centers are just a few of the essential facilities for which rid power systems may be configured to provide **emergency backup power**.

2.3 Research Literature

2.3.1 Nonvolatile Portable Power Supply, Performance Capabilities and Organization Principles in Continental Areas.

According to an article, optimizing the efficiency of renewable energy systems necessitates the careful consideration of several factors. The article highlights the significance of the dominant wind direction for wind generators, as it plays a crucial role in their year-round efficiency. In a similar manner, the inclination angle and placement of solar panels have a significant impact on solar energy production because they determine the amount of sunlight captured.

The article also observes that after the sun's peak hours, clouds have less of an effect on solar energy production. The author proposes the development of a hybrid renewable energy source system that incorporates wind and solar power in order to maximize energy production. The system seeks to increase energy supply reliability more than twofold by integrating both sources. In addition, the author intends to reduce the size and mass of the complex by a factor of two compared to conventional homogeneous systems. This hybrid approach could optimize energy production, improve system efficiency, and contribute to a more sustainable and reliable energy supply.

In this article, wind, hydro, solar, and petroleum are used to implement a hybrid renewable energy system. In relation to hybrid systems, two or more distinct types of energy resources may be utilized to ensure that the system generates more energy than conventional electricity generation. The flexibility of energy resources, as shown in Figure 2.9, is one of the advantages of hybrid renewable energy sources.

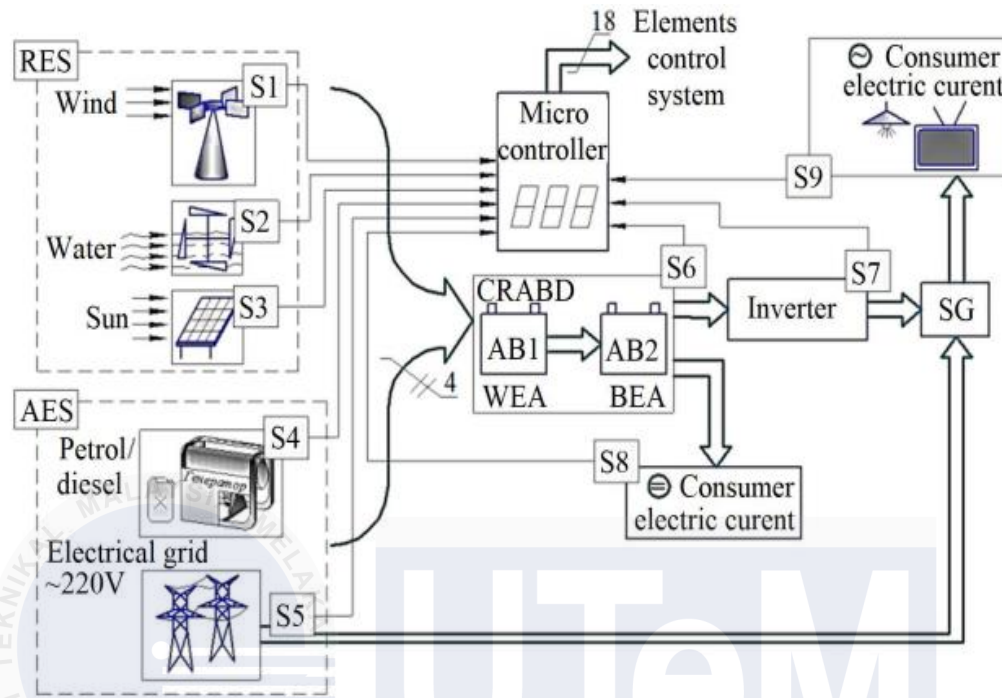


Figure 2.9 Renewable Energy Source (RES) in multichannel system functional diagram.[23]

The research article highlights the importance of portable power supplies, particularly in continental areas, and explores their potential for improved system performance. However, the limitations of a portable power supply include a smaller energy capacity compared to hybrid systems. The article suggests that combining solar and wind can improve energy efficiency by up to 42%. [23]

The project aims to contribute to developing independent portable renewable energy sources, emphasizing the need for lightweight and efficient construction while considering factors such as daily atmosphere analysis and panel area to ensure optimal system performance. The input and output ports should be compatible with end-users, meeting the portable power supply requirements. Ultimately, the research aims to improve the performance of hybrid renewable energy systems with storage for outdoor activities.

2.3.2 Portable Concentrated Sunlight Power Supply Using 40% Efficient Solar Cells.

The article demonstrates the significance of solar tracking for maximizing the generated power output. The fundamental axis of electronic tracking and manual adjustment support the concept of solar tracking. Figure 2.10 depicts a south-to-north-facing orientation for the sunlight-concentrating power supply. When the lens parquets are hit by sunlight, electricity is generated. In addition, a linear actuator used to rotate the solar modules from east to west has a variable-length north limb, and the control circuit in this instance is also adjustable.

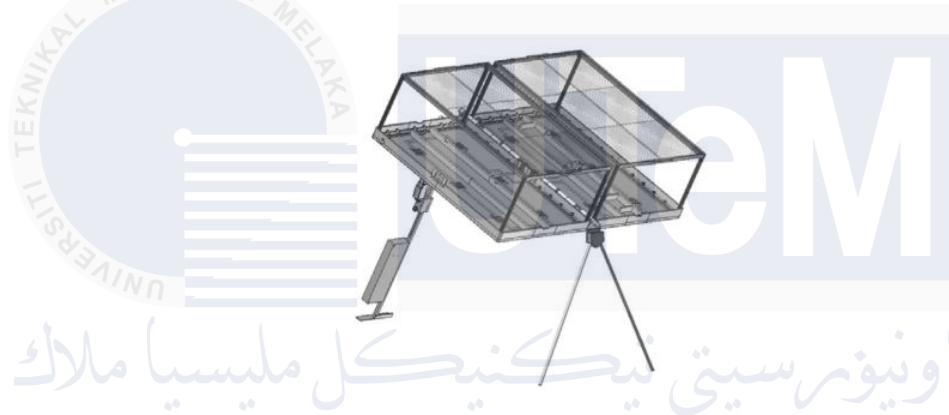


Figure 2.10 Deployed foldable 50-W CPV generator. [24]

The article describes how the rotation of the modules began from east to west using an electronically controlled linear actuator. When the module is rotated and the system encounters an angular problem, human intervention is required to manually modify the tilt of the module from the north to south evaluation angle once per day.

As a system that requires angle tracking, these rotational and incidence angles of the array must be included in this equation to ensure the angle is corrected and output power is maximized. The experiment described in the article demonstrates the percentage relationship between module temperature and maximum power efficiency. When the temperature of the module increases, the output power decreases in inverse proportion. The current also rises, as the impact of the temperature coefficient on the solar cell demonstrates.[27]

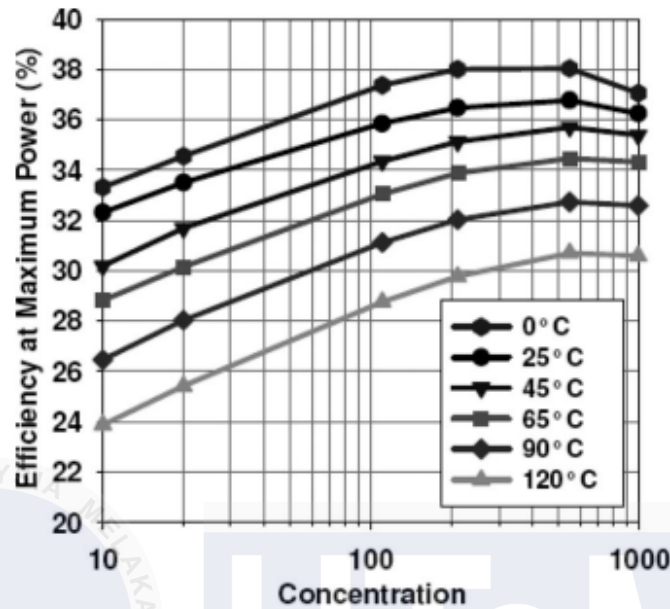


Figure 2.11 The Spectrolab C1MJ cell efficiency versus the sunlight concentration and temperature.[28]

The results of figure 2.11 are consistent with what the theory of solar energy predicts because the voltage should decrease as the temperature rises. Referring to the concept of solar energy, this experiment utilized a lens to transmit sunlight into a solar cell in order to obtain the cell's temperature. Accordingly, the experiment based on the article yields the same result as the solar energy theory.[26]

2.3.3 Design and Performance Analysis of a Portable Solar PV Power Supply.

In the article, the implementation of a 245-watt desert-type solar panel-based solar off-grid system is detailed. Two batteries are connected in series with a single charge controller and a DC-to-AC solar inverter. The purpose of this project is to design and measure system performance in relation to global solar irradiance, ambient and cell temperatures, array voltage and current, battery voltage, and energy produced.[30]

Before the author developed the hardware, simulation results should have been required as evidence to support the performance of the PV generation system and to demonstrate that the weather's impact is minimal.

Table 2.5 PV System Data[27]

Tilt and Orientation	Tilt: 25 degrees, south	
Cell Technology	Si-Poly, Model SM-D245, S-Energy Korea	
Modules	1	
Panel global power	Nominal: 245 W _p	
Panel operating	V _{mp} = 30 V	I _{sc} = 8.59 A

As shown in table 2.5 and 2.6 of the cited article, the charge controller datasheet included the panel Standard Test Condition (STC) value required for hardware development.

Table 2.6 The characteristic of solar PV charge controller and batteries[27]

Characteristic	I _{mp} = 8.18 A	Tem. Coefficient = - 0.458%/°C
	V _{oc} = 37.5 V	
Battery type	Model 6Y112	
Batteries	2	
Battery Characteristics	24 V, 130 Ah, 3.120 kWh	

The annual energy production in Saudi Arabia and the contribution of solar PV tilt angle are detailed in Table 2.7. From the data in Table 2.7, the authors demonstrate that the result was derived from their own experiment.

Table 2.7 Annual Energy Production Cost for Different Tilt Angle Optimization for Summer, Winter, and all seasonal[27]

Tilt angle	0° (Summer Optimization)	50° (Winter Optimization)	25° (Annual Optimization)
Annual Energy	361.37	375.16	403.10
Cost (SAR/kWh)	2.04	1.96	1.83
Solar Fraction (%)	86.7	90.0	96.7

As shown in Table 2.7, the author ran a simulation based on the climate in Saudi Arabia, which began with summer and ended with winter. The annual energy output is depicted by the difference between the three tilt angles of solar panels, which are 0 degrees, 25 degrees, and 50 degrees. As the above result is reflective of annual energy consumption in a season, it can be extrapolated to seasonal energy consumption. Summer has the lowest annual energy due to the solar fraction compared to winter and the annual optimization.

Solar energy is recognized as an indispensable and globally significant renewable energy resource. In an article, the author focuses on its potential in Saudi Arabia and constructs four distinct scenarios to simulate potential climate conditions in the region. By undertaking these simulations, the author aims to gain insights into the performance and viability of solar energy systems under varying climatic circumstances. These scenarios consider solar irradiation levels, temperature variations, cloud cover, and other meteorological parameters influencing solar energy generation.

Table 2.8 The effect of shading versus cleaning panel.[27]

Case	Radiation (W/m ²)	Ambient Temp. (°C)	Module Tem. (°C)	Vmp (V)	Imp (A)	Pmax (W)
Case 1: Panel with Dust	928	26.6	42.8	27.0	4.08	120.0
Case 2: Cleaned Panel at 968 W/m ²	968	26.6	42.0	24.1	7.40	177.0
Case 3: Cleaned panel with 1006 W/m ²	1006	27.9	43.1	25.6	7.01	179.9
Case 4: Panel with 25% shading	987	27.9	46.1	29.5	0.82	24.3

Table 2.8 provides a thorough analysis of the effects of solar radiation, ambient temperature, and module temperature on the output power of solar photovoltaic (PV) systems. The

table contains numerous simulation-implemented scenarios that provide valuable insight into the observed variations. The correlation between temperature and solar radiation is a crucial factor affecting the output capacity of PV modules. Solar radiation tends to decrease as temperatures rise, affecting the overall performance of the PV system. By analyzing the data presented in Table 2.8, researchers and industry professionals can gain a deeper understanding of the complex interplay between solar radiation, ambient temperature, module temperature, and the resulting variations in power generation. This information can inform the design and optimization of solar photovoltaic (PV) systems, resulting in increased efficacy and performance in response to changing environmental conditions. [28]

2.3.4 Building of A Portable Solar AC and DC Power Supply.

Figure 2.12 depicts the formation of mobile electron hole pairs that are used to generate electricity from a p-n junction, where the excited electron is swept to the n-region and the holes are swept to the p-region to become majority carriers.

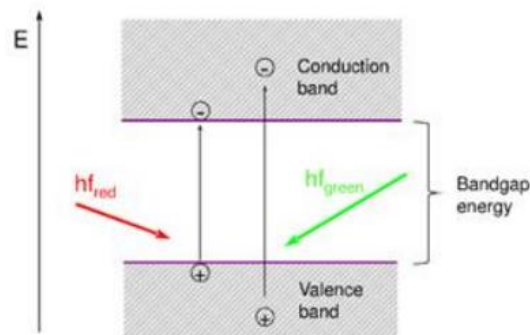


Figure 2.12 Photogeneration of electron-hole pair in a semiconductor.[29]

As depicted in Figure 2.12, photons with sufficient energy (greater than the material's bandgap) generate mobile electron-hole pairs in a semiconductor. Consequently, a solar cell converts photons into electrons to produce electrical energy. The term for this is photoelectric

effect. In terms of developing an external circuit to be connected between the solar cell and the external circuit to allow electrons to flow through the external circuit to combine with holes in the p-region, as shown in figure 2.13.

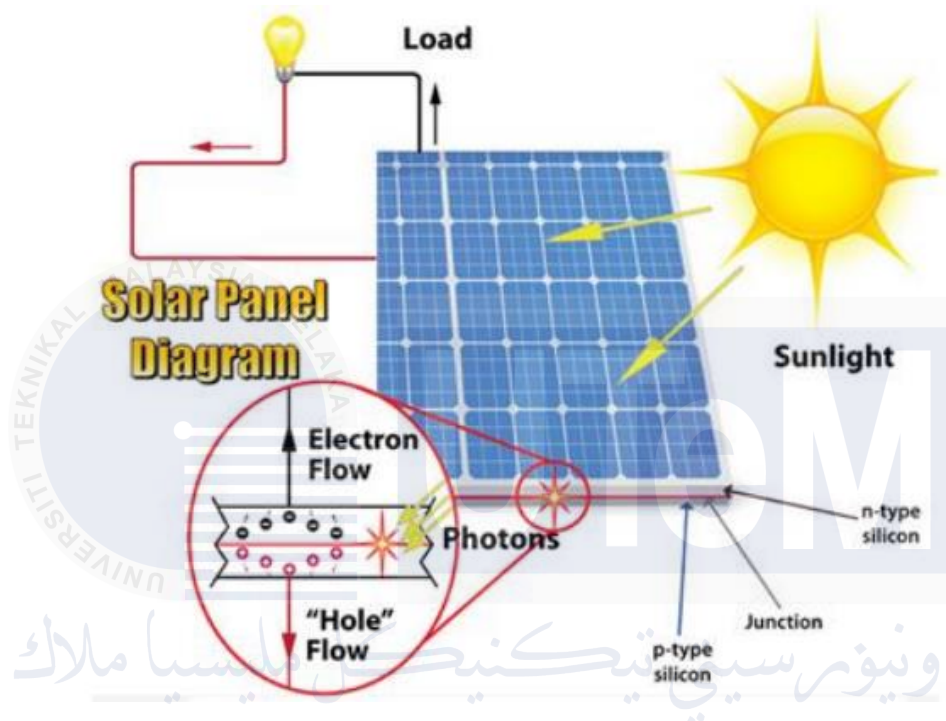


Figure 2.13 Conversion of sunlight to generate electricity.[29]

When the electron flows through the external circuit, the solar cell produces the electricity necessary to store energy in a rechargeable battery. According to solar energy, direct-current (DC) voltage will be generated. System components such as a charge controller, rechargeable battery, and inverter are required to develop a portable solar power supply.[30] Because more than one type of voltage source is required to meet the load limit.

According to Figure 2.14, the article's circuit design incorporated a portable power supply system in a circuit containing several essential components, including a solar panel, charge controller, voltage regulator, inverter, and battery indicator. However, since the input sources are distinct, this circuit can be used as a reference for a hybrid portable power supply. Inconsistent

solar panel voltage generation necessitates a voltage regulator to maintain a constant 5 V_{DC} power supply.

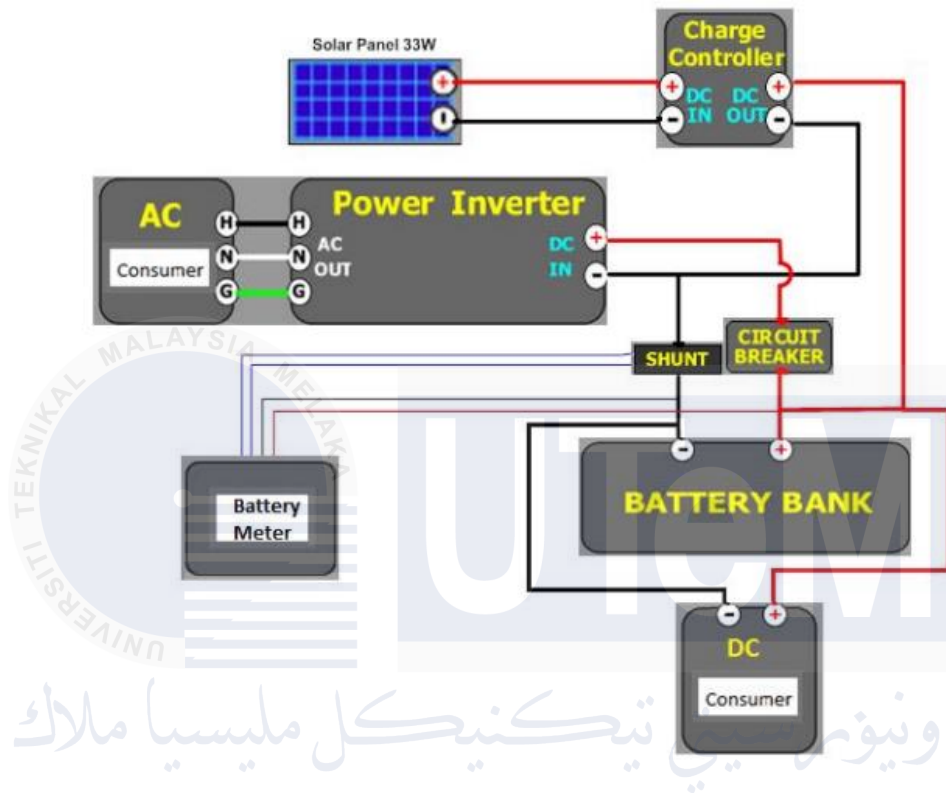


Figure 2.14 The system integrated for a portable power supply.[29]

Before proceeding to the hardware design phase, specific calculations must be performed based on the circuit shown in Figure 2.14. Using Ohm's Law, the current across an electronic component in a circuit should be directly proportional to the applied voltage while the resistance remains constant. [31]Consequently, the calculated value of the capacity required to operate some low-wattage devices with a 230 V_{AC} supply.

Table 2.9 depicts an experiment that analyzed the performance of a power supply system by simulating a household's average power consumption. The authors discovered that the system could provide power for two days at 230 W per day by directly extracting power from the battery. This reserve energy source provides power even without solar energy, with a system designed to prevent battery discharge below 50 percent.

Table 2.9 The Power Consumption for selected hardware are devices.[29]

Description	Rating (Watts)	Usage	Consumption	Quantity
Solar Panel	30	-	-	1
Battery	12 Volt, 40 Ah	-	-	2
Fluorescent bulb	30	2	60	2
Filament bulb	50	2	100	2
Laptop	35	2	70	1

To maintain battery capacity, the writers suggest monitoring the system to ensure that the batteries remain consistently above 50 percent of their maximum charge. According to the authors, it is crucial to match the battery size to the electrical appliance's utilization. As power consumption and the number of concurrently connected devices increase, so does the discharge rate. For instance, the authors tested the system with a laptop, a fluorescent bulb, and a filament bulb all connected concurrently, resulting in a higher current draw and a quicker discharge rate.

2.3.5 Development of Portable Solar Power Plant Equipped with IoT Connectability.

According to research literature, the lack of electricity in rural areas has encouraged the development of portable solar power plants. Describe in the abstract the regularity of earthquakes in Indonesia. When disasters occur, the power will go out, and the communication system will lose connectivity. Developers created a portable power plant as an emergency energy source for remote areas to prevent this issue. In addition, portable power plants are advantageous when the installation area is disconnected from the infrastructure. The system can continue to function with a secondary energy storage system.

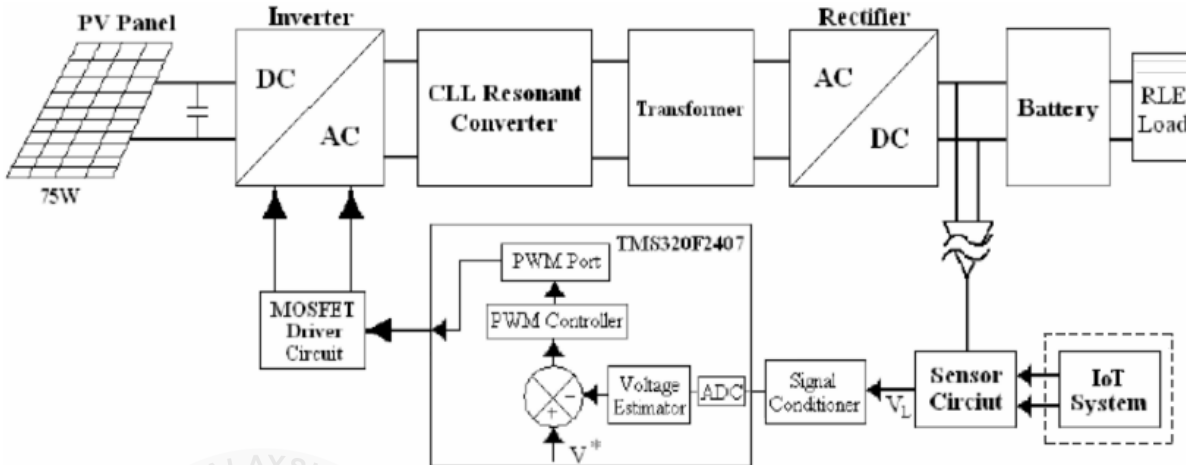


Figure 2.15 The block diagram of portable power supply to the battery storage system.[32]

The development of a portable solar power plant supply based on the Internet of Things (IoT) can provide reliable electricity sources in remote areas or as an alternative energy source during natural disasters such as earthquakes and tsunamis, as described by the authors. The portable power supply is beneficial during emergencies. [33]The IoT system connects to the off-grid system management, allowing for monitoring and control of transmission and distribution functionality. However, good internet connectivity is necessary for sending information to the receiver or transmitter, which may pose a challenge in rural areas.

Figure 2.16 depicts the method by which an Atmega328-based microcontroller displays the status of a portable power supply. Block A focuses on a control circuit for the energy storage system to transmit power to the Atmega328, whereas Block B has no power. In addition, Block B is a microcontroller circuit that enables the sensor signal to be transmitted as a pulse to the Atmega328 and records the grid status.

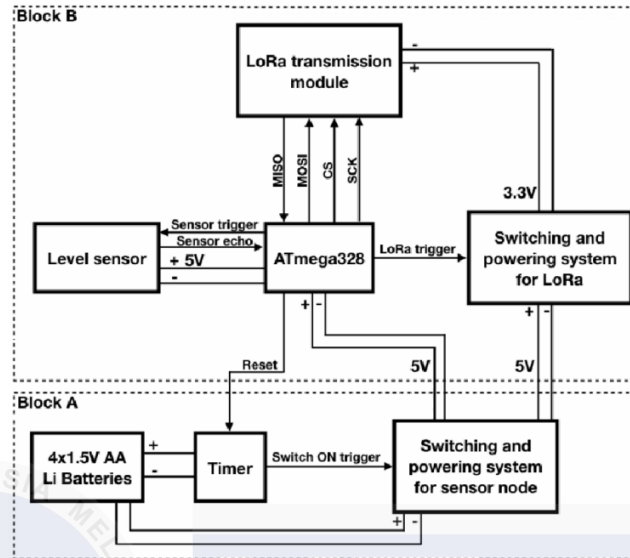


Figure 2.16 Block diagram of IoT system that use communicate with portable power supply.[32]

Figure 2.16 depicts an IoT system used for monitoring and control purposes to determine the status of a portable power supply. The Arduino ATmega328 is used to integrate all sensors in order to ascertain all system parameters that may be affected. The system requires an internet connection to communicate with specified IP addresses generated by the module for communication over the Internet. In addition, the sensor was used to transmit data to microcontrollers, after which the program would automatically upload the information to the cloud.

2.3.6 Magnet Dynamo

This article discusses the potential and limitations of using magnet dynamos to construct a hybrid portable power source. The article provides a concise history of electrical motors and the working principle of the dynamo, which generates electricity through the use of rotating magnets. [34]

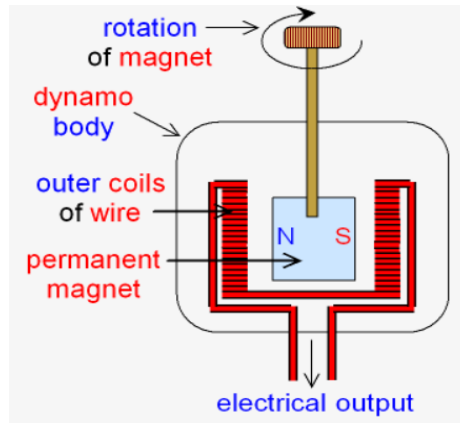


Figure 2.17 The schematic diagram of a dynamo.[35]

The electricity production by a dynamo is based on the rotation of a magnet in the center of several wire coils. Therefore, the absence of a slip ring eliminates the necessity for coils. Then produces electricity in the wire bundles. Otherwise, the rotating magnet should contact the tire's rotating circumference when the bicycle is in motion.[36]

The concept entails generating low-voltage DC with a bicycle dynamo or rotational magnet to support solar PV battery charges. The article highlights the significance of weight when replacing an alternator with a dynamo in a hybrid portable power supply. In addition, the article describes the benefits of using an alternator in terms of electricity generation consistency and the distinction between the types of electrical currents generated by an alternator and a dynamo.

2.3.7 A Novel Design and Fabrication of Energy Generating Oscillatory Swing – A Play way Technique for Public Parks.

According to the explanation in the article, oscillatory children's swings made of a specific material can generate electrical energy. The relationship between freewheels and a pendulum bar rotates the wheel arrangement while a rechargeable battery stores energy. However, the output power can also be used to power lighting lamps in public parks and charge communication devices such as cell phones, electronic devices, and children's toys.

Several aspects of the design of the proposed energy-generating oscillatory unit base swing have been completed. Table 2.10 outlines the materials employed in the development of oscillatory swing energy generation.

Table 2.10 Specification and dimension of material.[37]

Serial No.	Specification	Dimension
1	Stand	Height: 64-inch, Width: 50-inch
2	Swing	Height: 990.6 mm, Width: 647.7mm
3	Connecting Rod	Width: 673.1mm at right and at left 889mm.
4	Spur Gear	Big spur: 76.2mm in diameter Small spur gear: 50.8mm in diameter
5	Freewheel	Big Free wheel: 177.8mm in diameter Small Free wheel :76.2mm in diameter
6	Chain	Big:1346.2mm, Small: 1193.8mm
7	Battery	Lead acid battery: 12V, 7Ah
8	Convertors	9 volts dc to 18-volt dc converter, 12-volt DC to 230-volt AC converter

From material in table 2.10 its basic construction, the swinging action of the swing causes the horizontal beam member to rotate continuously at a certain angle and enables movement in both directions. This motion is transmitted to a link that converts the angular motion into a linear one and amplifies it. This motion is then conveyed to a freewheel through flexible links. The freewheel converts this linear reciprocating motion into a circular, unidirectional one transmitted to the flywheel. A specific transmission connects the flywheel to the generator in order to enhance the generator's end speed. The generator transforms mechanical energy into electrical energy, resulting in the production of electricity.

Table 2.11 The result of the experiment of oscillatory swinging.[37]

Load of swinger	Material made up of whole unit	Speed of the swing	Output (V)	Load	Status of load
35 40 45	Iron	Slow Average Faster	6 9 11	CFL bulb	Glow
35 40 45	Plastic	Slow Average Faster	12 18 22	CFL Bulb	Glow

Suddenly, the flywheel will be connected to the generator to increase the speed and output voltage that can be generated. In detail, the generator will convert mechanical power into electrical power and produce electricity. From the fabrication of the oscillator swinging, it can generate free energy or green energy sources.

2.3.8 A hybrid kinetic energy harvester for applications in electric driverless buses.

The article defines a hybrid system as a complex combination of multiple input energy sources. It focuses predominantly on three primary energy input modules, which will be elaborated upon in greater detail. This article aims to provide a comprehensive explanation of hybrid renewable energy systems, beginning with the transformation of kinetic energy into electrical energy. It emphasizes that the system can generate electricity whenever there is acceleration in the environment by utilizing this motion to generate electricity. Additionally, the article emphasizes that the hybrid system utilizes the combustion of the input sources in various ways to generate energy. Utilizing various techniques and technologies, such as thermoelectric conversion and internal combustion engines, the system maximizes the utilization of input energy sources. This comprehensive approach to hybrid renewable energy systems ensures efficient energy generation

by utilizing multiple input sources and providing increased flexibility and sustainability in meeting energy demands.

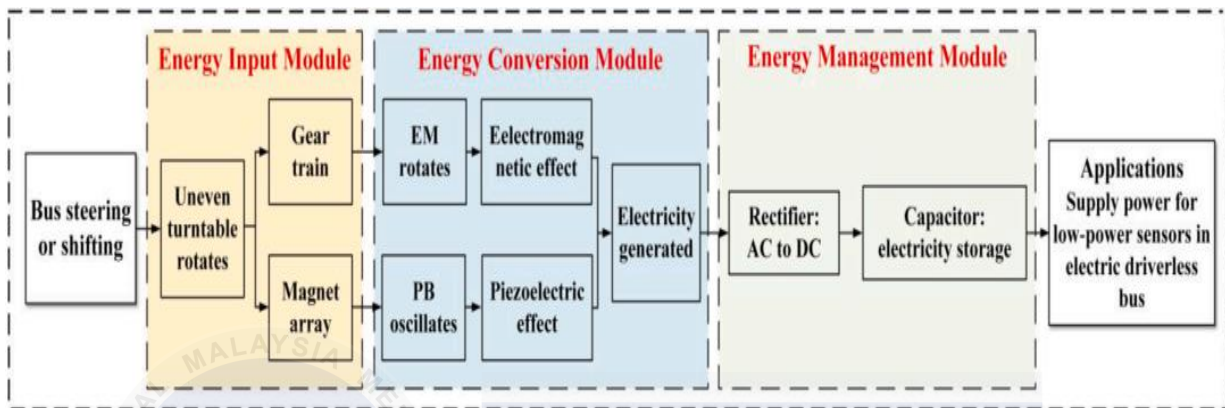


Figure 2.18 The hybrid flowchart to categorize the different energy conversions.[38]

Basically, the article does research by using technology that can harvest energy from environmentally and at the same time the energy automatically stores in the battery bank for design a driverless car or public transportation. Meanwhile, the challenge in this project is categorizing the different energy conversion mechanisms proposed to recover the available energy. From the article solution, the manufacturer design energy management circuits, and the control system sensor to implement self-powered.

Figure 2.19 illustrates the circuit layout of the autonomous bus. By converting AC voltage to DC voltage using a full bridge rectifier, energy can be stored in a battery bank. Since the energy must be direct-current voltage, the kinetic energy harvest (KEH) is alternating-current voltage. The administration of an energy circuit harvest is intended to convert unstable voltage to stable DC voltage, which can be stored directly in a battery and utilized directly to power a load.

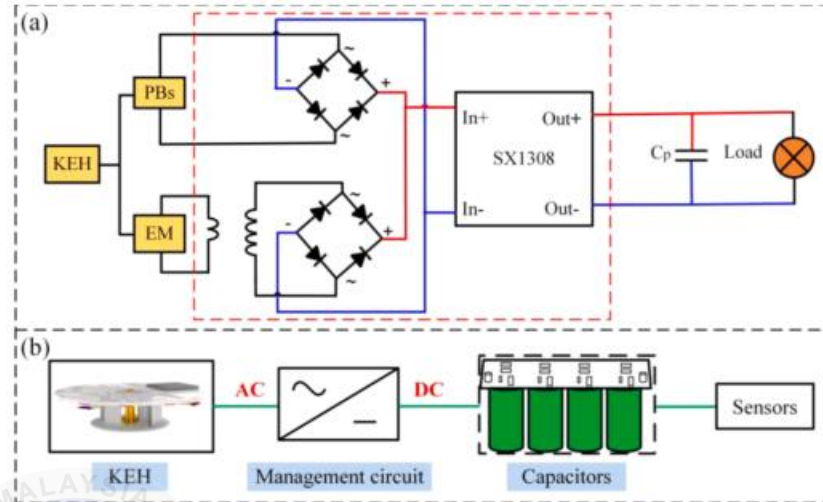


Figure 2.19 An electric driverless bus with equipment needed.[38]

For the energy management module, the inertial kinetic input will transfer the energy by converting an electromagnetic motor and piezoelectric beam. The system provides a voltage control circuit, a rectifier filter circuit, and a charging control chip to control the unstable voltage. To give a self-powered solution for low-power applications in driverless electric buses, this system will represent a piezoelectric, electromagnetic hybrid kinetic energy harvested (KEH) by the authors.[38]

2.3.9 Analysis of magnetic Rayleigh-Taylor instability in a direct energy conversion system which convert inertial fusion plasma kinetic energy into pulsed electrical energy.

The article explores the intriguing concept of converting plasma kinetic energy to electrical energy by means of magnetic flux compression (MFC). Utilizing the principles of Faraday's law, it investigates the intricate relationship between plasma kinetic energy and the generation of electrical energy. By examining this relationship, the study casts light on the potential for harnessing plasma's immense kinetic energy and converting it to an electrically usable form via MFC. This research paves the way for the future development of advanced energy

conversion technologies that capitalize on plasma's unique properties, providing new avenues for sustainable and efficient energy production.

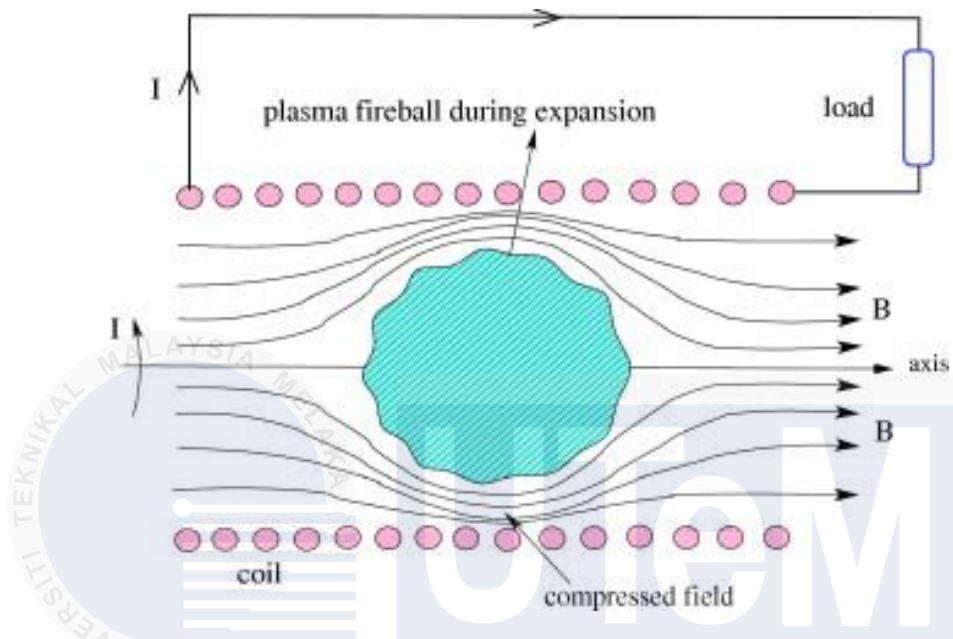


Figure 2.20 Magnetic flux compression during expansion phase. [39]

The article examines a direct energy conversion scheme for converting plasma kinetic energy in an Inertial Fusion system into pulsed electrical energy, focusing on the Magnetic Rayleigh-Taylor (MRT) instability and its application for magnetic flux compression. The authors provide simulation results of converting kinetic energy to electrical energy using MFC, with MHD simulations on different initial perturbation amplitudes and wavelengths.[39]

The experiment establishes a basis for comprehending the initial conditions of the investigated plasma system by referencing previously collected data. These initial parameters are crucial for describing and predicting the behavior and properties of the plasma throughout the experiment. Utilizing previously published data ensures that the experiment builds on existing knowledge and understanding, providing a basis for comparison and further analysis. By incorporating these initial plasma parameters, scientists can improve their comprehension of the

experimental system and its dynamics, thereby contributing to the advancement of knowledge in plasma physics.

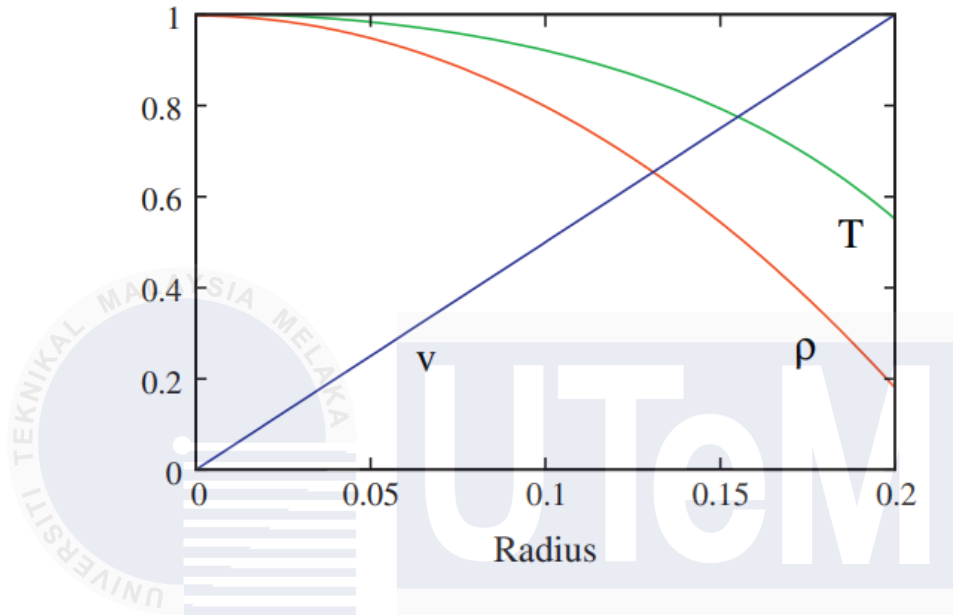


Figure 2.21 Data of initial plasma.[39]

The result of the author's simulation using plasma with an initial radius of 0.2 meters is shown in Figure 2.21. Nevertheless, the initial radial profiles for plasma density, temperature, and velocity are constructed using a separate 2D simulation that disregards the effect of B (free expansion up to a radius of 0.2 m).

2.3.10 Photovoltaics battery module power supply system with CIGS film applied in portable device.

The article compares the various varieties of photovoltaic systems, which are Cu (In, Ga) (S, Se)₂ (CIGS) films that must be implemented in a portable power source for electronic devices. Based on the experiment described in the article, the CIGS thin film solar panel type has been used. However, applying the system at a low temperature yielded the most significant performance.

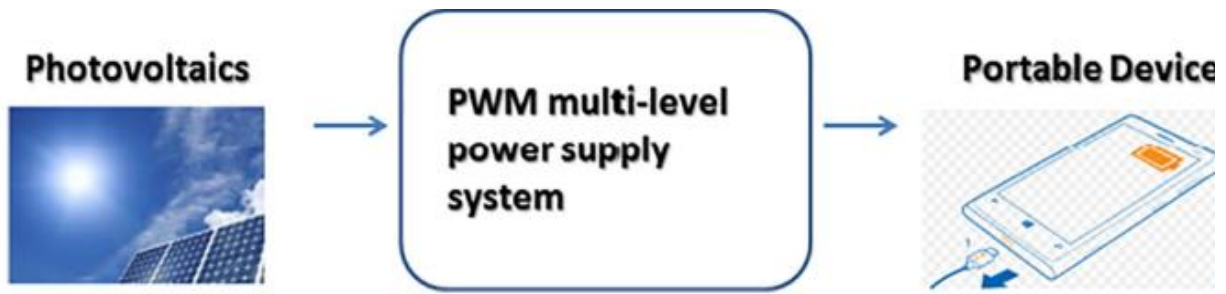


Figure 2.22 Block diagram of the photovoltaic battery module power supply system with CIGS film applied in the portable devices. [40]

The article introduces a multiplexer device instrumental in developing a multi-channel and multi-level power supply system, as shown in Figure 2.22. The semiconductor contained several essential features, such as "data latches" and "shift registers," to facilitate high-speed data signal processing. Utilizing these capabilities allowed the system to process data signals quickly and efficiently. The chip was designed to contain a clock fast-counting device, which played a crucial role in converting the input signal string into a parallel output for the infrastructure. This feature allowed for the simultaneous, seamless administration of multiple channels.

Figure 2.23 depicts the architecture of a semiconductor, highlighting its intricate design and functionality. The architecture consists of multiple cells, denoted by identifiers such as D11, D21, D31, and DN1, which correspond to discrete portable load systems. This advanced multiplexer processor and its associated features have revolutionized power supply systems by facilitating the development of a resilient and flexible infrastructure. The processor excels at managing multiple channels efficiently and satisfying diverse load requirements. With its versatility and adaptability, this semiconductor architecture has paved the way for improved power supply solutions that can seamlessly handle a variety of portable loads, ensuring optimal performance and dependability across a broad spectrum of applications.

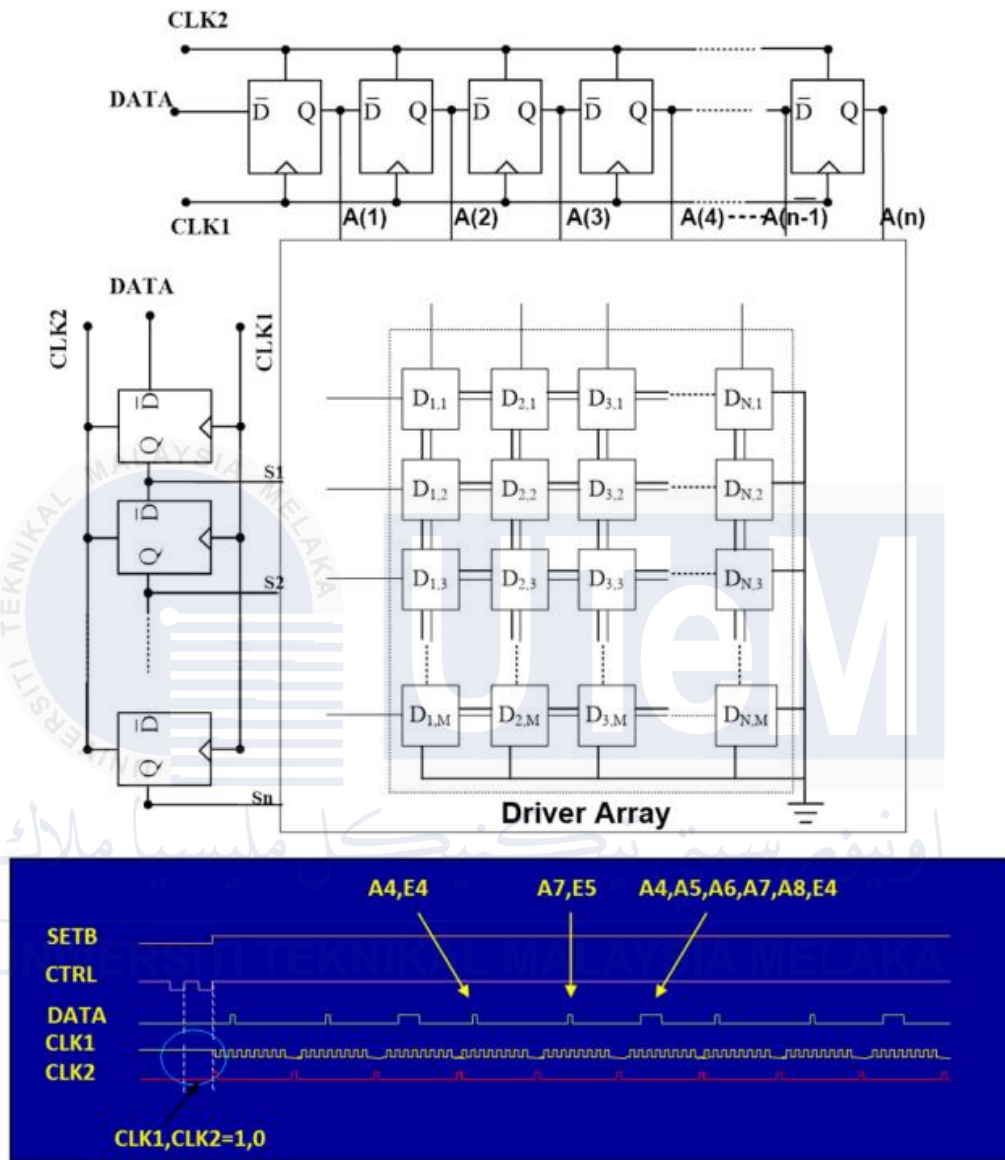


Figure 2.23 Multiplexer on chip. [40]

Regardless of the number and complexity of voltage-supplying electrical systems involved, the device described in the article demonstrates an exceptional capacity to convert multiple channels and voltages within a single integrated system. This remarkable device introduces a flexible and effective method for simultaneously managing multiple voltage levels and channels. By consolidating these functions into a unified solution, the system architecture is simplified and streamlined.

2.4 Research Summary.

Table 2.12 Summary of the research article.

No.	Authors	Title	Application	Remark
1.	Oleg Berg and Sergey Prischepov	Nonvolatile Portable Power Supply. Performance Capabilities and Organization Principles in Continental Areas.	<ul style="list-style-type: none"> i. The system is usually used in the continental area. ii. The combination of RES multichannel system. iii. The improvement of autonomous portable power supply. 	<ul style="list-style-type: none"> i. The system is more focused on side construction. ii. The system is specific uses for residential power consumption.
2.	Lewis Fraas, James Avery, Leonid Minkin, Han Xiang Huang, and Parvez Uppal	Portable Concentrated Sunlight Power Supply Using 40% Efficient Solar Cells.	<ul style="list-style-type: none"> i. Use for outside activities as an example is nowadays, soldiers also use more electronic devices more and carry heavy batteries to the camp. ii. Focus on point lenses and incorporation tracking. 	<ul style="list-style-type: none"> i. Uses for low power rate electrical consumption such as laptops, mobile phones, bulbs, etc. ii. The design of the portable power supply focuses on reducing the weight and number of batteries. iii. Mainly focus on outdoor activities.
3.	Mounir Bouzguenda, Abdullatif A.Al-Omair, and Abdurhman A. Al-Yamani.	Design and Performance Analysis of a Portable Solar PV Power Supply.	<ul style="list-style-type: none"> i. Large-scale power plant for the off-grid system. ii. The PV generation is based on the simulation used for rural areas. iii. Use for a low voltage to a medium voltage potential. 	<ul style="list-style-type: none"> i. The system is more focused on an off-grid system. ii. The project design simulated the low to medium voltage potential. iii. Focus on the performance of off-grid system efficiency.
4.	Luo-Qi Soh and Chee-Chiang	Building of A Portable Solar AC and DC Power Supply.	<ul style="list-style-type: none"> i. The design of this system is more about how to make the portable power 	<ul style="list-style-type: none"> i. Use for low power consumption.

	Derrick Tiew.		<ul style="list-style-type: none"> ii. supply fulfill outdoor purposes. To power up the lower-power home appliances. 	<ul style="list-style-type: none"> ii. The system can use for outdoor activities.
5.	Dicky Dwi Putra, Abdurrauf Irsal, Muhammad Alif Mi'raj Jabbar, Adelia Kurniadi, Agus Purwadi, and Achmad Munir	Development of Portable Solar Power Plant Equipped with IoT Connectability.	<ul style="list-style-type: none"> i. Using for the high possibility to remote sources area. ii. Focus on the earthquakes and tsunamis that occur. iii. Contribute to the IoT system to monitor and control transmission and distribution. iv. For the off-grid system. 	<ul style="list-style-type: none"> i. As a backup power supply when earthquakes and tsunamis occur. ii. Use for low voltage potential.
6.	Hugo Kim.	Magnet Dynamo	<ul style="list-style-type: none"> i. An explanation of how the dynamo can generate electricity. ii. How the dynamo can store energy in a battery. 	<ul style="list-style-type: none"> i. Low DC voltage devices.
7.	S.Yathavan, G.Ramesh Kumar, and S. Gokulraj	A Novel Design and Fabrication of Energy Generating Oscillatory Swing – A Play way Technique for Public Parks.	<ul style="list-style-type: none"> i. On oscillatory swing by the children. ii. Applied the different types of material to generate electricity. iii. The swing will be connected to the freewheel. 	<ul style="list-style-type: none"> i. A very low DC voltage.
8.	Minfeng Tang, Hao Cao, Lingji Kong, Ali Azam, Dabing	A hybrid kinetic energy harvester for applications in electric driverless buses.	<ul style="list-style-type: none"> i. Use the RES hybrid system to store the batteries. ii. Low-power application of electric driverless buses. 	<ul style="list-style-type: none"> i. Use for the prototype of driverless buses. ii. The conversion of kinetic energy into electrical energy.

	Luo, Yajia Pan, and Zutao Zhang.		iii. Energy management of different types of hybrid sources.	
9.	C.D. Sijoy and Shashank Chaturve.	Analysis of magnetic Rayleigh-Taylor instability in a direct energy conversion system which convert inertial fusion plasma kinetic energy into pulsed electrical energy.	i. Plasma kinetic energy is converted into electrical energy based on magnetic flux compression (MFC). ii. The acceleration of MRT will generate electricity.	i. More focus on the acceleration of the MRT. ii. How to the kinetic energy converted into electrical energy.
10.	Jian-Chiun Liou and Cheng-Fu Yang.	Photovoltaics battery module power supply system with CIGS film applied in a portable device.	i. The experiment of CIGS thin-film solar cell to work in low temperature. ii. Apply to multi-level power supply system chip design. iii. Use the able devices.	i. The experiment of solar cell performance. ii. To fully charge the multi-level power supply. iii. Mostly used to power up electronic devices.

2.5 Summary

Hybrid renewable energy systems effectively generate stable and sustainable electricity by combining multiple renewable energy sources. These systems offer several advantages, including reduced carbon emissions and the ability to mitigate the impact of climate change. The primary goal of designing a hybrid system is to create a cost-effective, durable product capable of powering low or high-rate electrical appliances while being environmentally friendly and lightweight.

To achieve these objectives, a thorough analysis of simulation results becomes crucial. Simulation evidence allows for a comprehensive understanding of the system's performance under different conditions, enabling engineers to optimize its design and ensure its reliability. By analyzing simulation outcomes, engineers can identify and address potential challenges early in the design process, leading to more efficient and effective hybrid systems.

Designing hybrid renewable energy systems presents its own set of challenges. Integrating multiple energy sources requires careful consideration of their compatibility and efficient coordination. The system must be designed to handle the variability and intermittency of renewable energy sources, ensuring a stable and reliable power supply. Moreover, balancing the power output from different sources and optimizing energy storage and management systems are critical to designing a successful hybrid system.

Despite these challenges, hybrid renewable energy systems offer a promising solution for a more sustainable energy future. By harnessing the benefits of different renewable energy sources, such as solar, wind, hydro, or geothermal, these systems can provide a reliable and continuous power supply while reducing reliance on fossil fuels. This contributes to mitigating climate change and promotes energy independence and resilience.

CHAPTER 3

METHODOLOGY

3.1 Introduction

In this chapter, the software and hardware components of a project's development process will be explained. Regarding meeting the energy needs of hybrid renewable energy based on portable power supplies. The project must design a circuit for the simulation based on the hardware components that must be used. In addition, the project's flowchart and architecture will be described in this chapter. As a result, project management will be represented by the project's time management progress. Next, the methodology employed in this project intends to define a comprehensive and systematic strategy for achieving the project's objectives. In order to ensure accurate data collection and reliable analysis by selecting techniques and procedures with care. This section describes the methodologies used to collect relevant data, conduct the necessary calculations, and verify the findings. It also highlights the tools, instruments, and software used to facilitate data acquisition and analysis.

3.2 Methodology

A work progress methodology follows a structured approach to effectively plan, execute, and evaluate tasks to achieve specific objectives. The first and crucial step in this methodology is comprehensive planning. This involves identifying the project's goals and breaking them down into manageable tasks, creating a visual flowchart or project roadmap. Realistic timetables are established, considering dependencies between tasks and allocating resources appropriately. It is

also essential to anticipate and identify potential risks or challenges during the project and develop contingency plans to mitigate them. Thorough planning sets a strong foundation for the successful execution of the project.

Once the planning phase is complete, the project moves into the execution stage. This involves carrying out the planned tasks according to the established timeline and resource allocation. Regular monitoring and tracking of progress against the set timeframe are crucial during this phase. It enables project managers to identify deviations, bottlenecks, or delays and take appropriate actions to keep the project on track. Flexibility is essential at this stage, as adjustments or modifications may be required due to unforeseen circumstances or changes in project requirements. Effective communication and coordination among team members are vital to ensure smooth execution and timely completion of tasks.

After completing tasks, a thorough evaluation is conducted to assess the overall performance and outcomes. This evaluation phase involves comparing the achieved outcomes with the original goals and objectives set during the planning phase. It also entails evaluating the efficacy and efficiency of the methods followed and identifying areas for improvement. Lessons learned during the project are recorded and documented to enhance future developments and avoid repeating mistakes.

Based on the assessment and evaluation, necessary actions and modifications are taken to improve future approaches and maximize work progress on succeeding projects. The identified areas for improvement are addressed, and adjustments are made to the methodology, planning process, or execution strategies to enhance efficiency, productivity, and overall project outcomes. These improvements are incorporated into future projects to refine and optimize work progress methodologies continuously.

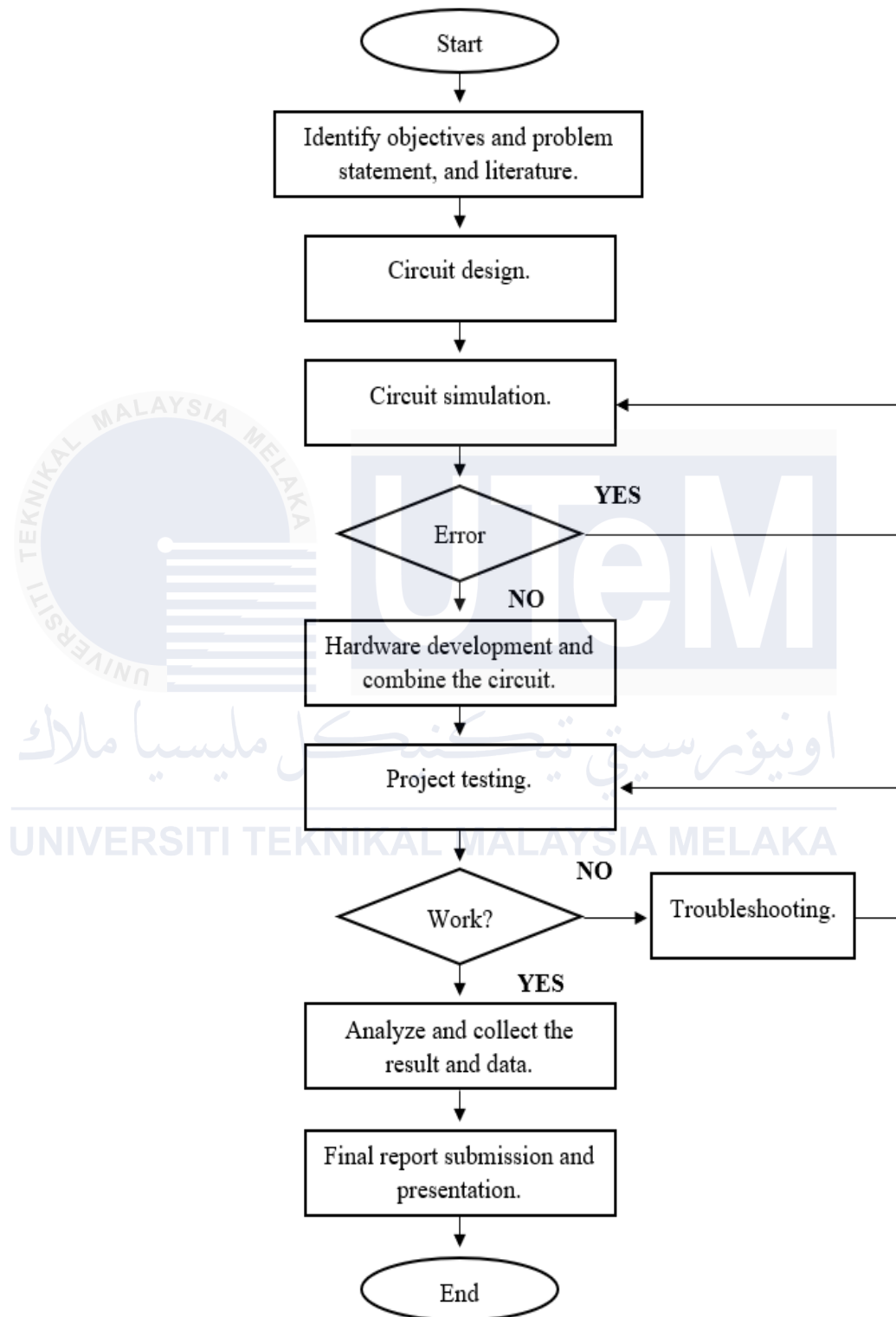


Figure 3.1 The project progress flowchart.

3.3 Project Architecture

In figure 3.2, a block diagram of the project's procedure based on the hardware's operation is shown. There is a combination of two distinct energy sources, namely solar and mechanical dynamos.

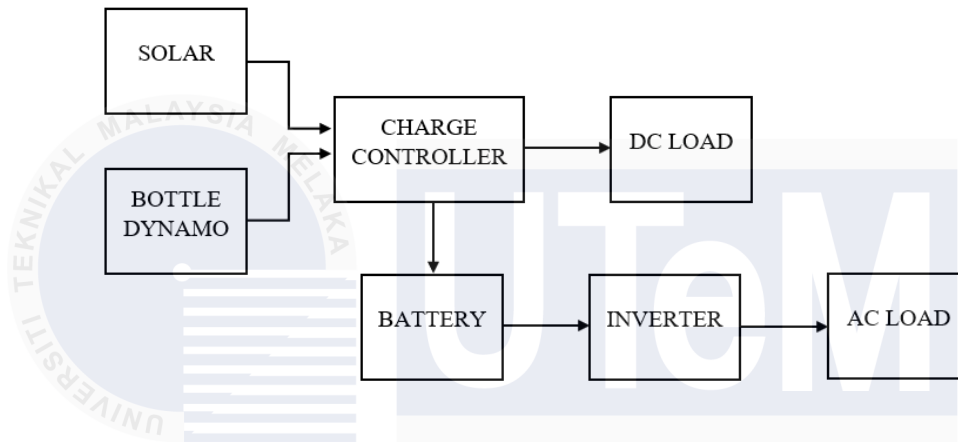


Figure 3.2 Block diagram of project.

According to the block diagram, this project's development utilized two distinct sorts of sources. Without the need for a converter to connect to a charge controller and store energy in a battery, solar energy provides direct current (DC). On the other hand, a mechanical dynamo will provide alternative current (AC), which a converter needs to convert into direct current (DC). Since the project's energy supply consists of more than two different kinds of energy sources, this arrangement will be regarded as a hybrid system. To provide 5 V_{DC} for direct-current loads and charge the battery bank, a solar controller is employed. Due to the various varieties of PWM charge controllers utilized for off-grid applications, the inverter will be connected to the battery bank. This means that the inverter will convert the DC sources from the battery bank and then send them to an AC application.

3.3.1 Parameters

Several characteristics must be carefully examined when developing a project using AC or DC input voltage sources such as solar PV, mechanical dynamo, and battery. First, the minimum rated voltage and current of these sources should be calculated, taking into consideration the project's unique needs. Furthermore, input and load control must be considered to ensure that voltage and current levels stay steady even in changing situations. Temperature stability is another significant consideration since temperature variations may impair the performance of these voltage sources. Finally, the design should include dependable short-circuit prevention systems to protect the system from any flaws and assure the safety of the components and users. A well-designed project may maximize the performance, efficiency, and reliability of the AC or DC input voltage sources by addressing these aspects.

3.3.2 Project Equipment

All the hardware and software required to properly finish a certain project are included in the project equipment. The project in question includes both software and hardware components. To enable precise simulations and practical implementation, it is crucial to make sure that the software (PSCAD) and hardware components of the solar off-grid arrangement are compatible and appropriately integrated.

3.3.2.1 Software

This project decides to develop the simulation section with the PSCAD program. PSCAD software has the benefit of allowing users to model themselves schematically using a hybrid

system, run simulations, examine the results, and manage their data in a fully integrated graphical interface.

3.3.2.1.1PSCAD

PSCAD, or Power System Computer Aided Design, is an excellent choice for designing the system's circuit configuration, running simulations, analyzing the results, and managing data in a fully integrated, graphical environment. Regardless of the user's skill level, this program provides the most recent features. PSCAD will be used to create a schematic of the ultimate product, which will depend on the circuit layout.

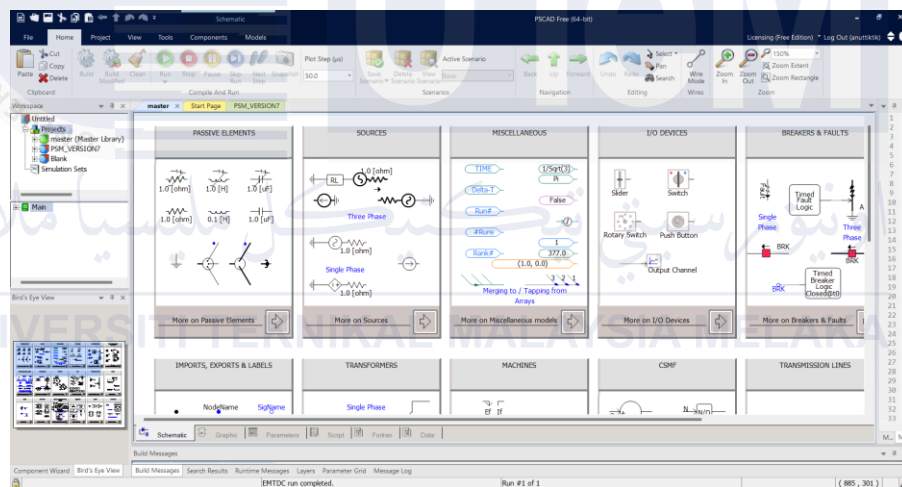


Figure 3.3 PSCAD V5 software.

The user must primarily comprehend how the system works while constructing the hybrid circuit. A library of preprogrammed and well-verified simulation models is included with PSCAD, ranging from basic passive parts and control functions to more complex designs like electric machines, fully functional FACTS devices, gearbox lines, and cables. In the event of a lack of an existing model, PSCAD offers options for creating unique models. For example, primitive models may be built from scratch in a flexible design environment, or existing models can be pieced together to build a module to create bespoke models.

3.3.2.2 Hardware

In order to operate the system, which maximizes performance, efficiency, and indications, the hardware components of the solar off-grid system, including the microcontroller, must be employed.

3.3.2.2.1 Solar PV panel

A solar panel is also known as a photovoltaic module or PV panel. A photovoltaic panel is a device that converts sunlight into electricity. Solar cells should comprise multiple interconnected materials like silicone that can absorb sunlight and generate electricity. When sunlight hits the surface of photovoltaics for electricity generation, the cells inside absorb the energy and release the electron.



Figure 3.4 Solar panel.

The working principle of a solar panel comprises multiple interconnected solar cells made of silicon or semiconductor material. As we know, sunlight will produce energy from the protons, causing electrons to be released from the atoms in the material of the solar cells. In addition, the electrons flow through the material, creating an electric current.

3.3.2.2.2 DC Motor

A DC motor is highly adaptable, as it can also operate as a DC generator, efficiently transforming mechanical energy into electrical energy by utilizing the rotational motion of its

shaft. The capacity of DC motors to effortlessly switch from converting electrical power into mechanical motion and vice versa is a result of their inherent electromechanical reciprocity. DC motors in generator mode utilize electromagnetic induction to convert the rotational kinetic energy of the shaft into a practical direct current (DC) electrical output.



Figure 3.5 12V 30W DC Motor.

The interaction between two wire coils and a small permanent magnet generates electricity in a dc generator. As the magnet rotates, it generates a magnetic field, which induces an electric current in the wire coils. This phenomenon, known as electromagnetic induction, is the fundamental principle underlying the functionality of a machine that converts mechanical energy into electrical energy.

In order to accomplish this, the electric current is sent through wires that are linked to the generator. This allows the lights to get electricity while simultaneously recharging the batteries. In order to transform the direct current motor into a direct current generator, the motor shaft must be rotated in order to transfer mechanical energy into electrical energy. Utilizing the mechanical pedal, which is human powered, allows for this. In any case, the direct current generator is able to recharge the battery by creating the voltage and current that should be followed as the minimum needed for the voltage and current rating of the charge controller.

3.3.2.2.3 Seal Lead Acid Battery

Rechargeable batteries, such as Seal Lead Acid Batteries, often provide a dependable, maintenance-free power supply. SLA batteries are often used in backup systems, emergency lights, UPSs, and other applications requiring a dependable power source, because of the SLA battery's cheap cost, safety, wide temperature range, and long lifespan. To keep the SLA battery operating at its best, it requires extensive periodic charging and maintenance.



Figure 3.6 Seal Lead Acid battery.

Numerous cells comprise the battery, each with a positive and a negative plate. This implies that the plates must be kept from contacting one another. A chemical process must occur within the cells to stop the elect must be sealed entirely too late from seeping out of the cell. The battery receives electrical energy when charged. Each cell's electrolyte and lead plates combine to form lead sulfate and water. During discharge, the lead sulfate and water undergo the reverse process, turning back into lead plates and electrolytes.

3.3.2.2.4 Charge Controller

In a photovoltaic (PV) system, a charge controller controls the voltage and current from the solar panels stored within the batteries bank. In further detail, the charge controller is designed to limit the amount of energy delivered to a battery and guard against the overcharging and over-discharging of the battery bank. To guarantee a secure and effective charging procedure, the device

may monitor the battery voltage and modify the charging rate. A charge controller is crucial in a solar PV system for several reasons.

The first is a gadget that aids in preventing overcharging and over-discharging of the battery. The second point is that the charge controller may maximize solar PV performance when a system requires high performance to guarantee that the battery is charged at the proper pace. Regarding charging rate, the system also requires safeguards against risks to people and equipment, including voltage spikes, short circuits, and reverse polarity. A charge controller may reduce the cost of a solar PV system, ensuring a reliable and effective operation system.



Figure 3.7 Charge controller.

In terms of its operation, a PWM solar charge controller will work by connecting the battery storage directly to the solar panels. The PV array output voltage is pulled down to the battery voltage during bulk charging when there is a constant connection from the PV array to the battery bank.

3.3.2.2.5 Solar Inverter

A solar inverter is a power converter that changes direct current (DC) into alternating current (AC), which is then supplied to a commercial electrical system linked to the grid or operating independently. The solar inverter offers unique capabilities, such as Maximum Power Point Tracking (MPPT) and anti-islanding protection, that may be tailored for photovoltaic arrays. By turning the DC side on and off 120 times per second while reversing the voltage every other

cycle, a solar inverter may convert DC electricity to AC. Solar inverters may also increase a photovoltaic system's efficiency by reducing losses and guaranteeing that most solar energy is accessible for consumption.



Figure 3.8 Solar inverter

The idea behind a solar inverter is to transform the DC power produced by solar panels into usable AC electricity for household appliances. Converting DC to AC electricity is pulse width modulation (PWM). The inverter produces a sine wave that resembles the AC power from the grid by using a computer to manage power transistor switching.

3.3.2.2.6 Earth Leakage Circuit Breaker (ELCB)

In electrical installations with high Earth impedance, a safety device called an Earth-Leakage Circuit Breaker is employed to guard against electric shock. When a defect occurs, the device will identify it by detecting a small amount of stray voltage on the metal of electrical equipment enclosures and interrupting the circuit. The voltage detecting ELCBs offer several benefits, such as fewer nuisance trips and less sensitivity to faulty circumstances. Second, comparable problems with frequencies much higher than the minimum required will cause the ELCB to trip.



Figure 3.9 Earth Leakage Circuit Breaker.

According to the ELCB's operating theory, it can detect circuit leakage at around 30mA or 1mA. It will trip automatically and cut off the supply. This operation abruptly turns off the electrical supply to the main circuit. The ELCB is intended to safeguard people and electrical equipment to reduce the risk of electrical fires and shock.

3.3.2.2.7 Miniature Circuit Breaker (MCB)

A circuit breaker is an electrical safety device to protect humans and electrical appliances from electric shock. The design of MCB is to protect an electrical circuit from damage caused by the overcurrent. MCB is an essential safety device that protects electrical installations against overcurrent and overload, which can cause electrical fires and is a safety hazard device.



Figure 3.10 Miniature Circuit Breaker.

Every electrical appliance needs to be protected from overloading and overcurrent. The operation of an MCB is directly dependent on the rate current of an MCB. The circuit breaker must detect a fault condition and quickly start operating to trip and disconnect the supply to load. MCB

is designed to be fast-acting, which means the circuit will interrupt by the flow of electricity in an installation circuit.

3.3.2.2.8 Arduino UNO Rev3

A Microchip ATmega328P microprocessor is included on the open-source Arduino Uno microcontroller board. The board has digital and analog input or output pins that may be interfaced with other expansion boards and circuits. It is programmed using the Arduino IDE. A simple project based on programming; the Arduino UNO is a well-liked microcontroller board often used in electrical projects.



Figure 3.11 Arduino Uno Rev3.

Run " sketches " created in the Arduino programming language to program the Arduino Uno. To simplify programming for beginners, these sketches are created in a condensed form of C/C++. Using programming statements that let users choose whichever pin they wish to utilize. Arduino runs programs that regulate the board's multiple inputs and outputs.

3.3.2.2.9 Liquid Crystal Display with I2C module (LCD I2C)

Additionally, this gadget is a well-liked communication protocol for electrical devices and embedded systems. With the I2C board, connecting a 16 by 2 LCD is more straightforward than before, given the restricted inputs and outputs of an Arduino. The user may utilize two pins to link Serial-Clock and Serial-Data pins at A4 and A5 when using the I2C board.

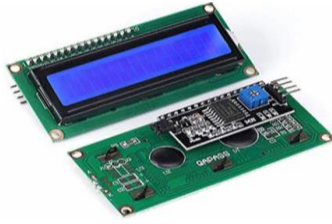


Figure 3.12 Liquid Crystal Display I2C.

The Serial Data (SDA) and Serial Clock (SCL) components of the I2C serial communication protocol, which enables many devices to interact with one another using only two cables, must be understood. The SDA connection carries data in both ways, while the SCL line synchronizes the clock between the enslaver and secondary devices during the data transmission.

3.3.2.2.10 Switch Socket Outlet.

We may plug in the electrical appliances to connect them to the electrical grid and power them up to learn what the switch socket outlet is. To put it another way, the switch socket outlet, sometimes a power outlet, is a gadget that supplies electrical power to gadgets and appliances. Many houses, workplaces, hallways, and other structures include switch socket outlets. Most home electronics and appliances receive AC power from the switch socket outlet. Additionally, the single country phase power source, whether 120 or 240V_{AC}, determines the voltage of a switch socket outlet.



Figure 3.13 Switch socket outlet

A switch socket outlet offers a secure and practical method of providing electrical power to gadgets and appliances. A switch socket outlet operates on multiple different principles. First, the switch socket outlet will send AC electricity from a power plant or generator source. The device is then physically connected to the socket when inserted into an outlet, completing the electrical circuit and enabling the source to the gadgets. Additionally, the switch socket outlet included safety measures like circuit breakers or fuses to guard against overloading, overheating, and overcurrent in the electrical circuit. Electrical dangers, electrical shock, and equipment damage may all be prevented using these safety measures.

3.3.2.2.11 AC Cable

The inverter's AC output is connected to the load via an AC cable that is designed to transmit alternating current safely and effectively. This cable is frequently used both indoors and outdoors, necessitating protective measures against environmental factors and possible damage. Commonly, protective conduits such as PVC conduit pipe, metal conduit, GI conduit, and PVC flexible tubing are used to preserve the integrity and longevity of cables. These conduits shield the cable from moisture, ultraviolet (UV) radiation, physical impact, and other external factors that may compromise its performance or pose safety risks. Installation location, durability requirements, and environmental conditions influence the conduit material selection.



Figure 3.14 AC cable for off-grid PV system.

The characteristics of the AC cable are similar to those of the DC cable, but since inverters have variable output currents, choosing the proper AC cabling is more complicated. Because the connection between cable diameter and ampacity is the main factor in choosing AC cabling, ambient temperature, voltage loss, and cable laying technique have little to no impact on the cable's ability to transport current. In terms of voltage loss in a solar PV system can be expressed as in (3.1):

$$\text{Voltage loss} = \text{passing current} \times \text{cable length} \times \text{voltage factor} \quad (3.1)$$

The length of the cable directly affects the voltage loss. If not, the current carrying table characteristics must be considered when calculating the cable carrying current capacity.

3.3.2.2.12 DC Cable



Figure 3.15 PV DC cable.

PV cables must be shielded against moisture, intense sunshine, extreme cold, and UV rays since they are often installed outside. In essence, PV-certified cabling must be chosen since regular cabling cannot replace it because it offers higher UV protection, insulation protection, and DC voltage resistance (often 600V_{DC}) than standard cables. PV1-F*4mm² cabling is more often utilized.

3.3.2.2.13 Grounding Cable

As its name suggests, a ground wire is an electrical cable that reaches into the earth underneath the building. Most contemporary houses have grounded outlets and electrical panels due to a phase-in of electrical code regulations that made ground wiring the norm in the 1960s.



Figure 3.16 Grounding cable.

An earth cable serves primarily as a conduit for excess electrical charges. As the earth possesses a negative electrical charge, it naturally attracts positive charges. Connecting to a ground wire facilitates the safe and controlled dissipation of these positive charges, thereby ensuring safety. The ground cable enables the direct discharge of electrical charges into the earth, thereby eliminating the danger of electric shocks and fires.

3.3.2.2.14 Electrical Panel Box.

Figure 3.17 represents an electrical panel serving as a distribution board. An electrical panel is essentially a utility unit that connects a primary power connection to a home and distributes electrical current to the home's numerous circuits. During the distribution of electricity to various circuits, circuit breakers and fuses prevent overcurrent from occurring.







Figure 3.17 Electrical panel box.






An electrical panel box, also known as a distribution board or electrical panel, is a crucial component of the electrical infrastructure of any building or business. It contains circuit breakers, fuses, and other components essential for the safe distribution of electricity. The primary function of an electrical panel box is to supply electricity to various circuits and devices throughout the structure, thereby effectively managing the flow of electrical power. The panel box guarantees the smooth operation of electrical systems, appliances, and devices within the building by organizing and distributing electricity in a controlled manner.







To ensure the safety and dependability of the electrical system, proper installation and maintenance of the electrical panel box are essential. Following industry standards and regulations, including proper wiring techniques, sufficient grounding, and ample clearances, constitutes proper installation. Regular maintenance of the panel box is also required in order to identify any potential problems or indications of wear and tear that could compromise its performance or pose safety risks. This includes checking for loose connections, damaged components, and overheating indicators.

3.4 Table of project equipment.

Table 3.1 List of project equipment.

No.	Items	Description	Remarks
1.	 <p>Solar PV Panel</p>	As a primary renewable energy sources.	Incorporate renewable energy sources for project and store the energy into batteries storage.
2.	 <p>DC Motor</p>	As a secondary renewable energy sources (dc generator).	As a secondary renewable energy source that can be used to store the battery bank.
3.	 <p>Solar Charge Controller</p>	To ensure the lifespan of the battery life and optimizing the efficiency of energy storage system.	To prevent the battery overcharging or discharging and maximize the performance of hybrid off-grid system.
4.	 <p>Solar Inverter</p>	Used to power electrical appliance by drawing the power from battery storage.	The off-grid hybrid power system needs an inverter to convert the DC output into AC output.

5.	 <p>2 Gang Switch Socket Outlet</p>	A switch that controls the flow of electricity to the socket.	To supply the 220-240V _{AC} in the system.
6.	 <p>MCB</p>	To prevent the overload or overcurrent of the system.	To cut-off the overcurrent and overloading of system.
7.	 <p>RCCB</p>	When dealing with SSO, the system needs to install a protective device that can be prevent from Earth leakage current.	A device that can quickly disconnect the power supply to prevent electric shock.
8.	 <p>Arduino UNO Rev3</p>	A microcontroller that can be used for creating hybrid system automation.	As a control system based on hybrid renewable energy.
9.	 <p>LCD with I2C module</p>	Ability to display the instruction from Arduino UNO.	Display the system status.

10.	 <p>Jumper Wire</p>	To transmit or receive the data from Arduino Uno and other devices.	For communication between microcontroller and LCD.
11.	 <p>AC Cable 2.5mm²</p>	To handle the power output of the inverter and the electrical appliance.	AC cable is a basic component to off-grid hybrid power system to carrying the AC output from solar inverter.
12.	 <p>DC Cable</p>	To deliver the DC output from solar panels to the charge controller and battery bank.	DC cable use for solar panel connect to charge controller and the battery bank to prevent the voltage losses in the system.
13.	 <p>Grounding Cable</p>	As a protection cable from the electric shock.	Every electrical equipment needs a safety grounding for aware in electrical shock.
14.	 <p>Rechargeable battery</p>	Use for storing the energy from solar PV and bicycle dynamo.	As a batteries storage system in portable power supply.
15.	 <p>Electrical panel box</p>	To ensure the portable power supply safe and reliable operation.	As a circuit protection and safety of the electrical system.

3.5 Project Quotation

The provided table provides a comprehensive listing of the required equipment for the development of this project.

Table 3.2 List of equipment of this project.

No.	Items	Description	Quantity /unit	Price (RM)	Total (RM)
1.	Solar Panel	A solar PV panel 18W.	1	28.70	28.70
2.	Solar Charge Controller	To regulates the voltage and current coming from a solar panel and mechanical pedal.	1	13.50	13.50
3.	Solar Inverter	300Wpeak Solar Inverter.	1	98.00	89.99
4.	2 Gang Switch Socket Outlet 3 Pin	Use for output AC load.	1	14.00	14.00
5.	MCB	Use as a protection for output AC load and system configuration.	1	8.99	14.00
6.	RCCB	Use as a protection from Earth-Leakage.	1	52.99	52.90
7.	Arduino UNO R3	For control the sub-system of the protection.	1	39.80	39.80
8.	LCD	16x2 Liquid Crystal Display Module with I2C Module)	1	12.90	12.90
9.	Electrical panel box	To ensure safe and reliable operation.	1	0.00	0.00
10.	Jump wire	For Arduino communicate with LCD with I2C module	1	0.00	0.00
11.	AC cable	Use for switch socket outlet and AC side connection.	3	0.00	0.00
12.	SLA Battery	As a solar energy storage batteries bank.	1	29.97	29.97
13.	Y-Shape Cable Lug	Equipment for attaching cables to other cables, surfaces, mechanisms, or electrical appliances	1	11.30	11.30
14.	Self-Tapping Screw	For holding the project equipment to case.	50	0.12	6.00
15.	Mechanical Pedal	Use as secondary electricity generation.	2	28.89	70.00
16.	DC cable	For connection between solar panel into charge controller and battery bank	4	0.00	0.00
17.	Grounding cable	Grounding purpose.	1	0.00	0.00
TOTAL					386.06

3.6 Project Design

To assure a comprehensive and well-planned approach, the project design incorporates the elements listed in Table 3.1 as well as the project budget. The items listed in the table provide the necessary components, materials, or resources for the successful completion of the undertaking. By incorporating these elements, the design intends to maximize functionality, efficiency, and overall project results.

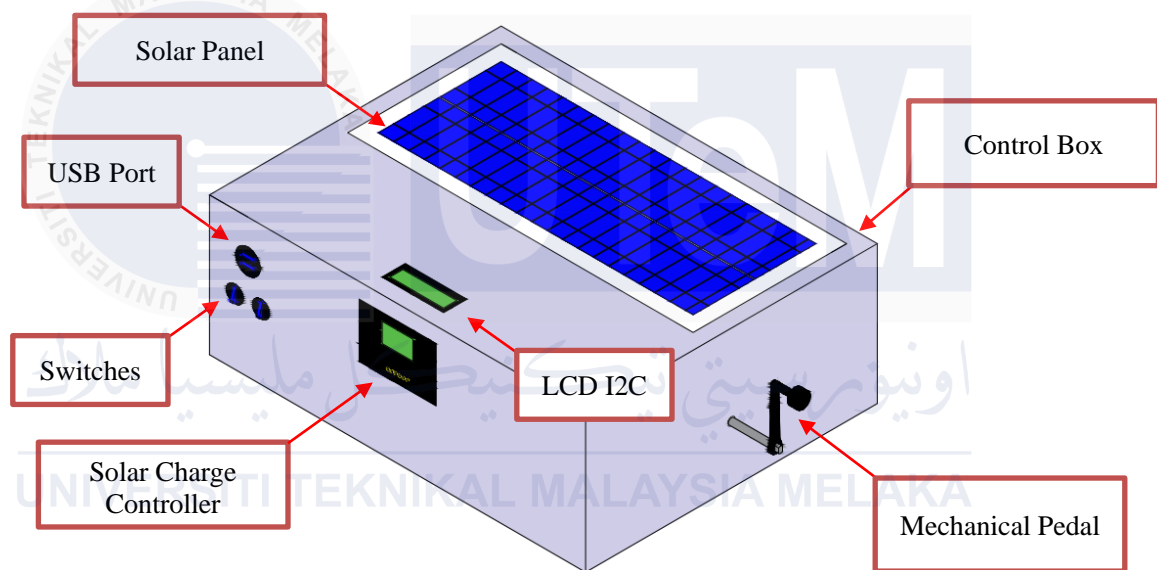


Figure 3.18 Project layout

Additionally, the design prioritizes the protection of the device from potential user harm by incorporating the structure and placement of equipment. This includes the careful placement of apparatus within the project's layout, the implementation of safety measures, and the incorporation of appropriate enclosures or protective mechanisms as required. By protecting the device from user injury, the design contributes to the overall success and sustainability of the project by promoting the device's durability, dependability, and seamless operation. The emphasis on apparatus protection in the design ensures that the project's objectives are met while the devices involved maintain their integrity and longevity.

3.7 Project Simulation

By taking into consideration the real component value, this section will discuss the circuit design of the simulation parts. In terms of the results of simulations that were used to monitor the functionality of the design in real-time. The project simulation may be used to determine which parameters should be increased or decreased to optimize the battery's rate of discharge in the simulation circuit.

3.7.1 Solar Photovoltaic Circuit

The circuit design for the modeling of solar generation is based on figure 3.19. Regarding circuit design, PSCAD software is used to operate the circuit based on real-time solar generation monitoring. Considering the maximum and minimal input voltages at a particular time, the signal generator is used to generate the input source for the DC power supply.

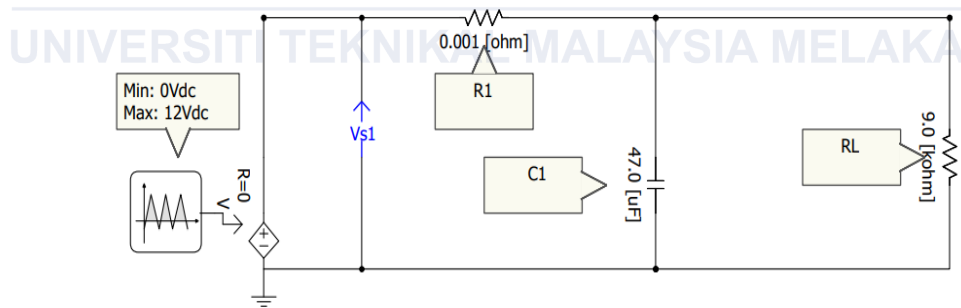


Figure 3.19 Solar Photovoltaic circuit.

The minimum and maximum voltage settings for signal generators are essentially 0 V_{DC} and 12 V_{DC}, respectively. Since the design must maintain an average capacitor voltage of 6 V_{DC}. In terms of resistors, R1 has a value of 1 milli-ohm so that the current flow in the circuit can store as much energy as possible in the battery bank. As RL is considered the load in this system, to allow battery to discharge then the resistance value at 9 kilohms is optimal. In addition, the

capacitor plays a crucial role in the charging and discharging of batteries, and once its value is determined, it functions well to match the burden. To accelerate battery depletion, the capacitor's value is also decreased.

3.7.2 Dynamo Circuit

For this project's secondary sources, dynamo energy generation will be utilized. This circuit has provided two distinct situations of dynamo speed, frequency, and voltage by simulating the performance of the generated energy using PSCAD. In the first scenario, the dynamo has supplied 12 Vac at 100 Hz with a 0-degree phase difference. In the second scenario, the dynamo is operating at its slowest speed, resulting in a voltage and frequency of 6 volts and 50 hertz, respectively.

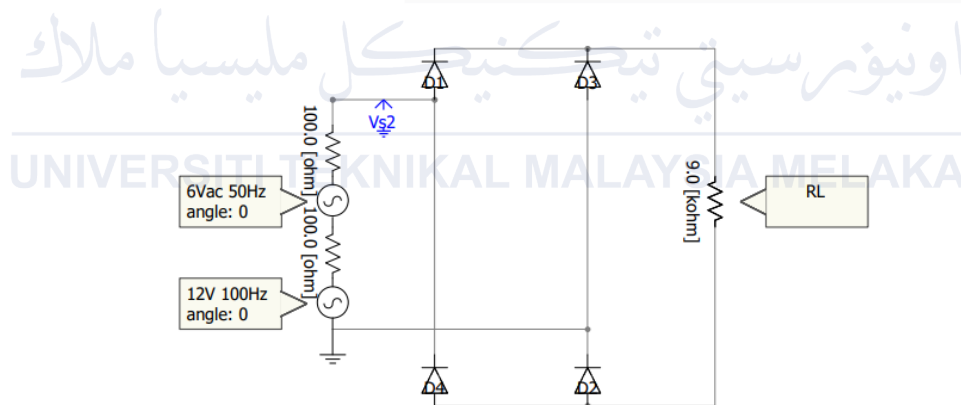


Figure 3.20 Mechanical dynamo circuit.

Although the full-wave rectifier performs a similar function to the half-wave rectifier, the average current from the AC source is zero in the full-wave rectifier, preventing problems that would otherwise occur if the average current was not zero. Full-wave rectifiers are constructed to have less output disturbance than half-wave rectifiers. The circuit will be converted to direct-current (DC) voltage using a full-wave rectifier, allowing the battery to be charged. Figure 3.20

demonstrates that there is no filtering of alternating-current (AC) voltage because the capacitor in the converter circuit supplies the filtering current.

3.7.3 Battery Circuit

Using two IGBTs as switches for the converter circuit, the battery circuit depicted in figure 3.21 was developed. This circuit utilizes a battery with 12 V_{DC}, 7.5 Ah, and 20 milli-ohm of internal resistance. In terms of the rate of internal battery discharge, a minimum capacity of 20 percent is stated. If the value of the resistor is less than 1 micro-ohm, the output waveform may be affected if the current in the circuit can reach 200 amperes and the value of the resistor is less than 1 milli-ohm.

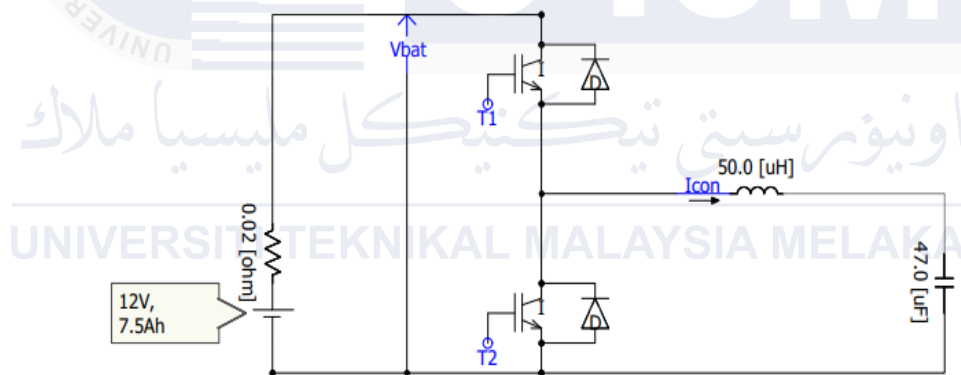


Figure 3.21 Battery circuit.

Two IGBTs are used in this circuit to switch electric current as quickly as possible with the least amount of switching losses. IGBT drivers are parts that quickly charge and discharge the IGBT gate in response to control signals, enabling the gate to turn on and off properly. In actuality, the IGBT driver's primary job is to magnify the battery current's control signals. The level of audible noise is decreased while dynamic performance and efficiency are improved using IGBT. It works well with resonant-mode converter circuits as well. IGBTs that have been optimized for both low conduction loss and low switching loss are available.

3.7.4 Switching Control Circuit

In this simulation section, the IGBT switching control circuit is depicted in Figure 3.22. However, the switching control circuit previously provided a switching pulse to the battery circuit's IGBT gate. Considering the value of an inductor and the resistance of the solar and dynamo circuits, the constant value of this circuit at 6.0 V_{DC} is used to maintain the average capacitor output voltage.

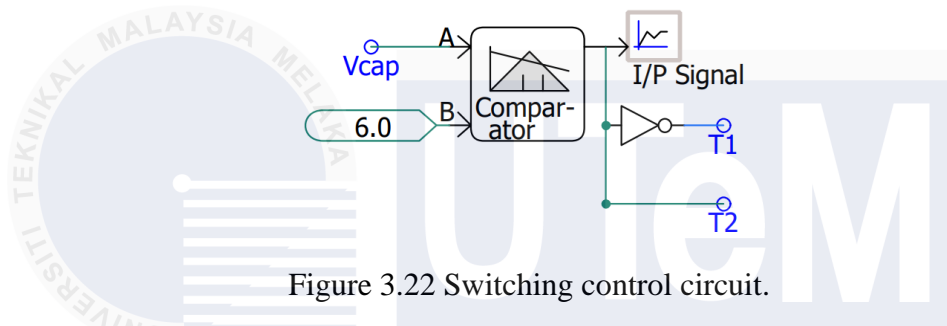


Figure 3.22 Switching control circuit.

The terminal A of the comparator in switching control circuit is used to record the capacitor voltage result. The comparator tool enables rapid and practical visual comparisons between module component specifications. The constant with a value of 6.0 is attached to terminal B because it is used to keep the circuit's average voltage at 6 V_{DC}. The comparator's output side has a connection to an output channel, which displays the simulation's ongoing graph. The NOT gate may also do logical negation on its input. In other words, the result will be false if the input is true. A false input causes a true output waveform, and vice versa. The IGBT receives its pulse using the denoted values for T1 and T2.

3.7.5 Full Circuit Design

For the complete circuit design represented in figure 3.23, solar PV and dynamo energy sources are combined. To achieve hybrid renewable energy, the system must contain at least two renewable energy sources. This circuit will simulate the actual project environment. First energy

resources from solar PV that provided 12 V_{DC} and 0 V_{DC} at the minimum voltage in order to simulate a cloudy or rainy day. Next, the secondary energy that supplies alternating-current (AC) voltage must be designed into a full-wave rectifier to reduce non-zero voltage and convert it to direct-current (DC) voltage. Aside from that, the off-grid system is the primary focus of this endeavor. In other words, the portable power supply required the battery to store energy after it was generated from solar PV and other renewable energy sources.

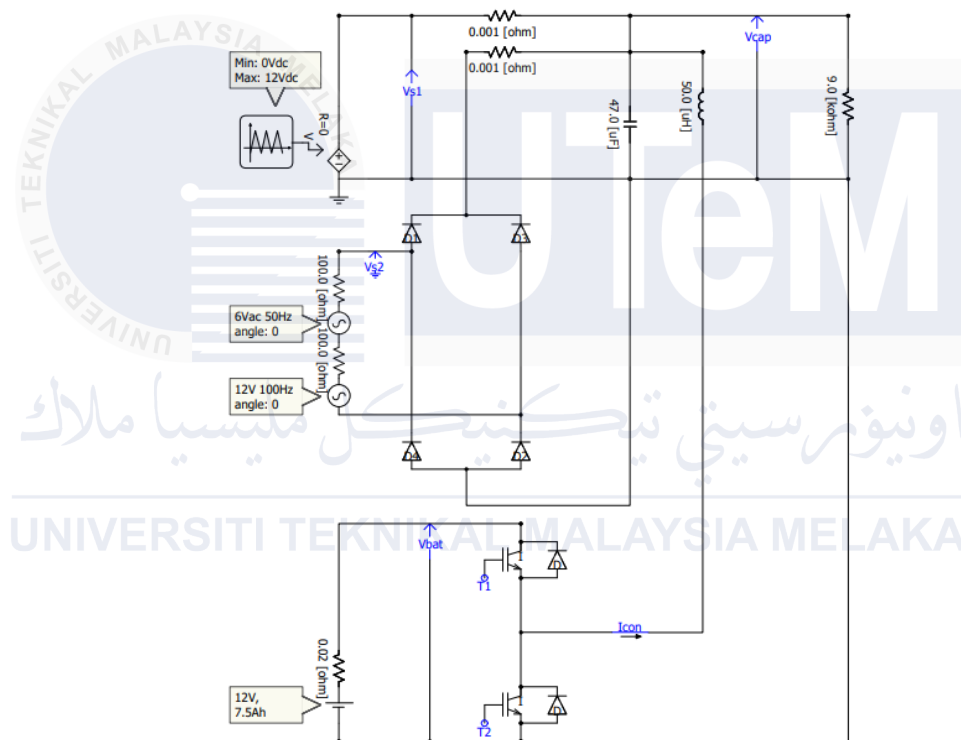


Figure 3.23 Full circuit layout.

A portable power supply must meet a set of minimum requirements in order to supply energy for loading. For example, a system may be able to provide energy for a few hours. This project can ascertain the number of hours required to charge and discharge the battery bank using the simulation circuit. The value of the battery must match the minimum capacity requirement for portable power supplies in order to meet the minimum requirements. Meanwhile, the capacitor and an inductor value must be 47 micro-Farad and 50 micro-Henry.

To effectively store and distribute energy within a circuit, it is necessary to connect every component between the power source and the capacitor. Capacitors are transient energy storage devices that are capable of dissipating energy faster than batteries. In addition, the battery circuit is directly connected to the inductor in order to generate a stable electromotive force and reduce fluctuations when a various current is present. The inductor facilitates the transformation of electrical energy into magnetic energy, ensuring a constant flow of current. In addition, inductors play an essential role in the production of direct current (DC) by sustaining the energy storage circuits utilized in switching-mode power supplies. By supplying energy to the circuit, inductors enable topologies in which the output voltage exceeds the input voltage, and they maintain current flow even during switching-off periods. Consequently, the combination of capacitors and inductors increases the efficiency and stability of energy storage and distribution within the circuit.

3.8 Project Hardware

In this subtopic, we will cover the hardware parts that have been planned for the project. Essentially, the component will visually present the physical arrangement of the project's hardware from different angles (front, top, and side) to choose the final version of the prototype. Nevertheless, it is crucial to emphasize that the project's hardware played a vital role in achieving the study objectives. Alternatively, the hardware part must be constructed to assess the efficiency of the portable power supply system that relies on hybrid renewable energy sources. This includes tasks such as battery recharging, load discharging, evaluating performance, and ensuring the completion of the project architecture as originally intended.

Figure 3.24 below demonstrates the top view of the project hardware, which includes a solar panel, an I2C LCD, and a mechanical pedal located next to the control box.



Figure 3.24 Top view.

Figure 3.24 represents the top view of the project's hardware, which includes a solar panel and an I2C LCD display. The solar panel serves as the primary source of renewable energy for recharging the lead-acid battery. The I2C LCD display shows the measured voltage, current, and power of the portable power supply that relies on hybrid renewable energy sources.

Figure 3.25 presents the frontal perspective of the control box for a portable power supply that utilizes hybrid renewable energy. The control box includes a solar charge controller, a mechanical pedal, a USB port, and two switches.

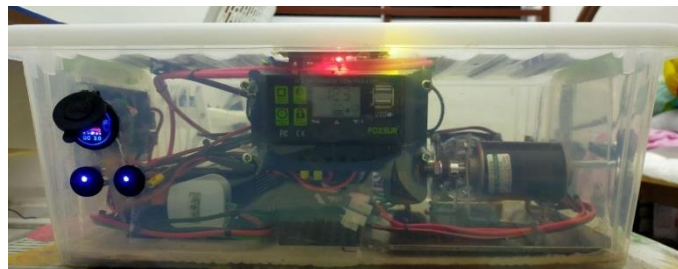


Figure 3.25 Front view.

The primary purpose of a solar charge controller is to assess the condition of the battery and track the solar PV or mechanical pedal charging potential. During the battery recharging process, the solar charge controller LCD will show the solar panel icon. Campers can utilize the USB connector for recharging their electronic devices. The primary purpose of two switches is to

activate or deactivate the solar charge controller and the inverter. The left-hand side switch is used to independently turn on and off the inverter, separate from the solar charge control. This is done to protect the inverter from potential damage during the recharging process. Alternatively, the appropriate switch is utilized to turn on or off the solar charge controller. During the charging process, it is necessary to switch off the inverter in order to minimize the charging time.

Figure 3.26 depicts the side view of the mechanical pedal. The mechanical pedal serves as a secondary source for recharging the battery. However, located at the rear of the control box is an exhaust fan designed to lower the temperature within the control box.

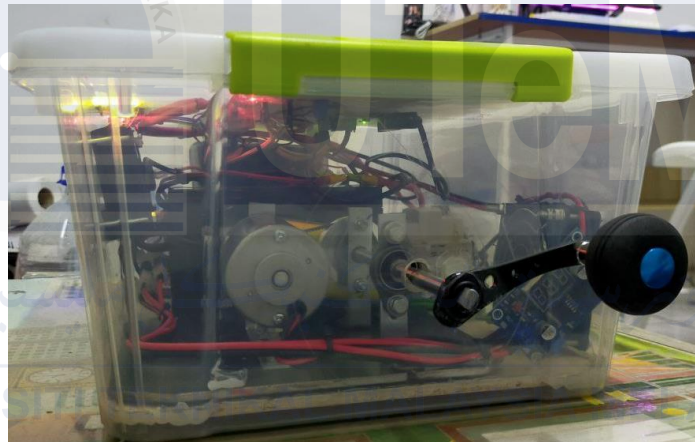


Figure 3.26 Side view.

When viewed from the side, the mechanical pedal serves as a secondary renewable energy source for recharging the battery during periods of electricity shortages at night. Nevertheless, the exhaust fan is employed to decrease the temperature of the control box. Upon activation of the inverter, the temperature within the control box rises. In the absence of an exhaust fan, the inverter, battery, solar charge controller, and Arduino UNO may incur damage.

3.9 Gantt Chart

This Gantt chart illustrates the flow of work progress by referring to the project schedule in terms of date and task, thereby ensuring that this project remains on track. Time management will be more effective and organized if the following is planned:

No.	Title	Week	PSM 1														PSM 2													
			W 1	W 2	W 3	W 4	W 5	W 6	W 7	W 8	W 9	W 10	W 11	W 12	W 13	W 14	W 1	W 2	W 3	W 4	W 5	W 6	W 7	W 8	W 9	W 10	W 11	W 12	W 13	W 14
1.	Briefing for PSM 1 by JK PSM, FTKEE																													
2.	Project Title Confirmation and																													
3.	Briefing with Supervisor																													
4.	Study the Project background																													
5.	Drafting Chapter 1: Introduction																													
6.	Task progress evaluation 1																													
7.	Drafting Chapter 2: Literature Review																													
8.	Table of summary literature review																													
9.	Drafting Chapter 3: Methodology																													
10.	Work on the Software/Hardware																													
11.	First draft submission to Supervisor																													
12.	Task progress evaluation 2																													
13.	Submission report to the panel																													
14.	Presentation of BDP 1																													
15.	Drafting Chapter 4: Analysis Data and																													
16.	Data Analysis and Result																													
17.	Record the result																													
18.	Drafting Chapter 5: Conclusion and																													
19.	Compiling Chapter 4 and Chapter 5																													
20.	Submit the latest report to Supervisor																													
21.	Finalize the report																													
22.	Presentation of BDP 2																													

3.10 Summary

The project summary concentrates on providing a thorough overview of the software and hardware involved in the development process. The initiative's primary objective is to meet the energy needs of a hybrid renewable energy system with portable power sources. Based on the identified hardware components, a circuit design will be constructed in order to simulate and implement the system. The summary also emphasizes that the project will include a detailed description of the flowchart and architecture, which will facilitate a clear comprehension of the operation of the system.

In terms of project management, the executive summary emphasizes the importance of time management as a vital indicator of the project's progress. The methodology employed in the project seeks to establish a comprehensive and systematic approach to achieving the project's objectives. The project ensures accurate data collection and dependable analysis through meticulous selection of techniques and procedures. This section describes the methodologies used for data collection, calculations, and validation, as well as the instruments, tools, and software used to facilitate these operations. The summary sets the stage for a successful and well-executed project by providing an overview of the software and hardware components, as well as the methodology employed for efficient project management and dependable results.

CHAPTER 4

PRELIMINARY RESULTS AND DISCUSSIONS

4.1 Introduction

This chapter presents the preliminary results and analysis pertaining to the design of a circuit configuration with potential future applications in hybrid renewable systems. The simulation findings serve as compelling evidence that the project holds promise for successful implementation. The output waveforms obtained from the simulation offer valuable insights for the future utilization of the system. By analyzing the data derived from the simulation, the potential system performance can be assessed, particularly in terms of the rate of charge and discharge of the battery storage within the hybrid renewable energy system. The peak voltage serves as a benchmark for comparing alternating voltage or current cycles to zero volts, enabling an understanding of the associated changes during each cycle. By maintaining the voltage at a steady 6 volts, the project can achieve optimal performance. These findings contribute significantly to the evaluation and optimization of the system, ensuring its effectiveness and viability in practical applications.

4.2 Simulation Results and Analysis

This part will go through the various simulations that were produced for this semester's tasks. The simulation results demonstrate the circuit design's functioning based on the real design for a DC load. Because the circuit was simulated using PSCAD software to meet the specific requirements of the hybrid system, which includes a solar PV, mechanical dynamo, and energy storage system (ESS), the findings of this simulation are primarily concentrated on direct-current (DC) loads.

The solar PV voltage is taken into consideration for the initial result of this simulation, and a signal generator from PSCAD was utilized as an external source for the voltage reference. Additionally, the signal generator is tuned to the solar PV's peak and lowest voltages of 12 V_{DC} and 0 V_{DC}, respectively. The design for this configuration circuit must match the solar PV module in order to keep the average voltage at 6.0 V.

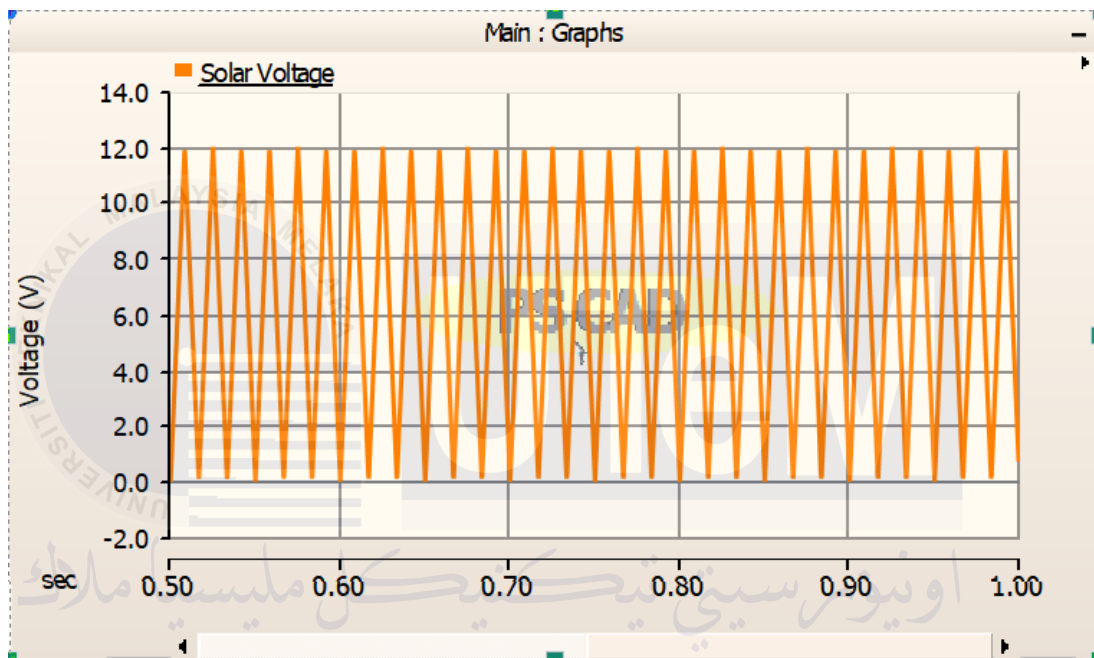


Figure 4.1 Simulation result of solar voltage.

The simulated value of the solar PV system's output voltage, which is provided via a signal generator and matches the setting, is shown in Figure 4.1. The solar voltage is shown with the peak and minimum solar PV voltages at 12.00 V_{DC} and 0.00 V_{DC}, respectively. In terms of the lowest voltage, shading is simulated as occurring when the system is operating with shade covering the PV module's surface.

Since a mechanical dynamo provided the alternating current (AC), it is considered the secondary source for this project. It will be possible to see the output waveform of the dynamo output voltage from the results below, which consider two different spinning magnetic flux speeds. Based on the various frequencies and input voltages of the dynamo,

this simulation will give an idea of the dynamo's speed. This system's peak input voltage is 12.0 V with a 100 Hz frequency in order to keep the output voltage at 6.0 V.

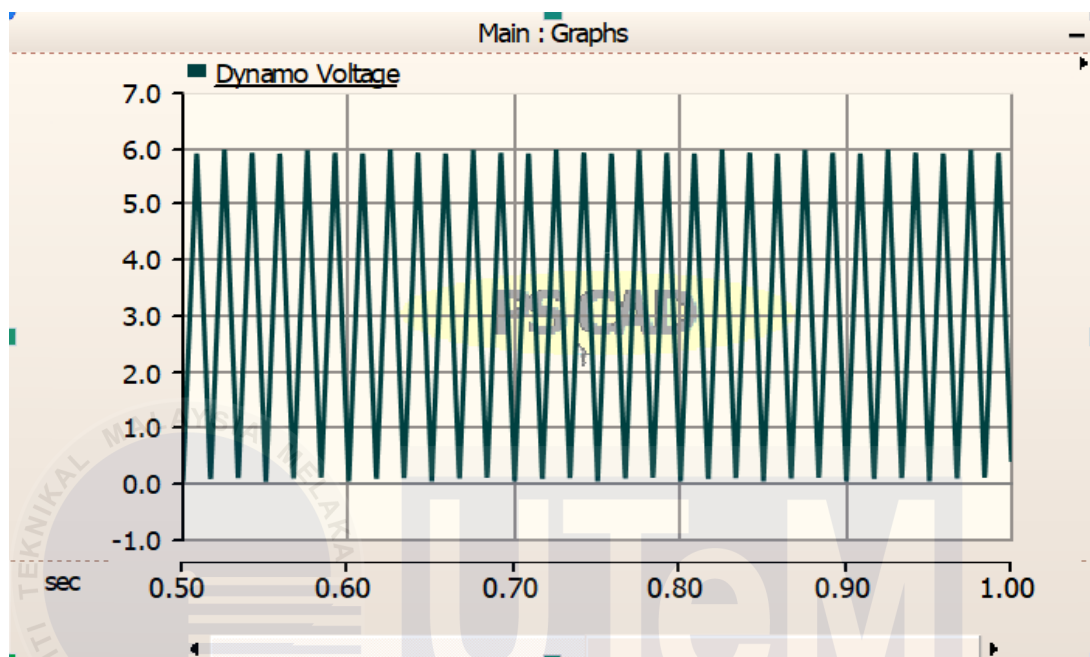


Figure 4.2 Mechanical dynamo waveform result.

The output voltage of the dynamo peaks at 5.996 V_{AC} and drops to 0.056 V_{AC}, according to figure 4.2. In order to accurately replicate the frequency and output voltage at different times during cycling, there are a few variations in the output voltage from the waveform. The secondary output voltage is listed as peaking at 5.996 V, whereas the main output voltage is described as 5.514 V_{AC}. The simultaneous waveform from the various dynamo frequencies at a given speed is shown based on frequency. If the waveform is generally used, the average output voltage that dynamos generate is 3.0 V_{AC}.

Figure 4.3 represents a simulation of the system's battery, which can be charged and discharged with the assistance of various circuit components. This simulation employs a 12-volt, 7.5-amp-hour battery. The high current may destroy a component in the circuit if the battery's resistance is less than 0.03 ohm, and the battery won't be able to discharge into the load. The design allows the battery to be discharged to a minimum of 20% of its capacity for an initial charge condition of 100%.

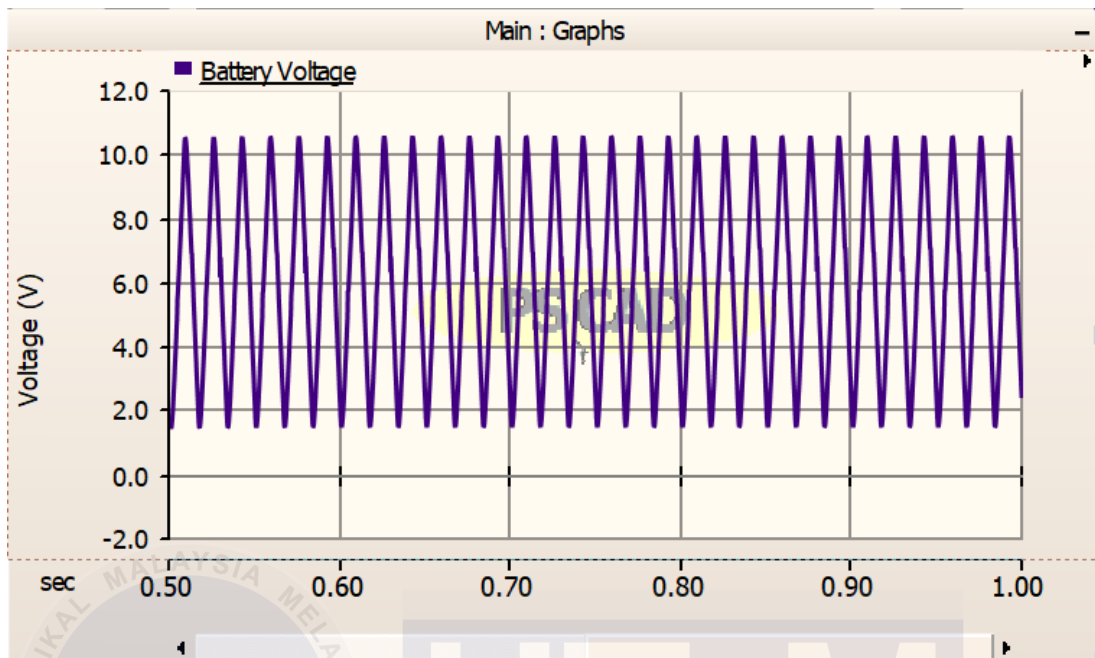


Figure 4.3 Battery voltage of circuit design.

The initial battery voltage at 0.00 V_{DC}, or the battery's state at 0% discharge, is shown in figure 4.3. The battery is charged to 7.488 volts in 0.04 seconds. Battery voltage is 10.159 V when time reaches 0.1 seconds, but it also drops at the same time to 0.231 V_{DC}. The charge controller regulates the charging process to provide a secure and effective charge for the battery. The battery is rising to 10.468 V_{DC} at 0.41 seconds, indicating that the system has successfully charged the battery bank.

The result of the simulation indicates that a capacitor value of 47.0 micro-Farad and an inductor value of 20 micro-Henry are needed to maintain a capacitor with an average output voltage of 6.0 V_{DC}. Because the greatest value of capacitor and inductor may filter the output voltage while maintaining the lowest capacitor voltage possible in the circuit design, the output waveform will be changed by the inductor value as it is raised.

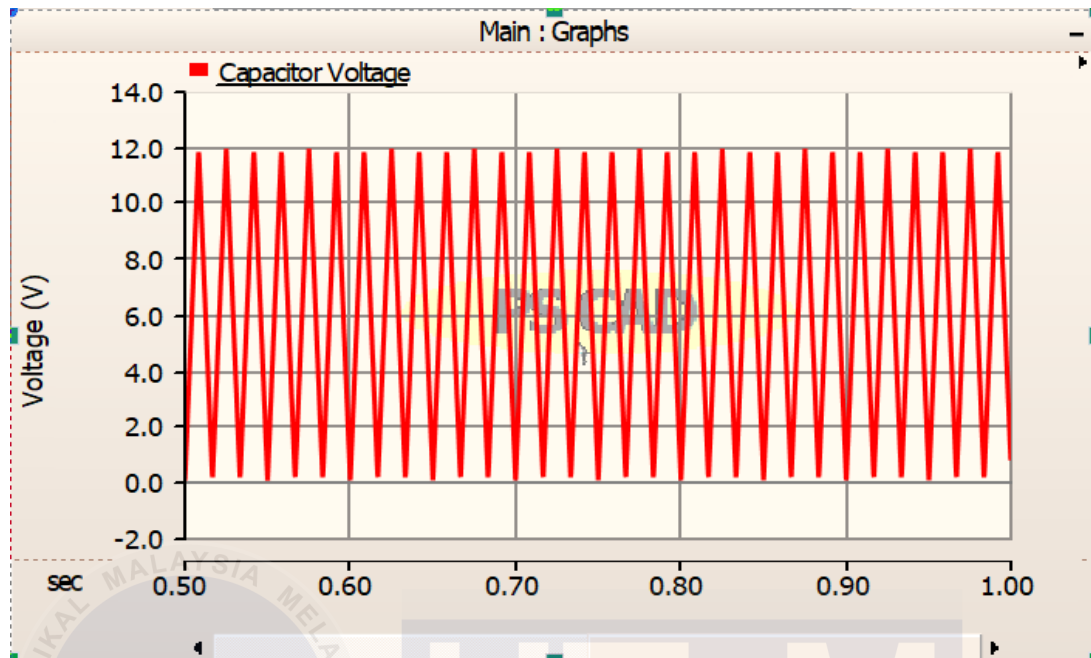


Figure 4.4 Result of capacitor voltage in circuit design.

The circuit design effectively maintains the average capacitor voltage plus/minus at 6.0 V_{DC} despite a peak voltage of 11.856 volts in 0.08 seconds. Based on the results, the minimum capacitor voltage is stated as being -0.004 V_{DC} per 0.02 seconds. However, before the output voltage drops to -0.004 V_{DC}, the peak voltage likewise drops from 11.856 V_{DC} to 11.738 V_{DC}. Due to its lower total energy storage capacity as compared to batteries, the capacitor discharges more quickly than a battery while in a charged or discharged condition. The constant value in the comparator in the circuit design must coincide with the average capacitor output voltage in order to maintain it.

Figure 4.5 output waveform illustrates the outcome of the current in battery storage being charged and discharged. Regarding the charging waveform, the graph will display a negative output current result, which is a negative number for a particular charging cycle. The waveform will be in the positive range for converter current discharge. However, the battery discharge rate also increased since the positive current was at its maximum.

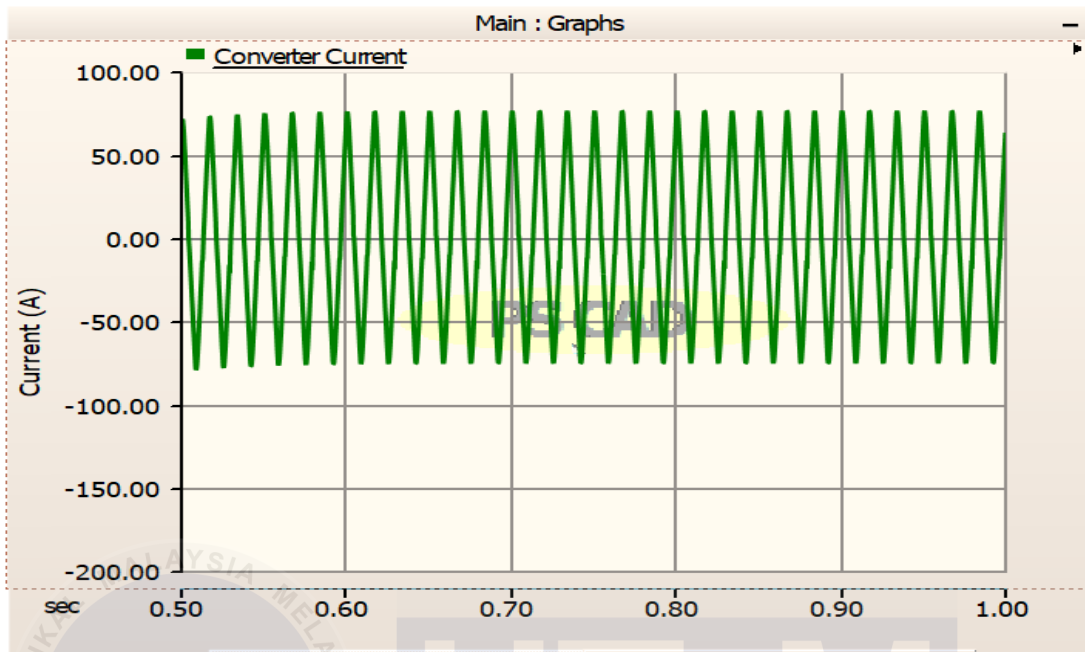


Figure 4.5 The converter current in simulation circuit.

According to Figure 4.5, the charging current of the converter begins at 0.01 seconds and -36.351 A. After 0.06 seconds, the charging rate decreased to -158.46 amps, where it remained for the next 0.20 seconds. However, the rate of discharge will increase by 0.22 seconds after the battery begins to deplete. Charge and discharge occur simultaneously within 0.35 seconds. In 0.6 seconds, the converter can deliver a maximum of 74.532 amps. In the meantime, the waveform is continuously charged and discharged at its maximum and minimum values of 74.532 amps and -74.532 amps, respectively. According to the simulation results, the project will complete the task successfully, as will the hardware components.

4.3 Hardware Result and Analysis

This section will discuss the outcomes of the hardware assembly, which involved collecting data from solar and mechanical pedal charging using cables of different sizes. The assembly also included a hybrid system and various load discharge, all aimed at achieving the project's objectives. Hence, the analytical outcome, which was utilized to validate the current flow through the cable, will be influenced by the diameter of the cable.

4.3.1 Solar PV Various Cable Diameter Charging

Findings reveal the significant role of time, solar irradiation, temperature response, and cable size within our investigation. The solar panel, with a capacity of 10 Watt and dimensions of 435 mm × 200 mm, may hinder the efficiency of charging time. The analysis uses different cable diameters to determine the various results of charging time. Larger diameters result in less resistance inside the cable, which can potentially lead to shorter charging periods. Research like these highlights how important cable diameters are for improving charging system efficiency.

In addition, the intricate relationship between module temperature and these various has an impact on current and voltage when exposed to sunlight. A small rise in module temperature leads to a modest increase in current, but at the same time causes a fall in voltage due to the temperature coefficient. Understanding this interdependent connection is crucial for grasping the complexities of energy production in different environmental circumstances. Understanding the complex relationship between temperature and the electrical property of the solar module allows us to improve our system's performance in a wide range of climates.

4.3.1.1 Solar PV Charging with Cable Diameter at 0.8 mm².

The result of charging the 12 V, 7.2-amp-hour battery with a wire size of 0.8 mm² is displayed in Table 4.1. Starting at 7:00 AM and ending at 7:00 PM, a total of 12 hours of data will be collected to demonstrate that this particular cable size is capable of charging the battery when used in conjunction with a solar charge controller.

Table 4.1 Solar PV charging with a cable diameter of 0.8 mm².

Solar PV Charging with 0.8mm ² Cable Diameter						
Time (Hour)	Solar Voltage (V)	Battery Voltage (V)	Solar Current (mA)	Power (W)	Temperature (°C)	Remarks
7:00	10.99	11.78	3.12	0.034	28	Sunny
8:00	11.45	11.80	9.00	0.103	29	Sunny
9:00	12.45	11.81	98.77	1.230	30	Sunny
10:00	12.56	11.82	219.60	2.758	32	Sunny
11:00	12.87	11.83	260.80	3.356	39	Sunny
12:00	12.98	11.93	274.40	3.562	44	Sunny
13:00	12.67	11.92	163.30	2.069	44	Cloudy
14:00	12.89	11.94	281.30	3.626	42	Sunny
15:00	12.99	12.01	271.10	3.522	41	Sunny
16:00	12.31	12.01	90.50	1.114	38	Cloudy
17:00	12.34	11.89	120.30	1.485	35	Cloudy
18:00	11.41	11.78	10.55	0.120	32	Sunny
19:00	9.11	11.67	0.00	0.000	30	Battery under 10%

At 3:00 PM, with a current of 271.1 mA, the maximum voltage recorded is 12.99V, as shown in Table 4.1. Despite the current temperature of 41°C, the charge controller is unable to fully charge the battery due to the short wire diameter, which results in the maximum internal resistance. The maximum solar current reaches 281.3 mA at 2:00 PM, resulting in a solar power output of 3.626 Watts. Otherwise, the solar panel utilized is 10 Watt, therefore the system's performance is only 36.26% to charged up the battery.

The battery can reach 12.01V between 3:00 and 4:00 PM, which is the highest reported value for a 0.8 mm² wire size. Following that, the battery self-drained due to the

solar system's performance being significantly lower than that of a conventional solar charge controller operational system. Because of temperature changes and wire diameter, it may take longer to fully charge the battery than usual.

Figure 4.6 illustrates the influence of solar voltage on the charging system, specifically the time response of climatic change. This graph displays the duration required to fully charge a battery with a capacity of 12 V and 7.2 Ah throughout a 12-hour period of data gathering.

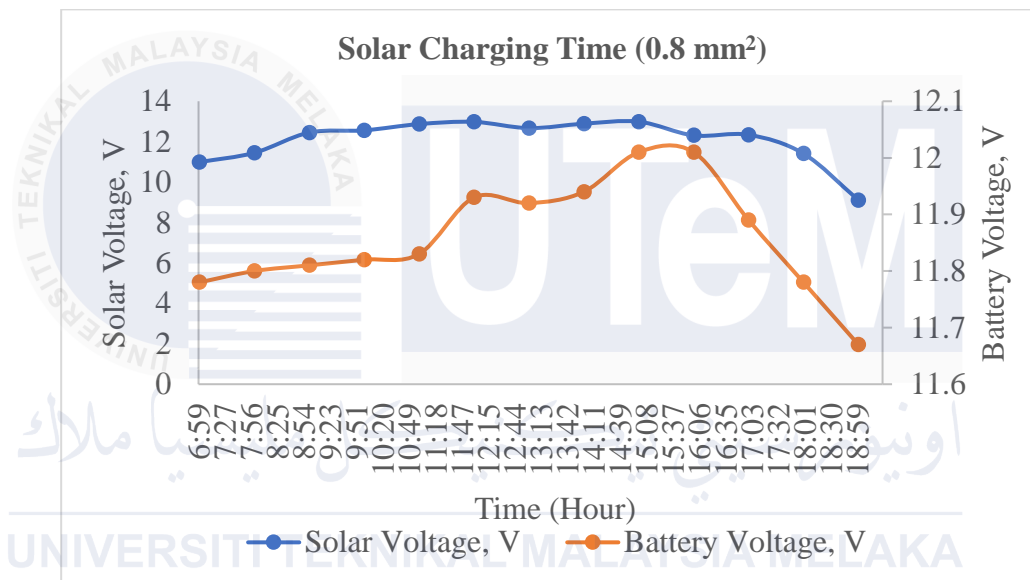


Figure 4.6 Solar charging time with wire diameter at 0.8 mm².

According to figure 4.6, the initial voltage measurement at 7:00 AM was recorded as 10.99 volts. The investigation of the battery voltage for the 0.8 mm² wire began at 11.78 volts. As a result, the battery voltage hits 11.80 V at 8:00 AM. It requires one hour to achieve a battery capacity of 0.02 volts. During the early morning, the current is quite low due to the limited amount of radiation, and the observed temperature is 29°C. The solar power has been measured to be 0.103 W by a calculation.

During the peak sun hour in Malacca, which is from 11:00 AM to 2:00 PM, the solar panel was able to meet approximately 33.56% to 35.62% of its wattage needs. The solar power experienced a rise from 2.758 W at 10:00 AM to 3.356 W at 11:00 AM.

Consequently, it is an opportune moment to recharge the battery using a wire with a cross-sectional area of 0.8 mm^2 . Within that timeframe, the battery's voltage increases from 11.82V to 11.83V at 10:00 AM. At 12:00 PM, the solar voltage was measured at 12.98V, while the battery voltage was 11.93V. This increase in solar voltage caused the battery voltage to rise. The maximum battery voltage recorded is 12.01V, occurring at both 3:00 PM and 4:00 PM. This coincides with solar voltages of 12.99V and 12.31V, respectively. By 4:00 PM, climate change had impacted the solar panel. After reaching its highest voltage of 12.01V at 4:00 PM, the battery voltage of 0.8 mm^2 gradually decreases owing to changes in climate and the presence of clouds.

Figure 4.7 illustrates the correlation between panel temperature and solar current for data analysis conducted on a 0.8 mm wire. This graph provides a detailed analysis of the effects of panel temperature coefficients on the generated current of a solar PV system. The duration of this experiment is approximately twelve hours, and it determines whether climate change causes the current to increase or decrease.

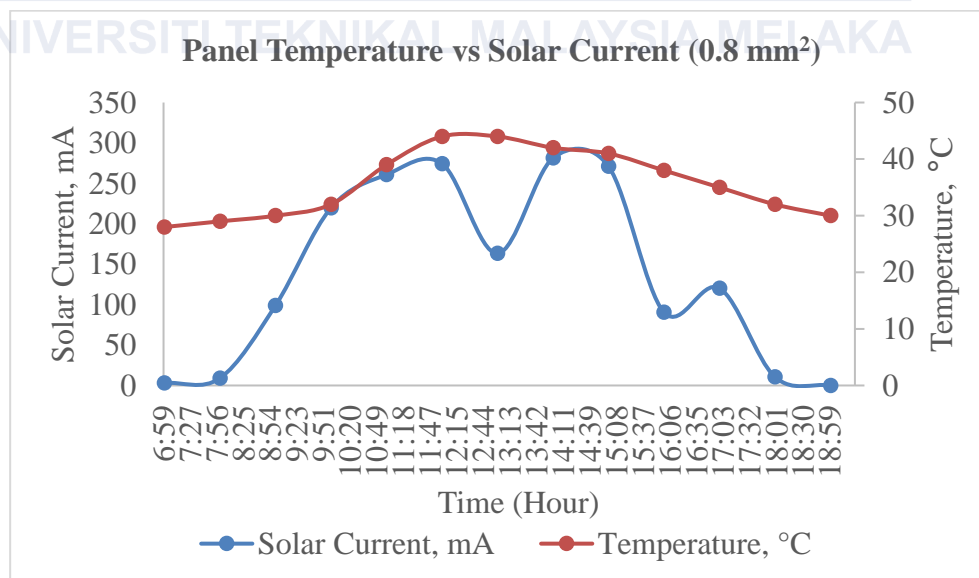


Figure 4.7 The relationship between temperature and current for wire diameter at 0.8 mm^2 .

At 7:00 AM, the current is lower than usual due to the low sun irradiation, and the temperature is also approximately 28°C to 29°C at 8:00 AM. Further elaboration on this link may be found in Figure 4.7, located above. As the panel temperature rises, the current gradually increases in accordance with the panel temperature. According to the data in Table 4.1, the panel temperature reaches its highest point at 44°C at both 12 PM and 1:00 PM. However, there is a slight variation in the present generation. The current generated at 12:00 PM was 274.4 mA, whereas at 1:00 PM it decreased to 163.3 mA. This is due to the correlation between solar irradiation and climate change.

According to figure 4.1, the current reached its highest point at 2:00 PM, with a value of 281.3 mA. The panel temperature of 42°C indicates that the system's operation does not exceed 44°C. Therefore, this method can be safely utilized in the future. According to the results, the highest temperature will correlate to the current generation as well.

The correlation between solar power and its effectiveness in charging a battery is crucial, particularly when taking into account the particular needs of lead-acid batteries. These batteries require a minimum state of charge at 20% in order to achieve optimal performance. Hence, the duration needed to fully recharge the battery utilizing solar photovoltaic (PV) power becomes a crucial determinant.

Based on the climatic variables depicted in the graph, it is clear that the effectiveness of solar PV generation is influenced by environmental factors. Having a clear comprehension of this concept is crucial in accurately forecasting the duration needed to achieve a complete recharge, considering the fluctuations in solar power generation and its consequent influence on the charging current and voltage. Essentially, this comprehensive strategy enables well-informed decision-making in maximizing the performance of solar energy systems for the purpose of charging lead-acid batteries in a dependable and efficient manner.

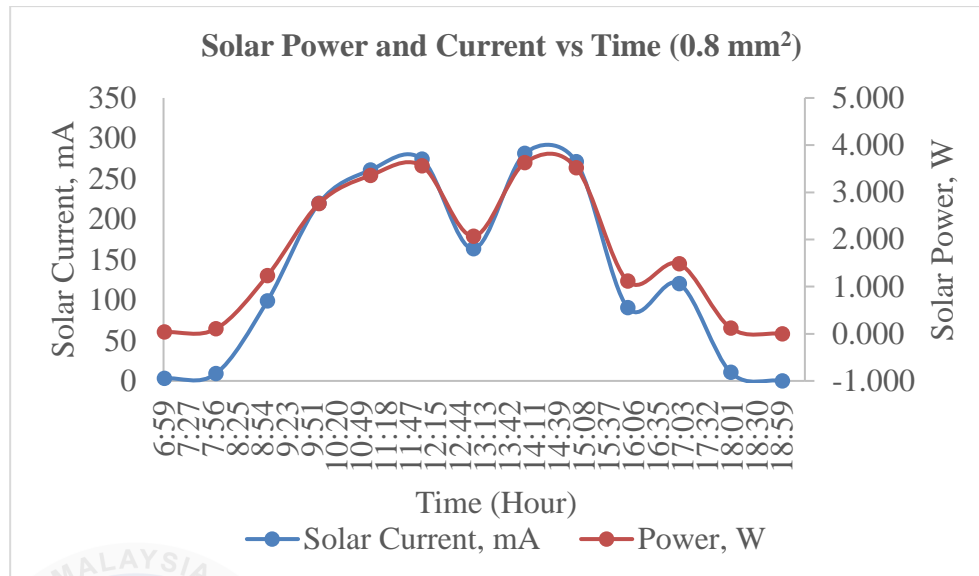


Figure 4.8 The solar power, respectively, is proportional to the current and time for the wire diameter at 0.8 mm^2 .

Figure 4.8 demonstrates a distinct correlation between PV power and current, emphasizing a straight proportionality in their connection. The slope of the graph clearly illustrates the direct relationship between the current and PV power, showing that as the current grows, the PV power also rises. The phenomenon is especially evident at 9:00 AM, with solar power measuring 1.23 watts and the equivalent current being 98.77 milliamperes. The graph's positive trajectory can be attributed to climate change, which is impacted by local weather occurrences.

An analysis of Figure 4.8 reveals the relationship between photovoltaic (PV) generation and meteorological conditions in Malacca over a period of time. The graph displays a strong surge in solar power during the hours around noon, increasing from 2.758 W to 3.562 W precisely at 12:00 PM. Weather conditions have a direct impact on the performance of PV panels, resulting in a decrease in power generation from 3.562 W to 2.069 W at 1:00 PM. The ensuing surge in solar power from 2.069 W to a maximum of 3.626 W at 2:00 PM indicates a rebound. However, at 3:00 PM, a slight decrease is noticed, with power generation dropping from a high to 3.522 W.

4.3.1.2 Solar PV Charging with Cable Diameter at 1.5 mm².

The outcomes of the conducted experiment, which measured the rate of battery charging over a period of 12 hours using a 1.5 mm² wire, are presented in Table 4.2. This result was utilized to compare battery charging with cables of varying sizes.

Table 4.2 Solar PV charging with a cable diameter of 1.5 mm².

Solar PV Charging with 1.5mm ² Cable Diameter						
Time (Hour)	Solar Voltage (V)	Battery Voltage (V)	Solar Current (mA)	Power (W)	Temperature (°C)	Remarks
7:00	10.56	11.85	2.21	0.023	28	Sunny
8:00	11.87	11.83	10.75	0.128	29	Sunny
9:00	12.44	11.90	37.36	0.465	30	Sunny
10:00	12.15	12.02	114.52	1.391	31	Sunny
11:00	12.31	12.24	270.50	3.330	45	Sunny
12:00	12.36	12.30	100.10	1.237	42	Sunny
13:00	12.28	12.21	49.29	0.605	28	Raining
14:00	12.30	12.24	150.30	1.849	35	Sunny
15:00	12.33	12.26	124.10	1.530	30	Cloudy
16:00	12.45	12.37	218.90	2.725	43	Sunny
17:00	12.44	12.37	142.10	1.768	40	Sunny
18:00	12.32	12.25	11.52	0.142	34	Raining
19:00	1.09	12.21	0.03	0.000	28	Sunny

Table 4.2 represents the solar PV voltage of 10.56 V, and the battery voltage is 11.85 V. The low solar radiation and temperatures in the early morning cause the current to be low. While the solar voltage is often lower at 7:00 AM, it reaches 11.87V around 8:00 AM, allowing the solar charge controller to function correctly. Due to the solar system's inability to function properly, the battery voltage drops slightly from 11.85V to 11.83V. Moreover, the system is unable to charge the battery because the power produced does not reach 1.000 W.

At 9:00 AM, the battery voltage increases from 11.83V to 11.9V because current increases during the charging process and there is no weather effect, which results in a

favorable panel temperature; a calculation reveals that the battery voltage increases by 0.07 V. At 12:00 PM, the generated voltage is 12.36 V, but the current is 100.10 mA, as shown in table 4.2. In terms of the outcome, the cloud cover over the panel at 12:00 PM may have caused the current to decrease. On the other hand, the battery voltage went up from 12.24 V to 12.30V. Therefore, the haze could appear at any point while charging. According to table 4.2, the peak PV voltage of 218.90 mA was recorded at 4:00 PM. Power output is proportional to input voltage and current. Table 4.2 shows that the solar panel produced a minimum voltage of 1.091 V and a current of 0.03 mA at 7:00 PM when the experiment was conducted, due to the rain that occurred during that time.

The graph in figure 4.9 indicates verified that the diameter of the cable has an impact on the current flow, and subsequently, on the correlation between the generated voltage and the battery voltage. The impact of climate on generated voltage, current, and power makes climate concerns vital in solar energy projects.

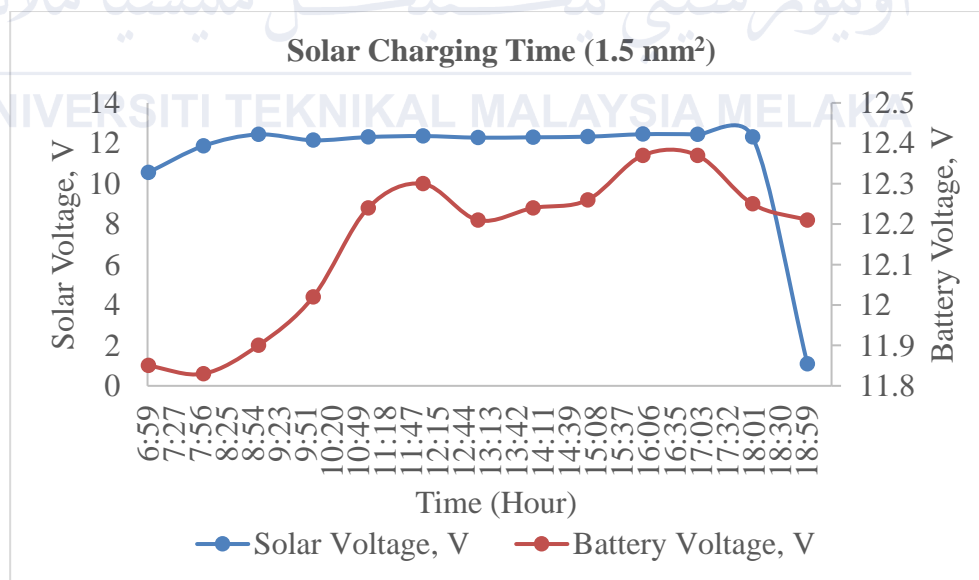


Figure 4.9 Solar charging time with wire diameter at 1.5 mm².

At first, the voltage produced was roughly 10.56 volts, whereas the voltage of the battery was 11.85 volts. Due to the lack of recharging between 7:00 AM and 8:00 AM, there was a noticeable drop in battery voltage at that time. The decrease in voltage is more

noticeable when the solar voltage generated drops below 12.0 volts, as shown by the values in Table 4.2 over the specified time period.

Figure 4.9 depicts a steady increase in battery voltage between 9:00 AM and 12:00 PM. The solar system maintains a constant voltage of 12.32 volts by computing the average voltage between 9:00 AM and 3:00 PM. Notably, the charging technique demonstrates efficacy by increasing the battery voltage from 11.83V to 12.30V during a duration of 3 hours.

Nevertheless, there is a following decrease in battery voltage, shifting from 12.30V to 12.21V between 12:00 PM and 1:00 PM. The system's inefficiency, which is a result of adverse weather conditions that affect the solar panel, is the cause of this issue. The occurrence of rainfall during this timeframe may lead to the self-discharge of the battery.

During the time period from 2:00 PM to 5:00 PM, the battery is being recharged. The recharging process starts at a voltage of 12.21 V at 1:00 PM and reaches its highest point of 12.37 V by 4:00 PM. The battery voltage reaches a stable level of 12.37 V at 5:00 PM. Although there was a minor decrease in voltage from 12.37 V to 12.21 V between 5:00 PM and 7:00 PM, the battery stays generally steady. Significantly, a transition to rainy weather is observed at 6:00 PM.

Figure 4.10 shows the relationship between the temperature of the solar panel and the volume of electric current that a standalone solar photovoltaic system produces. Figure 4.10 will also provide a more thorough explanation of the relationship between weather temperature and the rise in current.

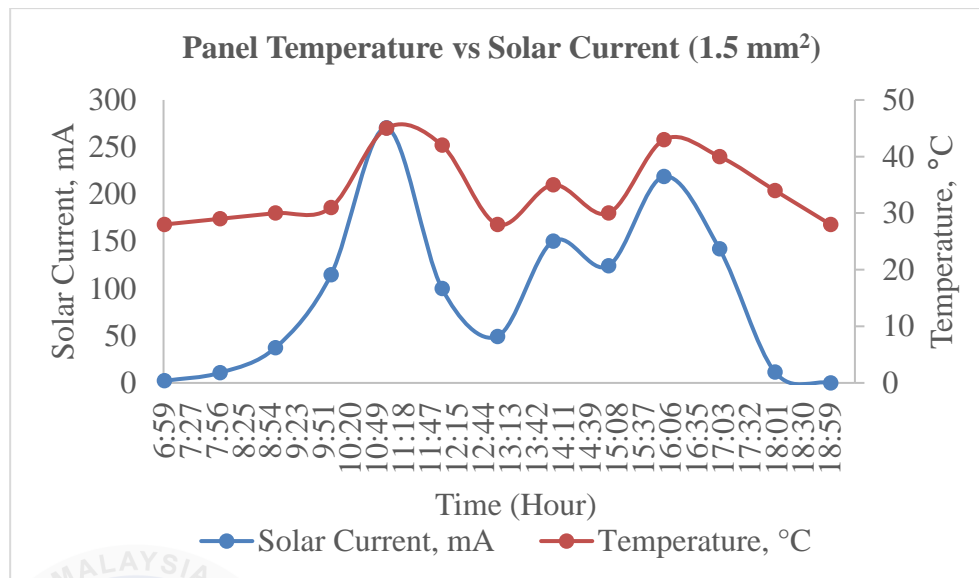


Figure 4.10 The relationship of panel temperature and current generated with cable diameter at 1.5 mm².

Based on the data presented in figure 4.10, the current reaches its highest point of 37.36 mA at 9:00 AM when the temperature is approximately between 28°C and 30°C. The graph depicts a gradual rise in temperature and its corresponding effect on the current. According to the experimental data, the maximum temperature recorded was 45°C at 11:00 AM, and the corresponding peak current was 270.50 mA. This result holds significant value when compared to the underlying theoretical principle.

According to the comparison, the 0.8 mm² cable has a maximum current of 281.3 mA when the panel temperature is 42°C. On the other hand, the 1.5 mm² cable is able to charge the battery from 12.02 V to 12.24 V in one hour. In contrast, the 0.8 mm² cable is capable of charging the battery from 11.92 V to 11.94 V. However, it takes one hour to boost the voltage by 0.02 volts.

This result can be utilized to clearly compare different options. The graph indicates a slight change in slope between 11:00 AM. and 4:00 PM, which can be attributed to the influence of weather conditions. Typically, rainfall causes a decrease in panel temperature, which might lead to a current correlation with the current. According to figure 4.10, the

graph shows a gradual change from 11:00 AM to 7:00 PM. This is due to the transition of weather conditions from sunny to cloudy and then from cloudy to rainy.

Essentially, figure 4.11 is a direct continuation of the experimental results presented in table 4.2. The graph below will illustrate the correlation between power and current over time. According to figures 4.9 and 4.10, an increase in panel temperature and solar radiation leads to a proportional increase in voltage and current. The output power of the solar PV system depends on the relationship between voltage and current.

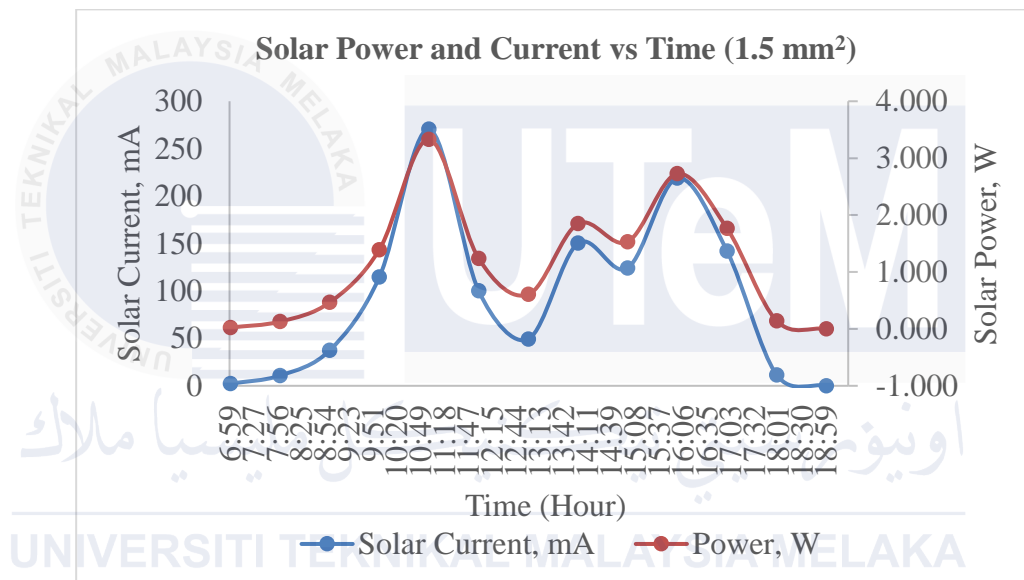


Figure 4.11 Solar PV generated power with cable diameter at 1.5 mm².

Figure 4.11 clearly illustrates a clear and positive link between current and power, emphasizing their proportional connection. During the time interval between 7:00 AM and 11:00 AM, both graphs display an upward trend. This indicates that as the current gradually rises, the photovoltaic (PV) power produced also increases, in accordance with the upward trend in current. Essentially, an increase in current results in a proportional increase in power output.

In order to improve the effectiveness of an off-grid solar system, it is crucial to increase the generated photovoltaic (PV) power when charging the battery. The reciprocal relationship suggests that as the power output grows, the duration needed for a complete

battery charge decrease. The maximum generated power reached a remarkable 3.330 W, peaking at approximately 11:00 AM and recording a current of 270.50 mA. A further maximum power of 2.725 W was measured at about 4:00 PM.

4.3.1.3 Solar PV Charging with Cable Diameter at 4.0 mm².

The project designed a hybrid renewable energy-based portable power supply and conducted an analysis of solar PV charging with a cable diameter of 4.0 mm². The following table below shows the results of the analysis using solar PV charging with a cable diameter of 4.0 mm².

Table 4.3 Solar PV charging with cable diameter of 4.0 mm².

Solar PV Charging with 4.0 mm ² Cable Diameter						
Time (Hour)	Solar Voltage (V)	Battery Voltage (V)	Solar Current (mA)	Power (W)	Temperature (°C)	Remarks
7:00	10.98	12.21	8.56	0.094	26	Sunny
8:00	11.25	12.18	56.71	0.638	27	Sunny
9:00	12.53	12.25	217.71	2.728	30	Sunny
10:00	12.31	12.29	111.72	1.375	32	Sunny
11:00	12.89	12.45	290.80	3.748	37	Sunny
12:00	12.91	12.57	300.80	3.883	41	Sunny
13:00	12.95	12.68	301.200	3.901	47	Sunny
14:00	12.92	12.76	289.9	3.746	47	Sunny
15:00	12.63	12.70	250.60	3.165	43	Sunny
16:00	12.89	12.89	300.20	3.870	47	Fully Charge
17:00	12.36	12.93	157.80	1.950	37	Rainy
18:00	12.15	12.61	58.19	0.707	34	Rainy
19:00	10.11	12.56	10.09	0.102	30	Rainy

Table 4.3 indicates that a 4.0 mm² wire diameter requires 9 hours to completely charge the battery by 4:00 PM. Table 4.3 demonstrates that the solar voltage remains stable at 12.22 V after 12 hours after the experiment is completed, indicating it as the average value. According to the data in Table 4.3, the maximum voltage produced by solar photovoltaic (PV) systems is 12.95 V at 1:00 PM. The solar photovoltaic (PV) system produces a

minimum voltage of 10.11 V at 7:00 PM due to the reduced solar radiation, which is below the peak sun hour in Malacca. Moreover, the battery voltage reaches its maximum capacity of 100% at 4:00 PM, with a voltage of 12.89 V. The device can achieve a maximum battery voltage of 12.93 V at 5:00 PM using a 4.0 mm² wire. Alternatively, the typical battery voltage measures 12.54 V, with a battery capacity of around 73% of 12.89 V. According to the data in the table, between 7:00 AM and 8:00 AM and between 5:00 p.m. and 7:00 p.m., the battery voltage experiences a modest decline. This decrease is attributed to the natural loss of charge over time.

Regarding solar-generated current, the maximum recorded current is 301.20 mA, precisely at 1:00 PM. Increasing the current results in a slight increase in voltage, which leads to a higher solar PV power output. In this scenario, the current and greatest temperature of the panel can reach up to 47°C, indicating that the solar radiation is greater, hence enhancing the efficiency of the panel. The mean photovoltaic (PV) current generated for the time period from 7:00 AM to 7:00 PM is 181.1 mA. The minimum recorded current at the start of data collection was 8.56 mA.

Figure 4.12 displays the relationship between solar PV charging time and cable diameter, specifically at a diameter of 4.0 mm². The horizontal axis represents time, while the vertical axis represents voltage. The graph in figure 4.12 depicts the solar voltage as the blue line and the battery voltage as the red line. The voltage measurements for both solar and battery voltage are graphed at different time intervals ranging from 7:00 AM to 7:00 PM.

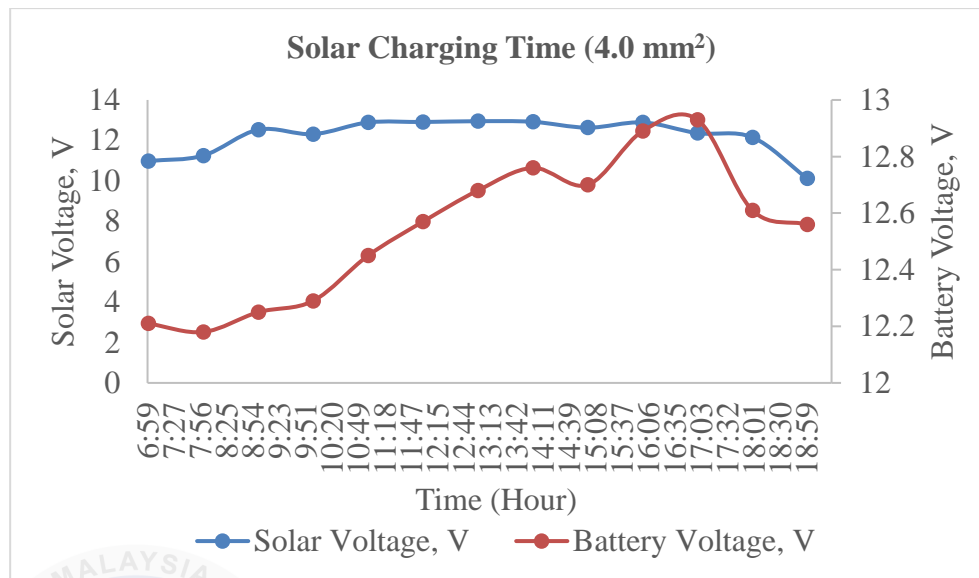


Figure 4.12 Solar PV charging time with cable diameter at 4.0 mm^2 .

Figure 4.12 depicts the progression of a battery's charging process over time, utilizing a solar panel. In addition, the red line illustrates that solar voltage first exhibits a relatively high value and thereafter diminishes gradually, suggesting a shift in solar energy accessibility, possibly attributable to variations in sunshine intensity. The graph illustrates that the battery voltage starts at a low level and gradually rises during the charging process. The battery's charge stabilizes, indicating that it has reached its maximum capacity around 4:00 PM. Alternatively, the graph indicates that it takes around 9 hours to completely recharge the battery given these circumstances.

The result indicates that the solar PV generated a peak voltage of 12.95 V, while the battery reached its peak voltage at 12.93 V. This suggests that the wire with a diameter of less than 0.8 mm^2 and 1.5 mm^2 takes less time to fully charge the battery. By utilizing "as a result" as a point of comparison for cable diameter, this graph demonstrates a significant initial difference between solar and battery voltage, emphasizing the charging process. Nevertheless, both lines exhibit slight changes, possibly because of variations in sunshine or charging efficiency.

Figure 4.13 is a graph that illustrates the relationship between the temperature of a solar panel and the amount of current that it generates within the solar panel.

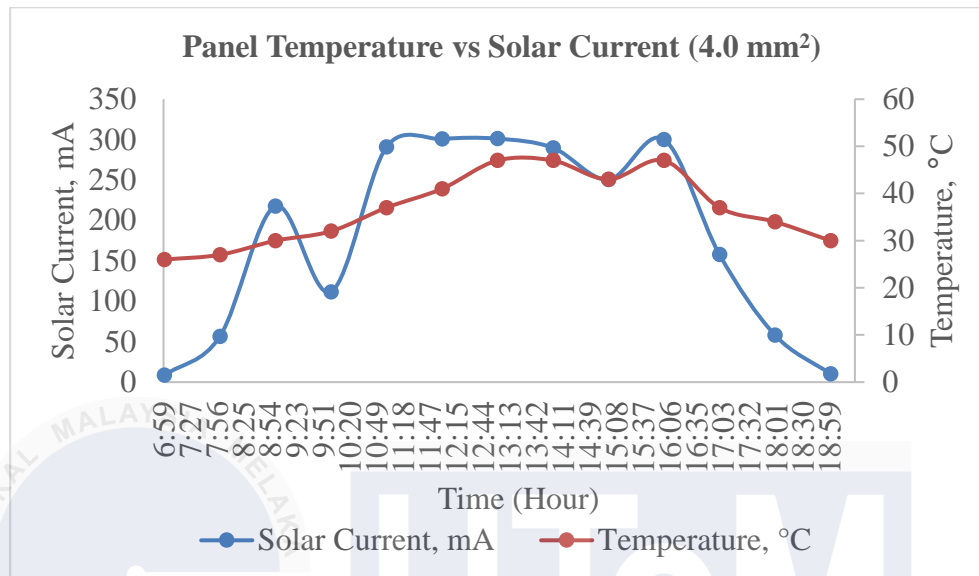


Figure 4.13 The panel temperature and current versus time with cable diameter at 4.0 mm².

The blue line in figure 4.13 represents solar PV current, whereas the red line represents panel temperature. This shows the relationship between time, panel temperature, and current. In addition, the solar current rises from 7:00 AM to 9:00 AM, drops at 10:00 AM due to weather, then rises again from 11:00 AM to 1:00 PM. Since panel temperature rises with time, the optimum current is at 1:00 PM.

Figure 4.13 illustrates the progressive rise in panel temperature, which peaks at 47°C between 1:00 and 2:00 PM, from 26°C. According to the graph, the solar panel is operating effectively under these circumstances. The temperature coefficient does not have an effect on the current output, and the temperature is not rising to a level that is higher than fifty degrees Celsius, which indicates that this system can be utilized without risky consequences.

The panel produced its maximum current and temperature at 47 degrees Celsius and 301.20 mA, respectively. This time period coincides with the prime sun hour, during which

the panels operate most efficiently. At 3:00 PM, the temperature decreases slightly from 47°C to 43°C due to atmospheric influences that may occur during the charging process. Consequently, the temperature of the panel reached 47 degrees Celsius between the hours of three and four o'clock in the afternoon. The panel temperature decreased from 47 degrees Celsius to 30 degrees Celsius between 5:00 PM and 7:00 PM due to the weather changing from sunny to rainy.

Figure 4.14 shows the relationship between solar PV power output and current over time. The horizontal axis shows hours, while the left vertical axis shows solar PV current. The right vertical axis displays solar PV power production. Figure 4.14 shows the graph, with the blue line representing solar current in mA and the red line representing solar PV power. Solar PV power is 0.000 to 5.000 Watts, and current is 0 to 350 milliamperes. The horizontal axis shows 12-hour time.

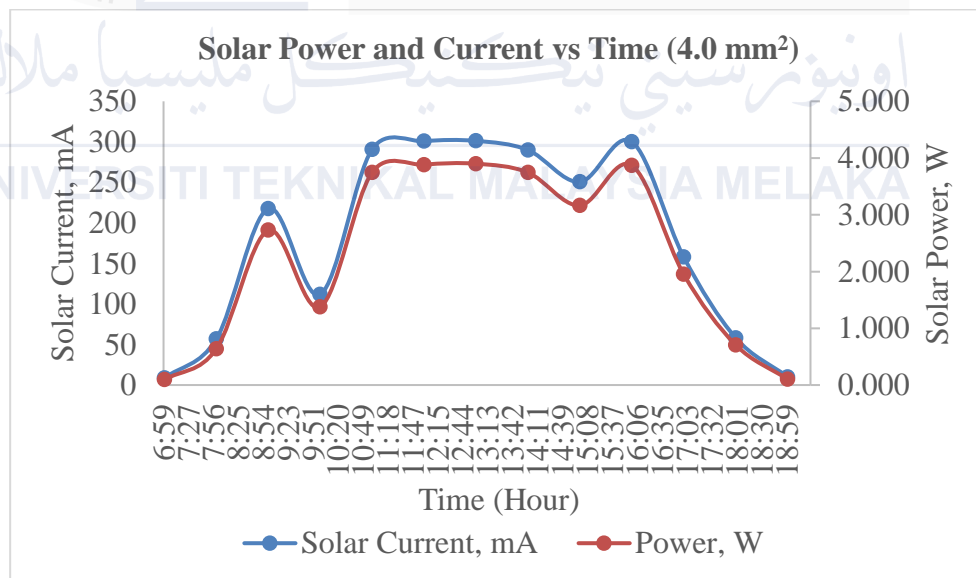


Figure 4.14 The solar PV generated power and current versus time with cable diameter at 4.0 mm².

The blue line, representing the solar current, starts at 8.56 mA and rises steadily beginning at 9:00 AM, reaching a peak of about 301.20 mA produced by solar PV at 1:00 PM. Nevertheless, the generated electric current does not experience a consistent increase

due to its manifestation of fluctuations, indicating possible fluctuations in sunshine intensity or other factors that impact the conversion of solar energy.

Figure 4.14 shows a straight relationship between solar power and current. As panel power increases, so does output. The fundamental relationship between current and power in electrical systems supports this. Power is theoretically defined as current, and voltage multiplied. The graphs show solar panels' power generation potential over time under certain conditions. The panel's highest power output is 3.901 W, and its early morning minimum is 0.094 W. This shows that 4.0 mm² cables create greater current than 0.8 and 1.5 mm² cables.

4.3.1.4 Solar PV Charging with Cable Diameter at 10.0 mm².

The data presented in Table 4.4 illustrates the electrical properties of a wire with a diameter of 10 millimeters during a period of twelve hours, beginning at seven in the morning and ending at seven in the evening. The following information regarding the steps involved in charging the battery is included in the table:

Table 4.4 Solar PV with cable diameter of 10.0 mm².

Solar PV Charging with 10.0 mm ² Cable Diameter						
Time (Hour)	Solar Voltage (V)	Battery Voltage (V)	Solar Current (mA)	Power (W)	Temperature (°C)	Remarks
7:00	11.87	11.81	10.81	0.128	28	Sunny
8:00	12.01	11.82	15.76	0.189	28	Sunny
9:00	12.78	12.07	201.20	2.571	30	Sunny
10:00	12.85	12.45	167.30	2.150	31	Sunny
11:00	12.57	12.47	10.37	0.130	31	Cloudy
12:00	12.98	12.58	309.60	4.019	44	Sunny
13:00	12.99	12.76	315.70	4.101	47	Sunny
14:00	12.85	12.89	219.90	2.826	46	Fully Charge
15:00	12.98	12.99	265.70	3.449	44	Sunny
16:00	12.76	13.15	98.70	1.259	45	Over Charge
17:00	12.44	12.99	189.20	2.354	44	Sunny
18:00	12.07	12.97	47.60	0.575	36	Sunny
19:00	10.07	12.89	7.98	0.080	35	Sunny

Between 7:00 AM and 9:00 AM, the solar voltage and current see a progressive increase, reaching their maximum values at 12.85 V and 201.2 mA, respectively. This solar system produces a power output of 2.571 watts. The battery voltage exhibits a concurrent rise, but with a tiny delay compared to the solar voltage. The temperature slightly rises from 28°C to 30°C.

From 10:00 AM to 11:00 AM, solar voltage and current decline somewhat, resulting in a 2.15 W power reduction. The battery voltage and temperature are stable. The 11:00 AM notes show cloudiness. Between 12:00 PM and 1:00 PM, solar voltage and current peak at 12.98 V and 315.70 mA, respectively. The highest power output is 4.101 W. The battery voltage peaks at 12.76 V, and the temperature rises from 44°C to 47°C.

Figure 4.16 shows the relationship between solar voltage, battery voltage, and time in a 10.0 mm² cable solar charging system. The blue line represents solar voltage in volts, and the red line represents battery voltage. On the horizontal axis, both variables were graphed from 7:00 AM to 7:00 PM.

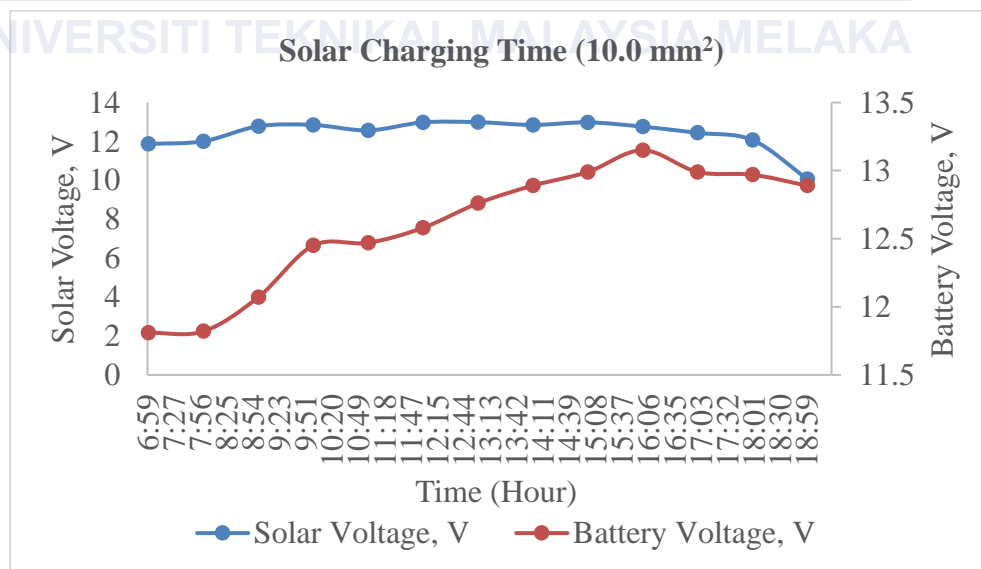


Figure 4.15 The solar PV system charging time over time with a cable diameter at 10.0 mm².

From morning to noon, solar and battery voltages rise, peaking about noon, and then slowly decrease. The solar voltage rose from 11.87 V at 7:00 AM to 12.85 V at 10:00 AM.

The notes column shows that at 11:00 AM, the solar voltage drops from 12.85 V to 12.57 V, suggesting weather is an influence. Solar voltage exceeds battery voltage all day, signifying charging. The difference between the lines represents the energy transmission and storage systems. The solar PV system generated 12.40 V over 12 hours during battery charging.

At midday, the solar and battery systems experience the highest voltage values, indicating the most favorable conditions for capturing solar energy. The graph illustrates the dynamic nature of solar charging and emphasizes the significance of comprehending voltage patterns for effective system design and management. According to the graph, the battery voltage rises from 11.81 V to 12.89 V over a period of 7 hours, indicating that the cable is capable of reducing the time required to fully charge the battery. After 2:00 PM, the charge controller continues to charge the battery to ensure it remains in a completely charged state.

Upon disconnection from the circuit, the battery retains a fully charged state with an overall capacity of 12.89 V. The use of cables with larger diameters can significantly lower the resistance within the cable, resulting in faster charging times.

Figure 4.16 shows the graph demonstrating the relationship between the panel's temperature over time and the current produced by solar energy. The vertical left axis depicts the solar current in milliamperes, ranging from 0 to 400 mA. The vertical right axis represents the panel temperature, ranging from 0 to 50 degrees Celsius, during the charging process. The horizontal axis represents time in hours, ranging from 7:00 AM to 7:00 PM, with a total duration of 12 hours.

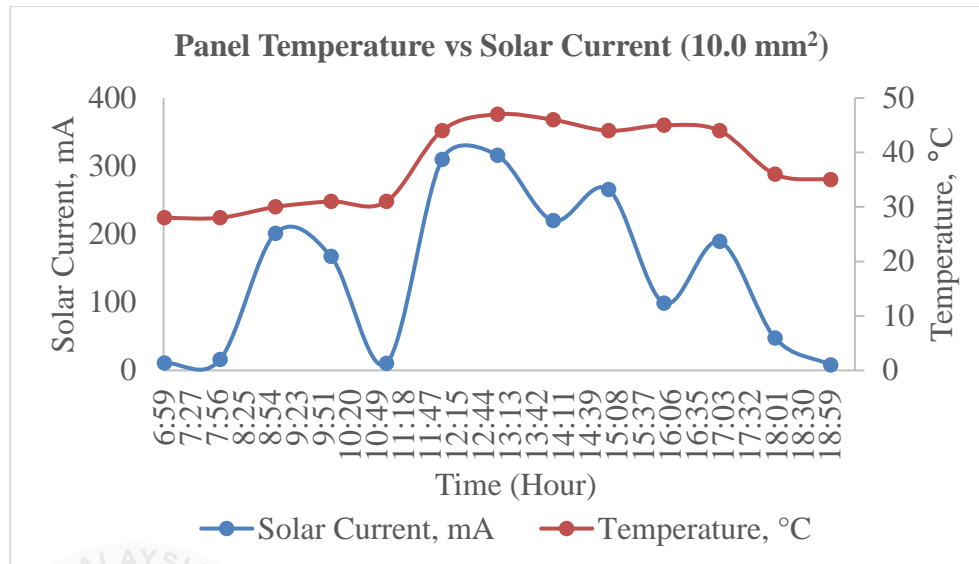


Figure 4.16 The solar PV generated current and panel temperature versus time with cable diameter at 10.0 mm².

Between 7:00 AM and 9:00 AM, both the solar current and panel temperature consistently increase, reaching a maximum current of 201.20 mA and a panel temperature of 30 degrees Celsius. The current generated between 10:00 AM and 11:00 AM was reduced due to the presence of clouds, as indicated in the remark column of table 4.4. This pattern closely tracks the trajectory of the sun across the sky, with the intensification of sunlight resulting in both increased current generation and panel temperature.

The solar current reaches its peak value of 315.70 mA at midday, while the panel temperature reaches its highest point of 47°C at the same time. The importance of peak sun hours in optimizing the power output supplied by the solar PV panel is emphasized. According to figure 4.15, the maximum recorded voltage during the battery charging process at 1:00 PM is 12.99 V, and the battery's charge capacity is at 90%.

Figure 4.17 illustrates the time-dependent solar PV power and current using a wire diameter of 10.0 mm². The left vertical axis is shown as a blue line, representing the solar current in milliamperes, ranging from 0 to 400 mA. The solar power is represented by a red line on the right vertical axis, with a range of 0 to 5 watts. The horizontal axis depicts the time in hours within a 12-hour period from 7:00 AM to 7:00 PM.

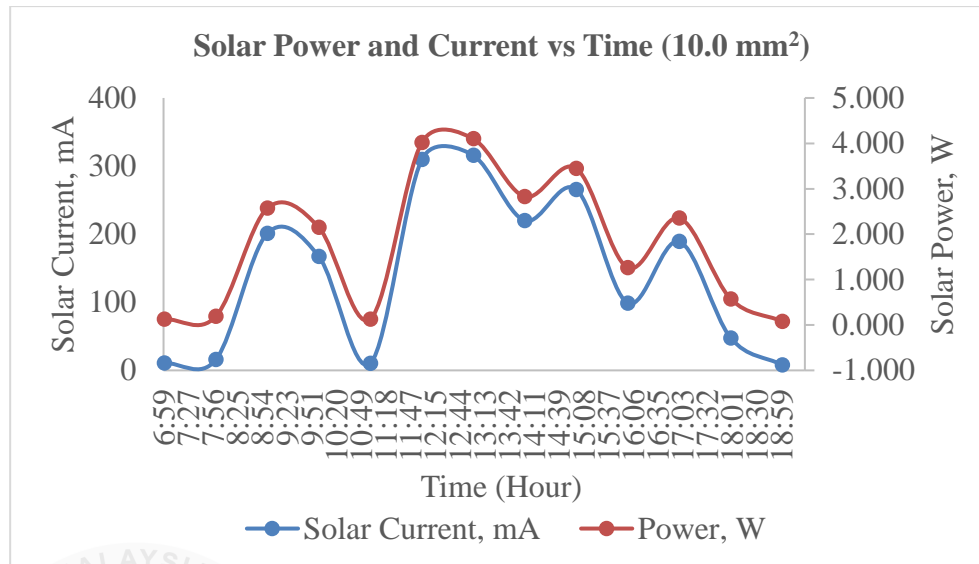


Figure 4.17 The solar PV generated power and current versus time with cable diameter at 10.0 mm^2 .

Figure 4.17 displays a Gaussian distribution, illustrating the patterns of solar current and power. Between 7:00 AM and 9:00 AM, both metrics consistently increase but then decrease from 9:00 AM to 10:00 AM. Unfavorable weather significantly reduces the efficiency of the solar panels between 10:00 and 11:00 AM, resulting in a significant drop in current from 167.3 mA to 10.37 mA when clouds appear. These weather-related variations also affect power generation.

Although there was a brief interruption at 11:00 AM, the solar panel quickly recovered its maximum efficiency during the middle of the day and afternoon, as indicated by current readings of 309.6 mA and 315.7 mA, respectively. Simultaneously, the production of electricity reaches its highest point of 4.101 W at noon. The strong parallelism observed between the two lines indicates a significant positive link between solar current and power. The relationship between current and power is one of direct proportionality, meaning that an increase in current leads to a corresponding increase in power and vice versa.

4.3.2 Summary of Solar PV Various Cable Sizing

Table 4.5 provides a comprehensive summary of the various cable sizing completed in this analysis presented in the following table:

Table 4.5 Table of Summary: Solar PV various cable size charging.

No.	Cable Size (mm ²)	Average Solar PV Voltage (V)	Average Solar PV Current (mA)	Average Solar PV Power (W)	Average Panel Temperature (°C)	Remarks
1.	0.8	12.08	138.67	1.77	35.69	20% to 35% SoC within 8 hours. (Not fully charge)
2.	1.5	11.30	94.75	1.17	34.08	20% to 55% SoC within 9 hours. (Not fully Charge)
3.	4.0	12.22	181.10	2.30	36.77	20% to 100% SoC within 9 hours. (fully charge)
4.	10.0	12.40	143.06	1.83	37.62	20% to 100% SoC within 7 hours. (fully charge)

4.3.3 Mechanical Pedal Various Cable Diameter Charging

This section seeks to explain the complex relationship between the conversion of kinetic energy into electricity through a mechanical pedal and the optimization of cable diameters for charging a lead-acid battery. The analysis of various cable size approaches is used to determine the current flowing through the cable diameter. The mechanical pedal's operation is closely related to the rotational velocity that human input generates. It is important to note that if the rotational speed continues below 3500 revolutions per minute, the generated voltage will decrease to a value below 12.0 V. This situation impedes the solar charge controller's optimal performance. On the other hand, if the rotor and stator rotational speeds exceed the designated threshold, the DC generator can generate a voltage of up to 15 volts.

4.3.2.1 Mechanical Charging with Cable Diameter at 1.0 mm²

Table 4.6 shows the expected outcome of charging a lead-acid battery using a mechanical pedal with a cable diameter of 1.0 mm². Time in minutes, voltage of the generator and battery, current of the generator, power, and a comment follow in the table.

Table 4.6 Mechanical Charging with cable diameter at 1.0 mm².

Mechanical Charging with 1.0 mm ² Cable Diameter				
Time (Minutes)	Generator Voltage (V)	Battery Voltage (V)	Generator Current (mA)	Power (W)
0	12.84	11.81	12.44	0.160
5	13.54	11.82	13.07	0.177
10	22.22	11.82	23.89	0.531
15	13.01	11.82	9.53	0.124
20	13.09	11.82	6.77	0.089
25	12.40	11.83	8.14	0.101
30	13.63	11.83	10.54	0.144
35	12.98	11.83	9.95	0.129
40	10.78	11.84	5.53	0.060
45	13.10	11.84	7.50	0.098

Table 4.6 illustrates the battery charging procedure using the mechanical pedal, which takes around 45 minutes. In order to maintain the generated voltage over 12.0 V, it is necessary to synchronize the generator speed and human rotation during the charging condition. Table 4.6's second column shows the results of the voltage generator that human pedal rotation produces. The average generated voltage of the generator is 13.78 V, with a low value of 10.78 V and a maximum voltage of 13.63 V.

Alternatively, the battery voltage is capable of rising from 11.81 V at a 20% level of charge to 11.84 V in a span of 45 minutes. The voltage generated by the generator is dependent on the speed of the pedal's rotation by the user. As the speed is enhanced, the resulting voltage also increases. The generator produces an average current of 10.74 mA, with the lowest current at 5.53 mA and the highest current at 23.89 mA.

The generator produces a peak power of 0.531 W and an average power of 0.161 W. Nevertheless, the generators only produced a minimum output of 0.060 W. While considering the process of charging, it may take a significant amount of time to fully charge while utilizing the mechanical pedal with human strength.

The graph in figure 4.18 illustrates the state of charge of a lead-acid battery being charged using a mechanical pedal. The charging process takes around 45 minutes. The graph depicts the generator voltage in volts on the left vertical axis and the battery voltage on the right vertical axis. The horizontal axis represents the time in minutes for which the analysis has been conducted. However, the blue line will reflect the battery's voltage, while the red line will show the generator's voltage.

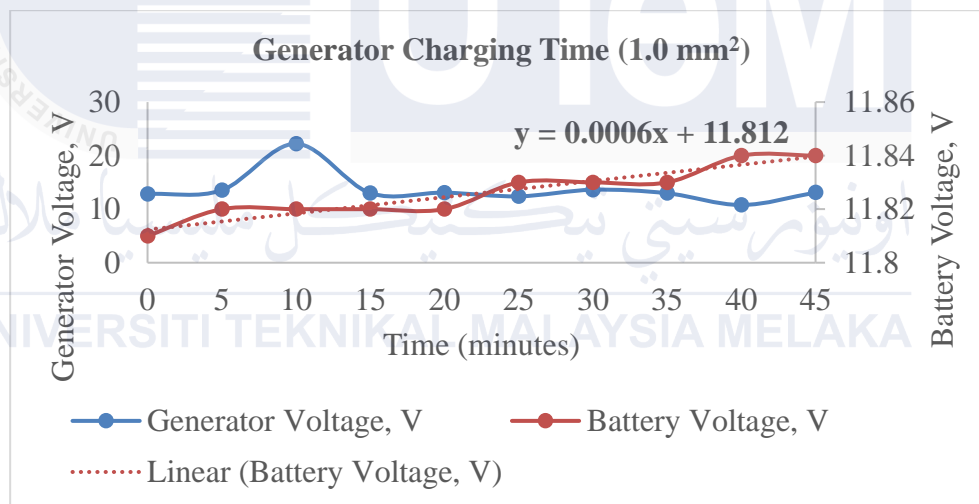


Figure 4.18 The mechanical charging using cable diameter at 1.0 mm².

The provided diagram indicates that the beginning voltage of the generator is 12.84 V. Within a duration of 5 minutes, the voltage increases to 13.54 V. Simultaneously, the rotational velocity of the generator also escalates. At the same time, the battery voltage undergoes a slight increase, rising from 11.81 V to 11.82 V in around 5 minutes.

Upon analyzing the data presented in figure 4.18, it is evident that the highest recorded voltage generated is 22.22 V, which occurred at the 10th minute. During the time interval of 5 to 20 minutes on the graph, the battery sustains a constant voltage of 11.82 V

for around 15 minutes, suggesting a stable level of charge. Significantly, around the 10th minute, the generator achieves its maximum voltage.

Over the next 25 minutes, although the generator voltage remains within the lower stability range of 13.01 to 13.1 V, the battery experiences a slight rise in voltage from 11.82 V to 11.84 V. This implies a dynamic interaction between the generator and battery, affecting the voltage levels and, subsequently, the rotating speed of the generator.

In order to estimate the whole charging time of the battery, we will utilize the equation derived from the data presented in figure 4.18. This equation reflects the projected duration required to completely charge the battery, measured in minutes, which will subsequently be converted into hours and minutes. The equation derived from the graph in figure 4.18 can be utilized to estimate the amount of mechanical pedal power required to fully charge the battery.

$$\begin{aligned}
 y &= 0.0006x + 11.812 \\
 12.89 &= 0.0006x + 11.812 \\
 0.0006x &= 12.89 - 11.812 \quad (4.1) \\
 x &= \frac{12.89 - 11.812}{0.0006} \\
 x &= 1796.667 \geq 29 \text{ hours } 57 \text{ minutes}
 \end{aligned}$$

By applying the derivation from equation 4.1, we can calculate that the overall charging time for the battery will be around 29 hours and 57 minutes. This computation is based on the premise that the cable diameter is 1.0 mm². It is important to note that the completely charged voltage of the lead-acid battery is 12.89 volts, which corresponds to the voltage value used in the calculation to calculate the total charging time, as previously discussed in this analysis.

The selected cable diameter is crucial in determining the efficiency and speed of the charging process. The equation's dependence on a cable diameter of 1.0 mm² is a critical

factor that influences the precision of the projected charging time. Furthermore, the fact that the fully charged voltage at 12.89 volts is equivalent to the voltage used in the charging equation strengthens the accuracy and dependability of the estimated duration for the entire charging process.

Figure 4.19 indicates the generator current in milliamperes on the left vertical axis, ranging from 0 to 30 mA. The generator's power is measured in watts and ranges from 0 to 0.600 watts on the right vertical axis. The horizontal axis represents the time span of the analysis, which is limited to 45 minutes.

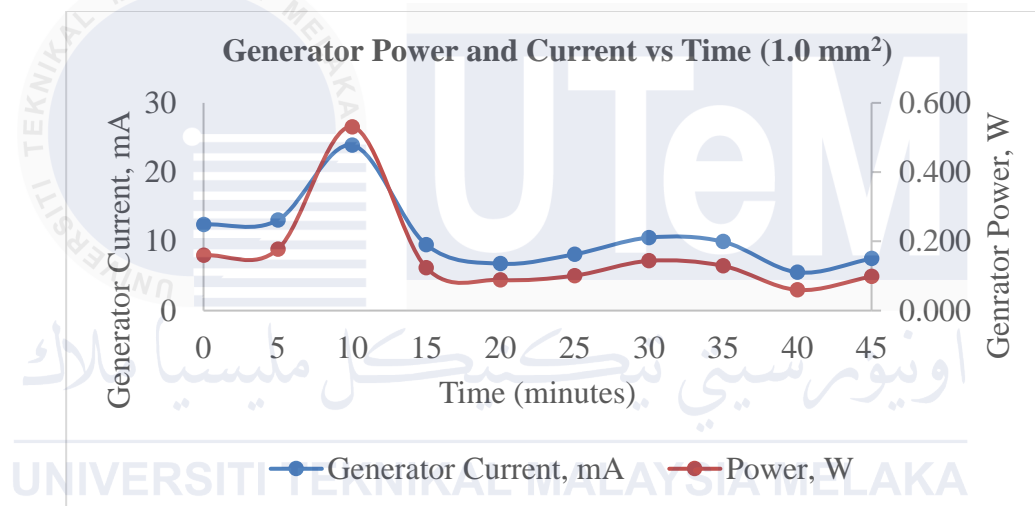


Figure 4.19 The power and current generated from mechanical pedal using cable diameter at 1.0 mm^2 .

According to Figure 4.19, there is a direct relationship between the current and power. However, at the 10th minute, the power is greater than the current due to the presence of a voltage of 22.22 V. Simultaneously, the generator generated a peak current of 23.89 mA. As the voltage rises, the current correspondingly increases due to their direct proportionality and the influence of power.

The current and power reach a maximum of approximately 10.54 mA and 0.144 W at approximately 30 minutes, after which they start to drop. The graph illustrates a positive correlation between two variables. As the generator's current output grows, so does the

power output. Such an outcome is predictable, as power is the result of multiplying current and voltage.

4.3.2.2 Mechanical Charging with Cable Diameter at 1.5 mm².

The results of a mechanical charging system with a cable diameter of 1.5 mm² are presented in the table in the following paragraphs. The following tables give details on how long it takes to charge a battery, the voltage of the generator and battery, the generator's current output, and the power.

Table 4.7 Mechanical Charging with cable diameter at 1.5 mm².

Mechanical Charging with 1.5 mm ² Cable Diameter				
Time (Minutes)	Generator Voltage (V)	Battery Voltage (V)	Generator Current (mA)	Power (W)
0	13.23	11.84	10.47	0.139
5	14.56	11.85	11.30	0.165
10	12.7	11.85	12.74	0.162
15	12.43	11.86	8.40	0.104
20	13.28	11.86	13.50	0.179
25	13.3	11.87	12.74	0.169
30	13.2	11.88	14.73	0.194
35	13.12	11.89	12.59	0.165
40	13.09	11.9	12.25	0.160
45	12.55	11.91	7.69	0.097

Table 4.7 provides a comprehensive breakdown of the duration it takes to charge, measured in minutes, throughout a 45-minute analysis period. This data is then compared to the voltage output from a mechanical pedal device. The second column presents the diverse voltage outputs generated in relation to the rotational velocity of the pedal. The data demonstrates that the mechanical pedal can produce a maximum voltage of 14.56 V, with a minimum voltage of 12.43 V attained with a cable diameter of 1.5 mm². The generator constantly sustains a voltage output of 13.15 V during the course of the 45-minute duration.

Although the generator's voltage shows little fluctuations, the battery voltage experiences a small rise from 11.84 V to 11.91 V after around 45 minutes. This indicates that the generator, functioning at a consistent current of 11.64 mA, faces difficulty increasing the current in accordance with the pace at which the human is spinning. According to theoretical predictions, an increase in the rate of acceleration should lead to a proportional increase in electric current. Nevertheless, the primary emphasis lies on the human ability to rotate the mechanical pedal shaft.

Figure 4.20 expresses the graph illustrating the correlation between the generated voltage from the generator and the process of charging the battery. The graph shows a blue line on the left vertical axis to represent the generator voltage and a red line on the right vertical axis to represent the battery voltage. Nevertheless, the horizontal axis denotes time measured in minutes.

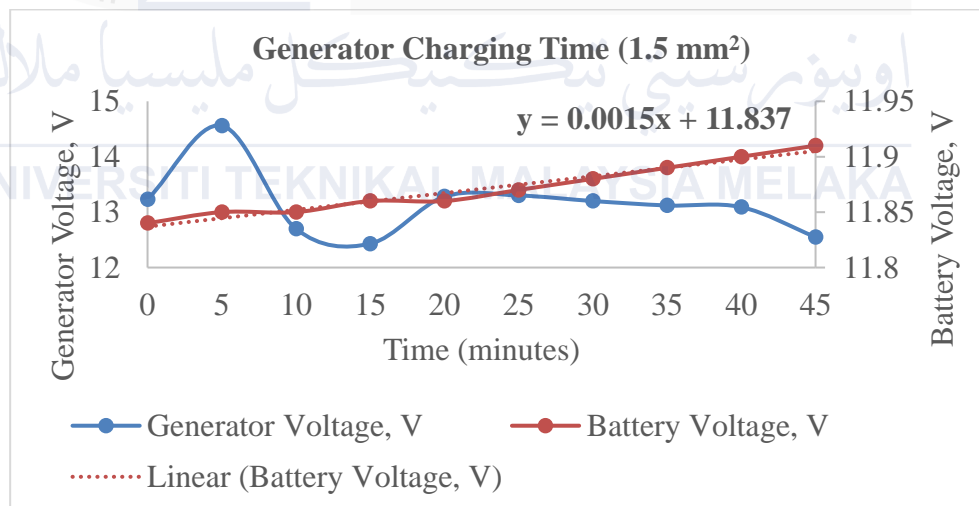


Figure 4.20 The mechanical pedal charging using cable diameter at 1.5 mm².

According to Figure 4.20, the graph displays the generator voltage measurement of 13.23 V at the start of the charging process. Additionally, it indicates a peak voltage of 14.56 volts at the 5th minute. The graph illustrates the correlation between the rotational speed of a person pedaling and the voltage generated for charging the battery. Between the 20th and

45th minutes, the voltage generated experienced a minor drop from 13.28 to 12.55. The generator's output voltage decreases in proportion to the pedal's reduced rotation.

The graph in figure 4.20 shows a minor increase in battery voltage from 11.84 V to 11.91 V around the 45-minute mark. Simultaneously, when observing the graph from 0 to 20 minutes, it becomes evident that the battery voltage is fluctuating due to the lack of synchronization with the generator voltage. Subsequently, during the time span of 20 to 45 minutes, the battery voltage had a gradual and steady rise without any noticeable variations.

The estimate of the lead-acid battery complete charge can be derived from the graph depicted in figure 4.20. By formulating the linear equation based on the graph, it is possible to determine the total duration required to fully charge the battery from 20% to 100%.

$$\begin{aligned}
 y &= 0.0015x + 11.837 \\
 12.89 &= 0.0015x + 11.837 \\
 0.0015x &= 12.89 - 11.837 \\
 x &= \frac{12.89 - 11.837}{0.0015} \\
 x &= 702 \geq 11 \text{ hours } 42 \text{ minutes}
 \end{aligned} \tag{4.2}$$

The linear equation above suggests that the overall time required to fully charge the battery using a cable with a diameter of 1.5 mm² is approximately 11 hours and 42 minutes. Otherwise, we use 12.89 V as the nominal number to consider while fully charging a lead-acid battery.

Figure 4.21 shows the relationship between generator power and current as it changes over time. The left vertical axis represents the generator current, while the right vertical axis represents the generator power. The horizontal axis of Figure 4.21 represents time in minutes, with the 45-minute mark shown. Hence, the blue line represents the current generated by cycling the DC generator, while the red line represents the power produced by the generator.

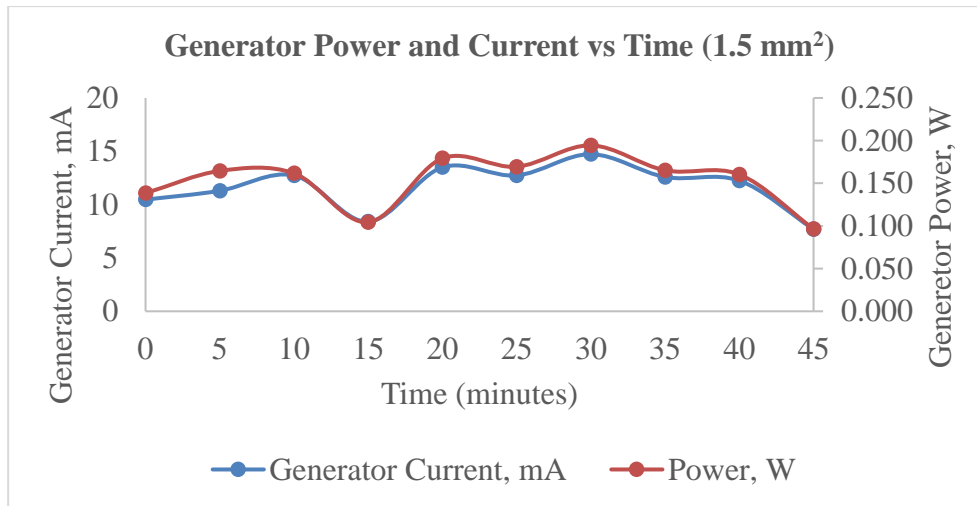


Figure 4.21 The power and current generated from mechanical pedal using cable diameter at 1.5 mm^2 .

Based on the data illustrated in Figure 4.21, the current output of the generator ranges from 0 to 20 mA, while the corresponding power generated ranges from 0 to 0.3 watts. Significantly, both curves show a parallel trajectory to the speed that human pedaling produces. The alignment of the current and power curves at the five-minute mark indicates an interesting synchronization point. The synchronization happens as the generated current, which is initially lower than the solar generation, gradually catches up.

According to an analysis of the data shown in Figure 4.21, the generator's mean output power is 0.153 W. Put simply, the mechanical pedal charging method depends on continuous human engagement to move the pedal, which enables the production of high voltage and current. As the voltage and current levels increase, the output power from the generator will certainly increase due to their straight proportional relationship.

4.3.2.3 Mechanical Charging with Cable Diameter at 4.0 mm^2 .

The results of mechanical charging using a cable diameter of 4.0 mm^2 are shown in table 4.8. The table includes data on the time taken in minutes, the voltage of the generator and battery, as well as the current and power.

Table 4.8 Mechanical Charging with cable diameter at 4.0 mm².

Mechanical Charging with 4.0 mm ² Cable Diameter				
Time (Minutes)	Generator Voltage (V)	Battery Voltage (V)	Generator Current (mA)	Power (W)
0	13.33	11.9	16.66	0.222
5	13.27	11.91	17.86	0.237
10	13.31	11.91	19.68	0.262
15	13.3	11.92	18.88	0.251
20	12.99	11.93	20.79	0.270
25	13.28	11.94	15.55	0.207
30	12.98	11.95	10.05	0.130
35	13.25	11.95	11.14	0.148
40	13.27	11.96	11.01	0.146
45	12.78	11.97	9.62	0.123

According to the observations, the table displays the complete period of cycling the generator, ranging from 0 to 45 minutes, in order to provide the necessary voltage and current for recharging the battery. The generator produces a peak voltage of 13.31 V and a minimum voltage of 12.78 V. The generator produced an average voltage of approximately 13.18 V and an average current of approximately 15.124 mA.

According to the data presented in Table 4.8, the battery, which has the capability to charge rapidly in around 45 minutes, had an increase in voltage from 11.90 V to 11.97 V. The battery started at an initial voltage of 11.9 volts. Approximately 5 minutes later, the voltage of the battery grew by 0.01 volts. For the following several minutes, the battery remained at a steady voltage of 11.91 volts until the 15th minute. At exactly 20 minutes, the maximum current was measured at 20.79 mA. The cable with a diameter of 4.0 mm² produced an average output power of 0.200 W. The maximum power production is 0.270 W at the 20th minute.

Figure 4.22 graph shows that the red line in the graph represents the voltage of the battery, while the blue line in the graph represents the voltage of the generator. The left

vertical axis represents the generator voltage, which ranges from 12.5 to 13.5 V. The right vertical axis represents the battery voltage, which ranges from 11.85 to 12.0 V. An examination was conducted on the overall duration of mechanical charging with a cable diameter of 4.0 mm², represented on the horizontal axis as time in minutes.

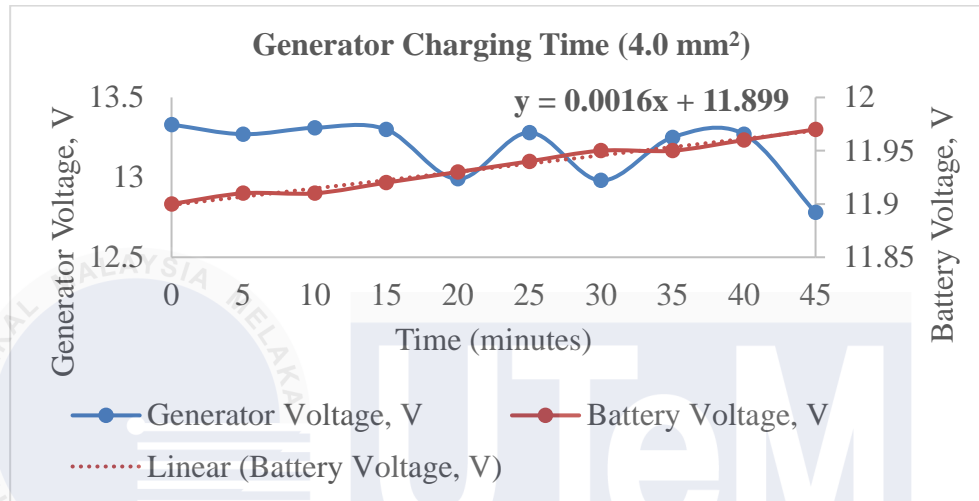


Figure 4.22 The mechanical charging process of cable diameter of 4.0 mm².

Upon examination, the graph illustrates the voltage created from mechanical pedaling, which fluctuates in accordance with the speed. However, the variations observed during the analysis are not deemed noteworthy. From 0 to 15 minutes, the voltage produced by the mechanical pedal remains consistent at approximately 13.3 V. Subsequently, the voltage experiences a decrease from 13.3 V to 12.99 V at the 20-minute mark. However, within a time frame of 15 to 45 minutes, the voltage generation from human-powered mechanical pedaling has the greatest variation.

According to the graph provided, the battery voltage exhibits a steady increase from 11.9 V to 11.97 V after around 45 minutes, despite some fluctuations in the generated voltage. The battery can recharge from 11.91 V to 11.95 V over a time frame of 10 to 30 minutes. This indicates that the generated voltage may be sustained at 13.17 V and increase by around 0.04 V after around 20 minutes. Utilizing a cable with a larger cross-sectional area

is an effective method to decrease the amount of time required for charging, which is a positive indication.

To determine the total time required to fully charge the battery using mechanical pedaling with a cable diameter of 4.0 mm², the estimation yields the following result as equation 4.3. The derivation equation can be obtained directly from the graph depicted in figure 4.22.

$$\begin{aligned}
 y &= 0.0016x + 11.899 \\
 12.89 &= 0.0016x + 11.899 \\
 0.0006x &= 12.89 - 11.899 \\
 x &= \frac{12.89 - 11.899}{0.0016} \\
 x &= 619.375 \geq 10 \text{ hours } 20 \text{ minutes}
 \end{aligned} \tag{4.3}$$

According to the calculation in equation 4.3, with a cable diameter of 4.0 mm², the estimated time to fully charge by cycling mechanically is roughly 10 hours and 20 minutes. Using a cable with a diameter of 4.0 mm² may reduce the charging time by 1 hour and 23 minutes compared to using a wire with a diameter of 1.5 mm². Additionally, the equation 4.3 mentioned above indicates that the battery's maximum capacity when fully charged is 12.89 V.

Figure 4.23 displays the graph depicting the relationship between the output power from the generator and the current over a period of time measured in minutes. A blue line on the left vertical axis that ranges from 0 to 30 milliamperes represents the generator current. The right vertical axis displays the generator's power output, which ranges from 0.000 to 0.3000 watts. However, the red lines also indicate the output power from the generator at that specific moment. The horizontal axis represents the duration of the mechanical pedal charging process, measured in minutes. This procedure utilizes a cable with a diameter of 4.0 mm².

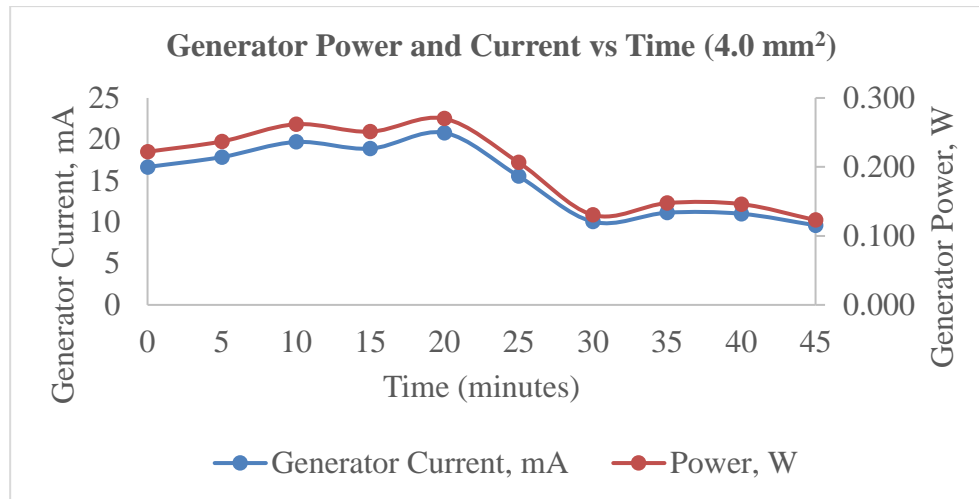


Figure 4.23 The output power and current over time of a cable with a diameter of 4.0 mm^2 .

Upon observation, both lines exhibit a synchronous relationship, where the generator's output power increases in direct proportion to the simultaneous increase in current. This establishes a clear correlation between current and voltage at that particular moment. Both trends show a gradual increase from 0 to 20 minutes during the mechanical pedaling-powered early stages of the charging process. Surprisingly, voltage drops are the cause of periodic changes that happen exactly every 15 minutes. Subsequently, the output power undergoes a slow decrease from its highest point, gradually decreasing until it reaches the lowest levels depicted in the graph.

4.3.2.4 Mechanical Charging with Cable Diameter at 10.0 mm^2 .

The project is related to the hybrid system of renewable energy that consists of solar PV and mechanical pedaling. Table 4.9 displays the results of mechanical charging with a cable diameter of 10.0 mm^2 . Table 4.9 includes time in minutes, generator and battery voltage, generator current, and power. However, the total period of cycling the generator ranged from 0 to 45 minutes.

Table 4.9 Mechanical Charging with cable diameter at 10.0 mm²

Mechanical Charging with 10.0 mm ² Cable Diameter				
Time (Minutes)	Generator Voltage (V)	Battery Voltage (V)	Generator Current (mA)	Power (W)
0	13.35	11.97	13.92	0.186
5	13.65	11.98	15.26	0.208
10	13.8	11.99	12.58	0.174
15	13.25	11.99	14.36	0.190
20	13.57	12	12.41	0.168
25	13.27	12	11.77	0.156
30	13.31	12.01	14.71	0.196
35	13.21	12.03	14.65	0.194
40	13.09	12.05	12.75	0.167
45	13.02	12.05	14.48	0.189

According to the observation, the generator initially generated a voltage of 13.35 V, while the battery voltage was 11.97 V. The peak voltage obtained at 10 minutes is indicated in Table 4.9. Hence, the wire with a diameter of 10.0 mm² produces a minimum voltage of 13.02 volts after 45 minutes. The mean voltage is roughly 13.352 V, according to the outcome. Nevertheless, the battery voltage exhibits a direct correlation with the voltage and current produced. During a charging process lasting 30 to 35 minutes, the battery voltage increases by approximately 0.02 V after 5 minutes, as a result of an average current of 13.689 mA.

According to the comparison, the generator's average output voltage was higher than 4.0 mm², while the current generated was lower. When both the voltage and current increase, the output power increases proportionally to the voltage and current. Alternatively, the highest measured power output in this investigation was 0.208 W, with a minimum of 0.156 W. The average output power is 0.183 W.

As can be seen in figure 4.24, the graph depicts the voltage of the generator and the battery as a function of time, measured in minutes. The blue line, which is at the left vertical

axis and has a range of 12.5 to 14 V, displays the generator's voltage. However, a red line on the right vertical axis shows the battery's voltage, which started at 11.95 milliamperes and continued to 12.1 milliamperes. With respect to the horizontal axis, the time expressed in minutes, of the overall duration of the analysis that was carried out is represented.

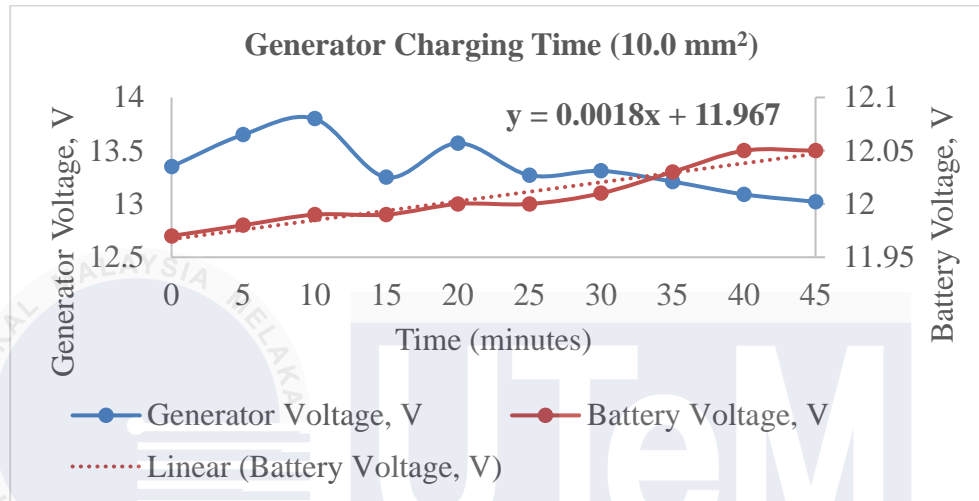


Figure 4.24 The graph of generator and battery voltage over time by using the cable diameter of 10.0 mm².

According to the graph shown in figure 4.24, it was seen that the blue lines experienced a minor increase between the 0- and 10-minute mark of the charging process. The blue of the generator voltage began to fluctuate anywhere between ten and forty-five minutes in the past. On the basis of the high voltage that was produced by mechanical pedaling at a time of ten minutes, which was 13.80 V. However, at twenty minutes, the voltage was 13.57 V, which was the second highest of all the voltages. Following that, there was a little fall in voltage, which went from 13.57 V to 13.02 V.

According to the findings presented in figure 4.24, the voltage of the battery grew somewhat from 0 to 45 minutes, which corresponds to the maximum battery capacity of 12.05 V on the battery. The battery voltage appears to decrease slightly between the tenth and fifteenth minutes of the charging process; however, when table 4.9 is taken into consideration, the battery voltage remains maintained at 11.99 V for around five minutes

without any increase in the charging process. The graph demonstrates that the voltage of the battery increases from 12.0 V to 12.05 V in a span of twenty minutes, with the process of mechanical charging taking between twenty-five and forty-five minutes.

An estimation of the amount of time required to fully charge the lead-acid battery can be obtained by deriving the equation from the graph depicted in figure 4.24. The derivation can then be utilized to determine the total duration of the mechanical pedal in comparison to the human pedal.

$$\begin{aligned}
 y &= 0.0018x + 11.967 \\
 12.89 &= 0.0018x + 11.967 \\
 0.0018x &= 12.89 - 11.967 \\
 x &= \frac{12.89 - 11.967}{0.0018} \\
 x &= 512.778 \geq 8 \text{ hours } 33 \text{ minutes}
 \end{aligned} \tag{4.4}$$

According to the derivation, it is determined that the complete charging process takes roughly 8 hours and 33 minutes. By contrast, the total charging time for a wire with a diameter of 4.0 mm² is around 10 hours and 20 minutes. By utilizing a charging diameter of 10.0 mm², it is possible to decrease the charging duration to 8 hours and 33 minutes. To decrease the overall charging time, it is necessary to maintain a consistent pace of pedal rotation that generates a voltage higher than 13.352 V, as indicated in table 4.9. The fully charged capacity of a lead-acid battery is roughly 12.89 V. Manufacturers typically measure a new battery's voltage between 13.05 V and 13.06 V at its highest point. The optimal pedaling pace for the battery to fully charge is around 8 hours and 33 minutes, as calculated using equation 4.4.

Figure 4.25 shows the graph that identifies the charging potential inside a 45-minute examination. A blue line next shows the generator current, which ranges from 0 to 20 milliamperes, on the vertical axis on the left. On the other side, the right vertical axis and red

line represent the power generated, ranging from 0.000 to 0.3000 watts. Alternatively, the horizontal axis represents time measured in minutes.

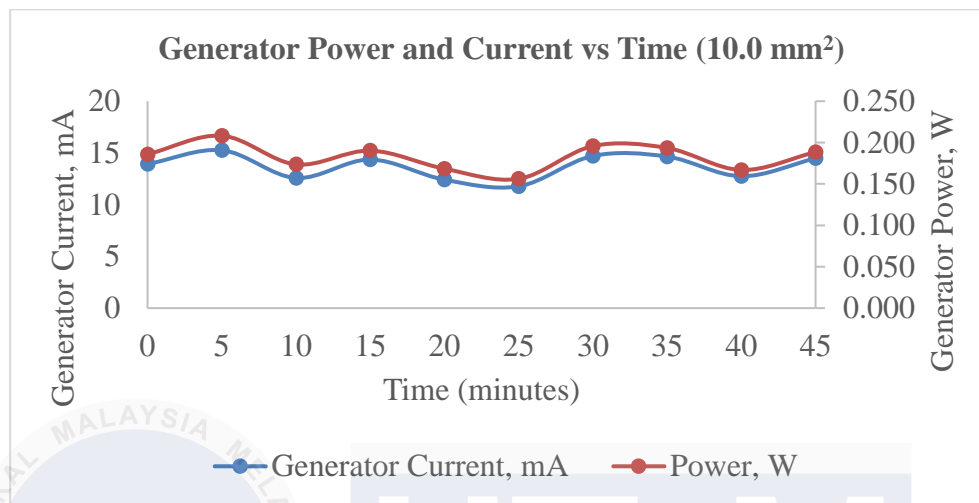


Figure 4.25 The output power and current from the generator over time in minutes by using mechanical pedal with a cable diameter of 10.0 mm².

Based on the observation, both lines exhibit dynamic fluctuations in generation due to variations in the current over the output power. This circumstance occurs when the generated current does not exceed the generated voltage. According to Table 4.9, the results indicate that the voltage is greater than the current. This is because the generator's current reaches a peak of 15.26 mA and has an average current of 13.689 mA. Consequently, in order to generate a higher current, it is necessary to increase the rotational speed of pedaling. As the mechanical pedaling rotation rate increases, the output power demonstrates a straight proportionality to the current and voltage generated, as depicted in the graph. The first current recorded in figure 4.24 above is 13.92 mA, whereas the final minute of data gathering shows a current of 14.48 mA.

From the observation, the graph trends similarly to the sinusoidal wave due to the current and power generated fluctuating due to the speed of mechanical pedaling, which is not consistent. However, the analysis of using mechanical pedaling, with a cable diameter of 10.0 mm², has the ability to recharge the battery as a secondary renewable energy source

for this project. As a secondary renewable energy source, the result of charging time can be used as a comparison to 10.0 mm² solar PV charging, which has a charging time of 7 hours, but mechanical pedaling needs 8 hours and 33 minutes to fully charge.

4.3.4 Summary of Mechanical Various Cable Size Charging

Considering a mechanical pedal analysis for charging a lead-acid battery with a 12.0V and 7.2 Ah capacity. Consequently, the charging procedure utilizing a mechanical pedal with varying cable diameter sizes is summarized in table 4.10.

Table 4.10 Table of Summary: Mechanical Pedal various cable size charging.

No.	Cable Size (mm ²)	Average Generator Voltage (V)	Average Generator Current (mA)	Average Generator Power (W)	Total Duration of Fully Charged, hours and minutes
1.	1.0	13.759	10.736	0.161	29 hours and 57 minutes
2.	1.5	13.146	11.641	0.153	11 hours and 42 minutes
3.	4.0	13.176	15.124	0.200	10 hours and 20 minutes
4.	10.0	13.352	13.689	0.183	8 hours and 33 minutes

4.3.5 Various Load Discharging

This subtopic will present the findings of the analysis conducted in order to determine the state of charge of a battery. The fan speed can determine the energy consumption of the load by measuring the resistance during its usage. The outcome of this subtopic allows for the determination of the duration required to reach a state of charge equivalent to 20% of the battery's total capacity.

4.3.3.1 Load Discharging at 19.5 W Power Rating

The analysis of the various load discharge of a fan speed at position 1 is presented in Table 4.11. The table displays the overall load discharge over a period of 2 hours, using a fan speed set at position 1, with an average load resistance of 1.97 kilohm.

Table 4.11 Various load discharge of a fan speed at position 1.

Fan Speed at Position 1 (≥ 1.97 kilohm)							
Time (Minutes)	Battery Voltage (V)	Load Voltage (V)	Load Current (A)	Power Usage (W)	Power Factor (θ)	Resistance (Ω)	Remark
20:00	12.39	243.4	0.128	18.7	0.58	1967.86	100% of battery is 12.89 V
20:15	12.34	243.2	0.128	18.7	0.58	1967.86	
20:30	12.29	242.8	0.128	18.6	0.58	1957.33	
20:45	12.22	240.9	0.130	18.6	0.57	1930.86	
21:00	12.2	242.2	0.132	18.7	0.56	1916.49	
21:15	12.16	242.5	0.129	18.8	0.56	2017.39	
21:30	12.09	243.5	0.128	18.7	0.58	1967.86	
21:45	11.92	242.7	0.128	18.7	0.57	2002.38	
22:00	11.81	243.4	0.128	18.7	0.57	2002.381	20% of SoC

Upon connecting the battery to the circuit, the battery's full charge of 100% gradually decreases from 12.89 V to 12.39 V as a result of the inrush current. Hence, from 08:00 PM to 08:30 PM, the battery voltage experiences a reduction of 0.05 units per 15 minutes. Subsequently, the battery exhibits a discharge rate ranging from 0.04 V to 0.12 V every 15 minutes. During the time period of approximately 2 hours, specifically from 08:00 PM to 10:00 PM, the load voltage remains constant at 242.733 V. When considering the efficiency of the inverter, the output voltage is approximately above 90%.

The load current, as indicated in Table 4.11, reaches a high of 0.132 A and remains steady at 0.128 A. By determining the fan speed, the power consumption of a load may be identified. The load has a peak power use of 18.8 W and an average power usage of 18.7 W. Alternatively, the power factor of the system was measured to be between 0.56 and 0.58, with an average value of 0.57. Essentially, the load resistance has the capability to reduce power consumption. When the fan is set to the lowest speed, it indicates that the resistance is higher. Based on the data in table 4.11, the greatest recorded resistance is 2017.392 ohm, observed at 09:15 PM.

Based on figure 4.26, the analysis graph shows that the various load discharging of a fan speed at position 1 is represented by the battery and load voltage over the duration of discharge until reaching a state of charge of 20% for a lead-acid battery. A blue line on the left vertical axis represents the battery voltage, and a red line on the right vertical axis represents the load voltage. Thus, the horizontal axis represents the duration of the battery discharge.

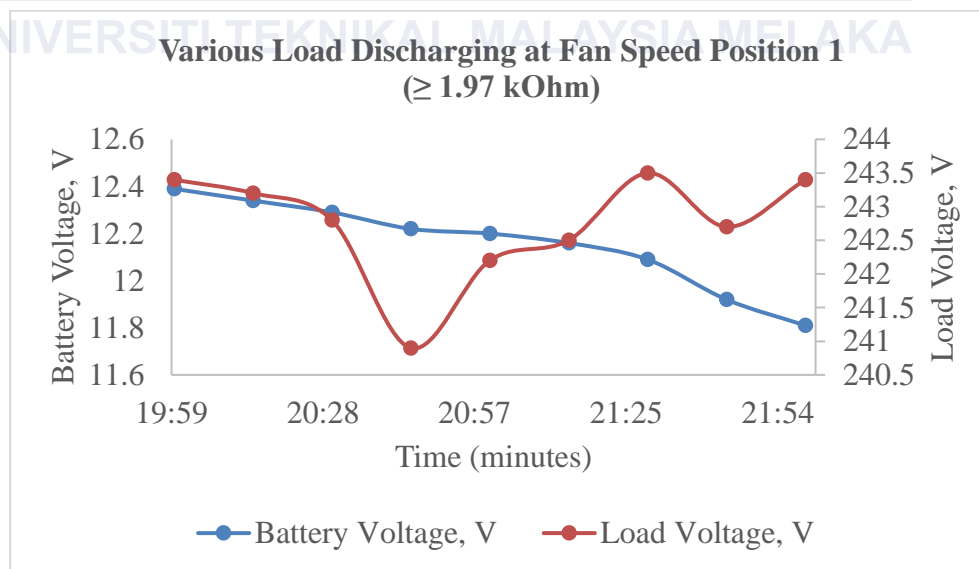


Figure 4.26 The battery and load voltage over duration of discharging.

According to the observation, Figure 4.26 depicts a graph illustrating a decreasing trend of the battery voltage, represented by the blue lines, from an initial value of 12.39 V

to 11.81 V after approximately 2 hours. During the initial phase of fan speed position 1 load discharging, from 08:00 PM to 08:45 PM, the battery discharge is lower compared to the period from 08:45 PM to 10:00 PM. According to the graph, the rate of discharge increases between 08:45 PM and 10:00 PM, with a discharge rate ranging from around 0.04 to 0.12 V.

Based on the graph provided, the load voltage experiences a minor drop from 243.4 to 240.9 V between 08:00 PM and 08:45 PM. From 09:00 PM to 09:30 PM, the efficiency of the inverter improves, as seen by the graph in figure 4.26, which shows an increase in the load voltage from 240.9 V to 243.5 V. Subsequently, the graph illustrates that the load voltage began to oscillate between 09:30 PM and 10:00 PM.

The graph below shows the load current on the vertical axis on the left side, with a blue line that covers from 0.127 to 0.133 A. The vertical red line represents power consumption, ranging from 18.6 to 18.9 W. The horizontal axis represents the overall time of battery discharge, ranging from 100% to 20%.

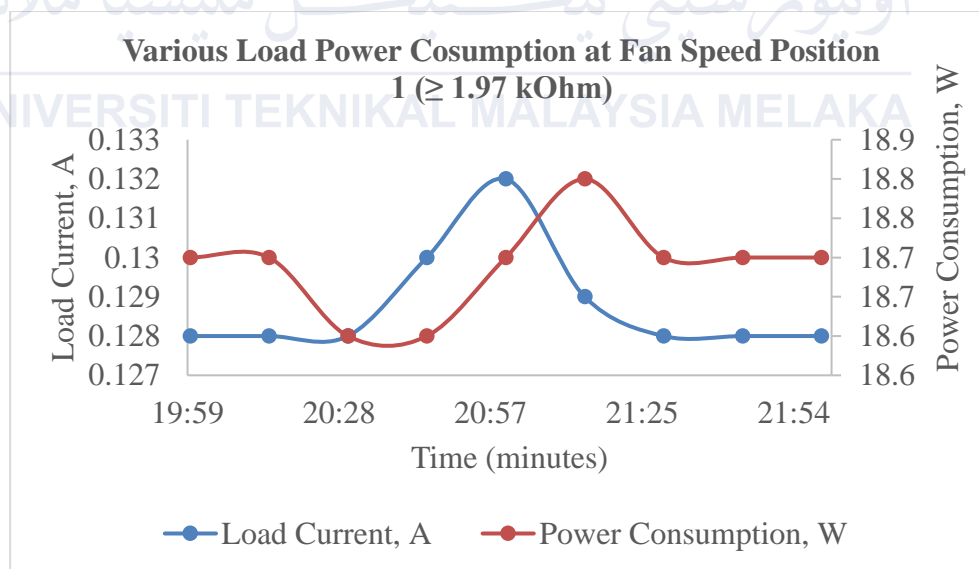


Figure 4.27 The power consumption of load current over the time of discharging.

Figure 4.27 is a graph illustrating a gradual decrease in power consumption over time. The load current initially begins at 0.128 A and gradually rises to 0.132 A within a span of 1 hour. The power consumption first stands at 18.7 W and thereafter reduces to 18.6

W for the identical time interval. Several potential reasons account for the steady decrease in electricity use. One potential cause is that the battery in the load is depleted, resulting in a decrease in voltage. Another potential explanation is that the load is gradually improving its efficiency. The graph indicates that the peak load current at 09:00 PM is 0.132 A. After 09:00 PM, the load current experienced a little reduction from 0.132 A to 0.128 A after reaching 20% of the state of discharge.

4.3.3.2 Load Discharging at 25.1W Power Rating

Table 4.12 shows the results of analyzing the various load discharge of a fan speed at position 2. The analysis data is collected at intervals of roughly 15 minutes to determine the rate of battery discharge and the power factor.

Table 4.12 Various load discharge of a fan speed at position 2.

Fan Speed at Position 2 (≥ 1.42 kiloohm)							
Time (Minutes)	Battery Voltage (V)	Load Voltage (V)	Load Current (A)	Power Usage (W)	Power Factor (θ)	Resistance (Ω)	Remark
20:00	12.35	242.1	0.182	25.1	0.57	1329.401	100% of battery is 12.89V
20:15	12.31	243.1	0.177	24.8	0.55	1439.271	
20:30	12.2	242.4	0.178	24.9	0.55	1428.883	
20:45	12.06	242.9	0.177	24.9	0.55	1445.074	
21:00	11.9	242.4	0.177	24.8	0.55	1439.271	
21:08	11.81	242.6	0.178	24.8	0.55	1423.144	20% of SoC

Table 4.12 demonstrates that the fan speed stays the same for 1 hour and 8 minutes. The battery drains from 100% to 20% throughout this period. However, the battery's inrush current reduces its capacity from 12.89 V to 12.35 V when connected to the circuit. According to Table 4.12, the battery voltage declines faster after 8:15 PM, from 12.31 V to

12.20 V in 15 minutes. Fan speed position discharge averages 0.09 to 0.16 V every 15 minutes.

Inverters must be over 90% efficient to power AC loads. The data show an average load voltage of 242.583 V. This means the inverter efficiency can maintain the output voltage. At 8:15 PM, the load voltage peaked at 243.1 V, while the first load discharge study started at 242.1 V.

Table 4.12 shows 0.182 A as the peak load current at fan speed position 2 at the commencement of load analysis. With 25.1 W of high-power usage, the average current sustained was 0.178 A. Inrush current occurs when an AC load is connected. The typical fan speed position power consumption is 24.9 W, with a power factor of 0.55 and a load resistance of 1417.507 Ohm.

Figure 4.28 shows the fan speed load at a lead-acid battery discharge point. A blue line on the left vertical axis shows battery voltage from 11.6 V to 12.4 V. The red lines on the right vertical axis represent the load voltage from 242 V to 243.5 V. The battery discharge time in minutes is shown on the horizontal axis.

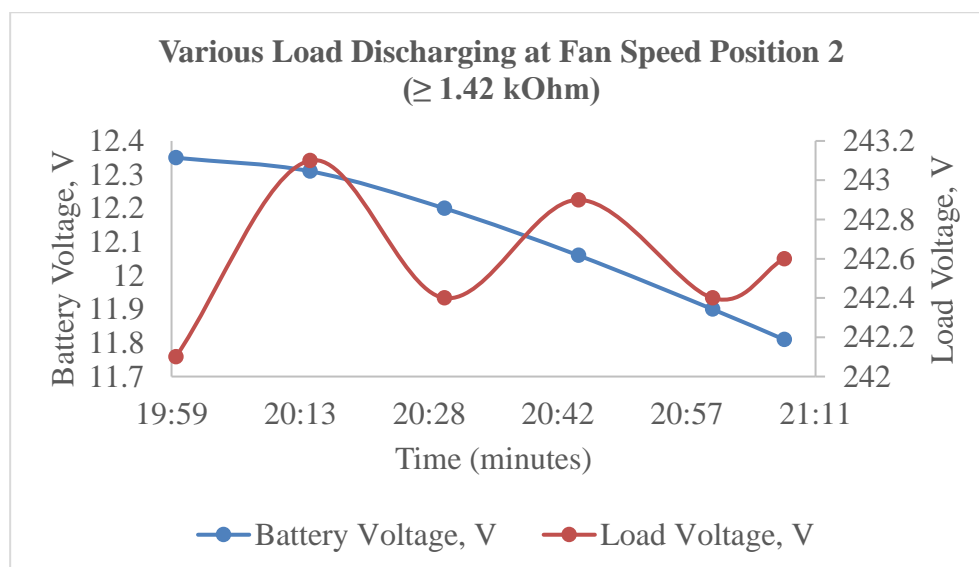


Figure 4.28 The battery and load voltage over time of fan speed position 2.

The graph in Figure 4.28 above illustrates the correlation between battery voltage and load voltage. The battery voltage was first measured at 12.35 V and decreased to 11.81 V after approximately 1 hour and 8 minutes. According to the graph in figure 4.28, the battery discharge rate increases after 08:15 PM. Specifically, between 08:15 PM and 09:08 PM, the battery capacity discharges rapidly. Alternatively, the load voltage exhibits a sinusoidal waveform as a result of the inverter's operation. The occurrence of this sinusoidal waveform can be attributed to the simultaneous factors of inverter efficiency and battery voltage. The total duration of fan speed discharge at position 2 is 1 hour and 8 hours. As power consumption increases, the discharge rate also increases proportionally.

Figure 4.29 illustrates the correlation between load current and power usage during battery discharge over time. The blue line on the left vertical axis is a representation of the load current, which ranges from 0.176 A to 0.184 A. The right vertical axis reflects power usage, as does the red line. Thus, the horizontal axis represents the time in minutes for the entire duration of the battery drain.

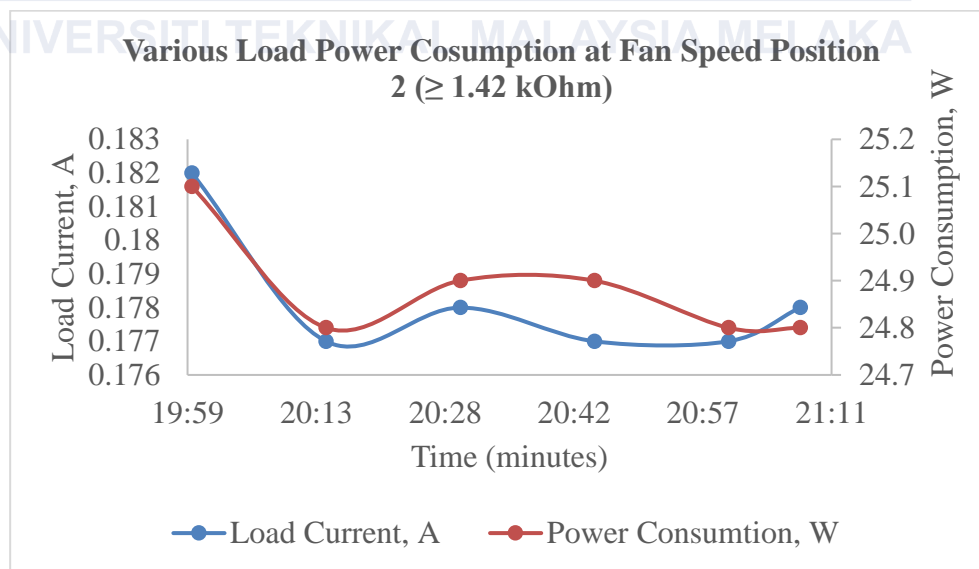


Figure 4.29 The load current and power consumption of fan speed position 2 over time.

The graph depicted in Figure 4.29 illustrates that the load current and power usage remain generally stable during the given time period. At the beginning of the analysis

conducted, both lines slightly dropped from 0.182 A and 25.1 W to 0.177 A and 24.8 W due to the fan operating having the greater starting current, or, in other words, inrush current. Subsequently, the load current and power consumption exhibited a direct increase for both lines, as depicted in the aforementioned graph.

The graph trends can be used to assess the performance of the hybrid renewable energy portable power supply by analyzing the variations in current and power usage over time. The graph demonstrates a clear proportionality between the load current and power usage. This implies that as the load power consumption increases, the rate at which a 12 V, 7.2 Ah lead-acid battery reaches its state of charge also increases. Nevertheless, this result can show a connection between the amount of power an electrical device uses and the current it draws. The total duration required to achieve the desired charge level for this load analysis is 1 hour and 8 minutes, specifically for the fan speed set at position 2.

4.3.3.3 Load Discharging at 33.7W Power Rating

The table below displays the findings of a battery discharge analysis conducted at fan speed position 3.

Table 4.13 Various load discharge of a fan speed at position 3.

Fan Speed at Position 3 (≥ 0.95 kiloohm)							
Time (Minutes)	Battery Voltage (V)	Load Voltage (V)	Load Current (A)	Power Usage (W)	Power Factor (θ)	Resistance (Ω)	Remark
20:00	12.35	242.4	0.268	32.5	0.49	923.459	100% of battery is 12.89 V
20:15	12.25	242.9	0.264	32.9	0.49	963.367	
20:30	12.05	242.6	0.264	32.8	0.49	960.439	
20:45	11.83	242.2	0.263	32.6	0.5	942.619	
20:47	11.81	241.9	0.262	32.5	0.5	946.915	20% of SoC

Table 4.13 includes data on the duration in minutes, battery and load voltage, load current, power usage, power factor, resistance, and any further comments. Table 4.13 displays the battery load discharging rate from 08:00 PM to 08:47 PM. It represents the entire time it took for the battery to discharge, from 100% to 20%. Nevertheless, the battery's rate of discharge initially begins at 0.1 V and subsequently rises to a range of 0.02 V to 0.22 V between 08:15 PM and 08:47 PM.

According to table 4.13, the load voltage remained constant at 242.4 V, with peak and minimum voltages of 242.9 V and 241.9 V, respectively. Alternatively, the maximum current flowing through the load was initially 0.268 A and gradually decreased to 0.264 A to 0.262 A between the time periods of 08:15 PM and 08:47 PM. According to the table, the peak power use occurred at 8:15 PM and reached a value of 32.9 W. The power factor of this analysis result remained consistently between 0.49 and 0.50, with an average value of 0.49.

The load resistance must be taken into account, as it directly affects the rate at which the battery discharges. Decreasing the load resistance will result in an increased battery discharge rate, as seen in Table 4.13. The study indicates that the battery discharged from 100% to 20% state of charge in roughly 47 minutes, as noted in the remarks column.

Figure 4.30 illustrates the relationship between the load discharging at fan speed setting 3 and the battery voltage, shown by the blue line on the left vertical axis. On the other side, the right vertical axis and red line represent the voltage of the load. Both vertical axes vary from 11.6 to 12.4 V and 241.5 to 243 V. Nevertheless, the horizontal axis represents the time in minutes it takes for the battery to deplete from 100% to 20%.

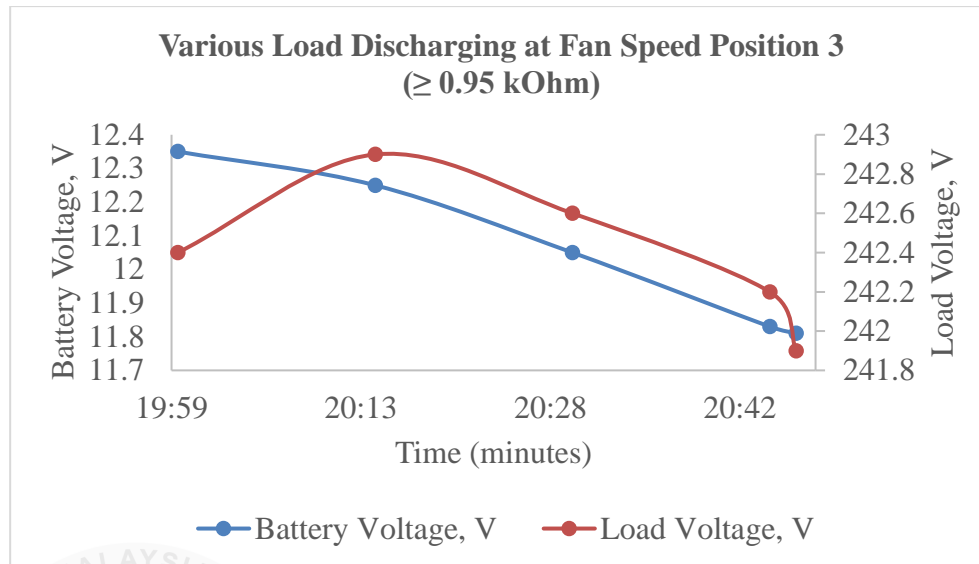


Figure 4.30 The discharging load and battery voltage over time of fan speed at position 3.

According to the graph provided, the battery voltage first measures 12.35 V and thereafter drops to around 11.81 V after around 47 minutes of 20% state of charge due to the fan operating at position 3. As the fan speed rises, the rate of discharge will also increase. Nevertheless, the graph depicting battery voltage clearly shows an escalation in the discharge rate from 08:15 PM to 08:47 PM. Nevertheless, the initial voltage upon loading was approximately 242.4 V and subsequently rose to 242.9 V at 8:15 PM. Subsequently, the load voltage experienced fluctuations from 08:15 PM to 08:47 PM as a result of the battery voltage increasing the rate of discharge.

The graph in figure 4.30 illustrates the discharge rate of a lead-acid battery when the fan speed is set to position 3. This graph is used to assess the operation of a hybrid portable power source and estimate the length of load utilization. Using this finding, it is possible to estimate the power consumption of camping appliances. When a load has a high-power consumption, the rate of discharge also increases.

Figure 4.31 displays the graph depicting the relationship between power consumption and load current during the discharge of a varied load over time. A blue line with a range of 0.26 A to 0.27 A represents the load current on the left vertical axis. On the

graph, the vertical axis on the right side and the red line indicates power usage, which varies between 32.4 W and 33.0 W. The horizontal axis represents time in minutes, indicating the duration of battery discharge from 100% to 20%. The discharge rate can be identified by referring to the graph displayed below.

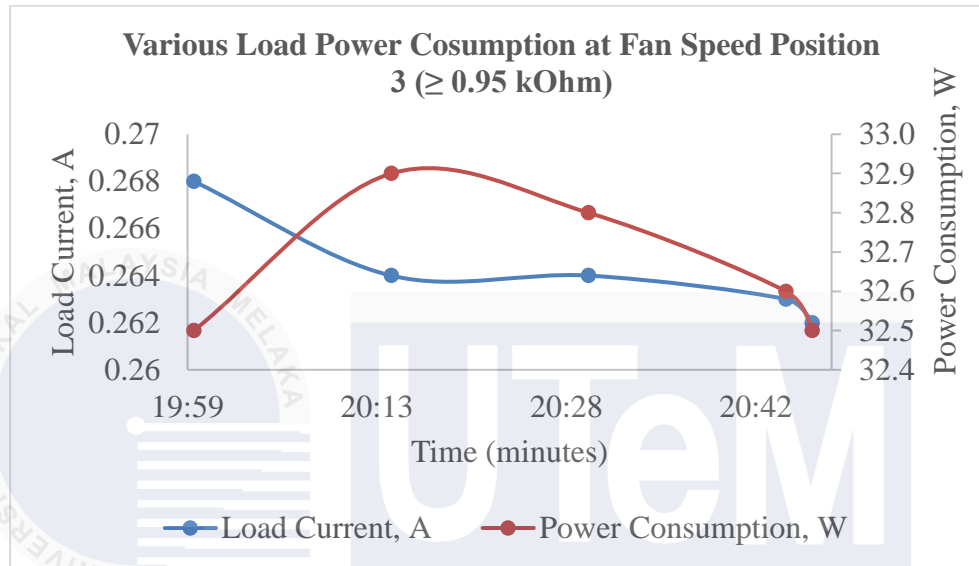


Figure 4.31 The discharging load current and power consumption for the fan speed position 3 over time.

Based on the graph in figure 4.31, the load current starts at 0.268 A during the initial analysis and decreases to 0.264 A at 8:15 PM. However, the initial power consumption is lower than the load current because the load voltage at that moment is 242.4 V. According to the graph, the power consumption rose from 32.5 W to 32.9 W at 08:15 PM and thereafter declined between 08:15 PM and 08:47 PM.

To determine the discharge rate, the hybrid power portable supply saw an increase in discharge rate after adjusting the fan speed to position 3. According to the graph, the portable power supply can operate the fan at position 3 for approximately 47 minutes. This is due to the discharge rate being inversely related to the power consumption of the fan. When the power consumption and current of the load exceed the capacity of the battery. The discharge rate will proportionally rise in accordance with the load power demand.

4.3.6 Arduino Signal Indicator

This section will clarify the role of Arduino UNO signal indicators in measuring voltage, current, and power for a hybrid portable power supply.



Figure 4.32 Arduino UNO signal indicator of voltage and current for the hybrid portable power supply.

Figure 4.32 demonstrates an I2C LCD display that shows the voltage and current. This display is used to determine the battery capacity and the current flowing to the inverter. Nevertheless, the Arduino UNO signal is capable of alerting individuals when camping in order to monitor the duration of power use. The use of signal indications can effectively mitigate the risk of power loss when utilizing the power supply. This is due to the fact that the inverter requires a minimum voltage of 11.81 volts from a fully charged lead-acid battery in order to function properly. Additionally, the signal indicators help avoid excessive usage that could potentially damage the batteries. Hence, it is crucial to monitor the present use of the circuit to guarantee the optimal functioning of the system and to safeguard the microcontroller, solar charge controller, and inverter from potential harm.

Figure 4.32 illustrates the power usage during camping activities and can assist in determining the power source and battery capacity.



Figure 4.33 Arduino UNO signal indicator of power for the hybrid portable power supply.

According to Figure 4.32, a portable power supply needs to have a signal indication in order to precisely assess the amount of power that is being used, the voltage, and the current. It is essential to do this in order to avoid any power outages that may occur while camping. When it comes to signal indications, it is essential to provide power usage as a monitoring page in order to ensure that the power source is able to supply electricity for the entirety of the night. A simultaneous indication of the amount of power that the battery is consuming will be displayed on the I2C LCD display whenever the load is being used. For this reason, it is possible to determine whether or not the battery is safe to use, and it also helps to prevent the battery from being damaged.

4.4 Summary

A circuit layout for a hybrid renewable energy system may be designed with the help of the findings and analyses offered in this chapter. These results also suggest possible uses for the simulation's output waveforms in the future. The simulation results provide important proof that the project will be successful in the future. Evaluation of the system's prospective performance is made practical by analyzing the simulations and hardware data. Based on the findings of the simulation, it is possible to assess the battery storage's rate of charge and discharge, which is a critical component of a hybrid renewable energy system. In order to compare an alternating voltage or current cycle to zero volts and determine the change that takes place during that cycle, peak voltage is used as a benchmark. For this experiment, it seems that keeping the voltage at 6 volts produces the best results. In the end, the simulation data analysis and inferences made provide significant new information on the planning and prospective efficacy of the circuit architecture for the hybrid renewable energy system. These results may be used to further investigate potential applications and enhance the system's charging and discharging efficiency. The hardware study provided identical results to the simulation results obtained in the previous semester, based on observation. Nevertheless, the analysis of various cable diameter possesses the capacity to ascertain the rate at which charging occurs and reduce the duration of the charging process.

CHAPTER 5

CONCLUSION AND RECOMMENDATIONS

5.1 Conclusion

The focus of the project is to develop a portable power supply that utilizes hybrid renewable energy. The main objective is to provide electricity for outdoor activities while ensuring portability. Conducting thorough research on previous projects related to portable power supplies will greatly contribute to improving this project. By reviewing previous research publications, the project may get significant insights into design concerns and the number of output ports necessary for camping reasons. This approach increases the project's chances of meeting the maximum requirements. Furthermore, it is critical to improve the performance of the portable power supply by investigating methods to make it lighter and ensuring user-friendly installation of input and output components. To achieve these objectives, a system with highly efficient inverters is ideal. Hybrid renewable energy systems are currently the most efficient option, as they are not reliant on a single energy resource. Hybrid systems enhance dependability and energy availability by integrating several renewable energy sources, such as solar, wind, hydro, and others.

According to preliminary results, system efficiency can be assessed through hardware implementation. This allows for feedback on less efficient components in the power supply. However, this semester's focus primarily lies on direct-current (DC) loads, as designing the inverter circuit poses greater challenges compared to developing circuits for solar panels, dynamos, and batteries. Constructing a hybrid circuit is significantly more difficult than working with a single type of energy because it necessitates careful consideration of converters and switching control circuits. When dealing with hybrid

systems, the energy produced is greater than that of a single renewable energy source, which may have implications for battery storage. Despite these challenges, the circuit design demonstrates that the system can function properly with two separate renewable energy sources.

The objective of the upcoming semester's thesis is to concentrate on the hardware development aspect of the project's configuration, focusing on the inventory of equipment needed for a portable hybrid renewable energy-based power supply. This initiative's primary objective is to achieve a cost-effective solution by designing and developing the essential hardware components at the lowest possible cost. By focusing on the hardware, the thesis intends to contribute to the overall objective of reducing the costs associated with hybrid, renewable energy-based portable power supplies. Through meticulous analysis, research, and design, the thesis will investigate novel techniques for optimizing the hardware configuration, considering such factors as component selection, manufacturing processes, and material utilization. The goal is to develop a practical and cost-effective hardware solution that supports the portability, reliability, and performance of the hybrid renewable energy-based power supply, thereby making it accessible and affordable to a broad range of users.

Even though this semester has been successful in accomplishing the goal of making a hybrid renewable energy power supply, which was the objective of this research. As a result of the analysis of the various cable diameter size, it is possible to find the varied charging times in order to accomplish the goal of reducing the charging process. Next, hybrid renewable energy has the ability to boost the potential of a portable power source by providing multiple ways to recharge a battery, regardless of whether it is daytime or nighttime. This is because, when camping, there is a greater possibility of experiencing

power outage in the middle of the night. The hybrid system makes it possible for the campers to recharge their batteries by using the mechanical pedal.

At the same time, the process of load discharge analysis is extremely significant in order to determine the effectiveness of the hybrid renewable energy-based portable power supply. The power consumption of the load, which can vary, can affect the battery's performance during load usage. The various load discharging has the potential to increase the potential for commercialization of the project and to maximize the demand for power usage during camping activities. This is necessary in order to achieve the goal. Additionally, the hybrid system has the potential to enhance the efficiency of recharging the battery, thereby reducing the amount of time required for the charging process. This is because, in the case of a standalone system, the capacity of the battery is crucial in determining the length of time that power is consumed and then lost.

Moreover, the project incorporates the microcontroller system in order to make it possible to utilize it as a monitoring device and to protect the hybrid portable power supply from being damaged. It is possible to lessen the likelihood of experiencing a power outage during the evening hours by utilizing Arduino UNO to measure the voltage, current, and power available during camping activities. The hybrid portable power supply will alert the camper when the battery reaches 20% of the battery state of charge, which will be indicated by a beeping sound coming from the inverter. This is necessary in order to prevent power losses during the nighttime hours. The voltage, current, and power will be displayed on the I2C LCD in order to protect the battery from being damaged. This will serve as a reminder to campers to avoid causing any damage to the battery.

According to the research, the cable with a diameter of 10.0 mm^2 is capable of reducing charging time due to its lower resistance when compared to cables with sizes of 0.8 mm^2 , 1.5 mm^2 , and 4.0 mm^2 . The comparison of cable sizes of 4.0 mm^2 and 10.0 mm^2 reveals

that the 4.0 mm² cable diameter requires 9 hours to fully charge the battery, while the 10.0 mm² cable diameter only requires 7 hours of the solar PV charging analysis. As a result, the charging method was reduced from 9 to 7 hours, resulting in a 2-hour time savings. Based on mechanical pedal charging analysis, the longest charging time was 29 hours and 57 minutes for a cable diameter of 1.0 mm². Otherwise, a cable diameter of 1.5 mm² determines the battery's charging time, which is 11 hours and 42 minutes. In comparison to both cable diameters, the 1.5 mm² cable has the ability to reduce charging time from 29 hours and 57 minutes to 11 hours and 42 minutes. This analysis compares the charging timings of various mechanical pedaling cable sizes to guarantee that the charging time is efficient and that the longest time to reach a state of charge from 20% to 100% is minimized. The highest charging rate, however, is 10.0 mm² cable, which is 8 hours and 33 minutes. Based on the solar PV and mechanical pedaling charging analyses, it was established that 10.0 mm² had a very good impact on the charging rate in order to reduce the duration of charge. As a result, solar PV and mechanical pedaling with a cable diameter of 10.0 mm² have the lowest charging times of 7 hours, 8 hours, and 33 minutes, respectively.

5.2 Recommendation

Based on the project's emphasis on producing a portable power source for outdoor activities utilizing a hybrid renewable energy strategy, many suggestions may be made to increase its performance. To begin, doing significant research on previous portable power supply projects will allow for advancements in battery capacity that fit the load requirements for camping. In addition, to enhance mobility and use, the power supply design should prioritize lightweight construction and user-friendly installation of input and output components. The most efficient types of inverters should be carefully chosen to increase efficiency. The advantages of hybrid renewable energy systems make them appealing

options for producing sustainable energy. The construction of a hybrid circuit demands careful analysis of the circuit improvement by utilizing MATLAB software to model the outcome before hardware implementation. Because hybrid systems generate more energy than a single renewable source, their impact on battery storage should be examined, and PSCAD circuit design is less efficient when compared to other software.

According to the current semester's project, the size of the hybrid portable power supply is larger than what was originally planned in the previous semester. Based on the project's advice, it is advised to reduce the dimensions of the hybrid portable power supply to enhance portability for campers during the camping season. Subsequently, the gear system's design aims to diminish the exertion of human effort in order to provide electricity for battery charging. When considering the process of charging through mechanical pedaling, it requires a significant amount of human effort to rotate the pedal and charge the battery. The creation of an effective gear system that lowers the generator's speed can accomplish this. Regarding the battery, employing a lithium-ion battery to decrease its weight may pose safety risks. This is because the system incorporates an inverter, and inadequate airflow within the control box might lead to explosions.

5.3 Future Works

In the future, the accuracy of the hybrid renewable energy based on portable power supply hardware estimate findings might be improved as follows:

- i) Begin working hands-on to create the model based on the project concept.
- ii) Include research to obtain a better and more accurate load and loss factor value to increase project efficiency.
- iii) Begin analyzing the project modeling results by referring to the electrical parameters.

- iv) Consider the impact of the imbalanced voltage produced by solar PV when the voltage regulator is used.
- v) Making use of the microcontroller to show system performance depending on battery capacity and power supply temperature.
- vi) Gear system design to minimize the speed of the generator for mechanical pedaling.
- vii) To reduce the size of the box on purpose in order to make it more convenient to carry when participating in camping activities.
- viii) Increasing the solar panel size from 10 W to 30 W, which is the same dimension, in order to reduce the recharging time.
- ix) Increasing the battery capacity from 12V, 7.2 Ah, to 12V, 14.4 Ah, by paralleling the battery circuit will ensure that the battery has the ability to increase load discharging time.
- x) Installing the resistor to reduce the inrush current of the battery capacity to ensure that it does not decrease while connected to the circuit.

5.4 Potential of Commercialize the Project

According to the findings of this experiment, hybrid portable power supply has the potential to be marketed in the future. The hybrid portable power supply should have the efficiency of the various cable diameter charging analysis to calculate the percentage of commercialized hybrid power supplies. This is done to ensure that the system can reduce the amount of time that campers need to charge their devices while they are participating in camping activities. However, the analysis of various load discharging is utilized to increase the project's marketability by ensuring that the system can provide power to the campers for the duration of the night. Additionally, the hybrid charging system is able to enable campers

to charge their batteries even during the night. The mechanical charging analysis with various cable sizes shows that to accomplish this, one must pedal the mechanical pedal to recharge the battery. In any other case, campers can use the solar photovoltaic system to recharge their batteries during the daytime hours, and they can also use the USB port to recharge their electronic devices, which is also included as part of the project prototype. The analysis revealed that different cable diameters were required to achieve a state of charge ranging from 20% to 100%. This was done to identify the minimal charging time, taking into account the various cable diameters and forms of charging. The analysis reveals that the fastest charging times for solar PV charging, and mechanical pedals are 7 hours, 8 hours, and 33 minutes. Based on the different loads being discharged, the fan speed at position 1, which is 19.5 W, has the lowest rate of discharge, reaching just 20% of the state of charge. The load study reveals that the fan speed at position 3 has its highest discharge rate, measuring 33.7 W. Additionally, it takes the battery 47 minutes to reach a state of charge of 20%.

UNIVERSITI TEKNIKAL MALAYSIA MELAKA

REFERENCES

- [1] "What is Power supply_ (Basics of Power Supply) _ Tech _ Matsusada Precision". (6/10/2023)
- [2] "Best Portable Power Stations for June 2023 - CNET". (6/10/2023)
- [3] "Choosing Solar Chargers for Backpacking _ REI Expert Advice". (6/10/2023)
- [4] "Portable Power Station vs. Generator: Which is Right for You?" [Online]. Available: <https://blog.ugreen.com/portable-power-station-vs-generator/#:~:text=Due> (6/10/2023)
- [5] "Ways to improve battery consistency Control of the production process." [Online]. Available: <https://www.grepow.com/blog/what-is-inconsistency-in-the-battery-packs-and-how-to-solve-it.html> (6/10/2023)
- [6] J. P. Lai, Y. M. Chang, C. H. Chen, and P. F. Pai, "A survey of machine learning models in renewable energy predictions," *Applied Sciences (Switzerland)*, vol. 10, no. 17. MDPI AG, Sep. 01, 2020. doi: 10.3390/app10175975. (6/12/2023)
- [7] "Light-plant-Fig1198-Page989-Ch45-Hawkins-Electrical-Guide - Hybrid power - Wikipedia". (30/5/2023)
- [8] "Hybrid power." [Online]. Available: https://en.wikipedia.org/wiki/Hybrid_power (2/5/2023)
- [9] S. Moghaddam, M. Bigdeli, and M. Moradlou, "Optimal design of an off-grid hybrid renewable energy system considering generation and load uncertainty: the case of Zanjan city, Iran," *SN Appl Sci*, vol. 3, no. 8, Aug. 2021, doi: 10.1007/s42452-021-04718-x.
- [10] Z. Milovanovic, "HYBRID SYSTEMS BASED ON THE SOLAR AND WIND POTENTIAL IN THE BANJA LUKA REGION PRIJEDLOG MJERA I AKTIVNOSTI NA UVOĐENJU OPTIMALNOG UPRAVLJANJA POKAZATELJIMA KONKURENTNOSTI ENERGETSKIH I PROCESNIH POSTROJENJA (UVOĐENJE ASSET MANAGEMENT-A NA NAJVIŠEM NIVOU)"-FAZA I View project ANALIZA MOGUĆNOSTI I PERSPEKTIVE KORIŠĆENJA KOGENERACIJE I TRIGENERACIJE U REPUBLICI SRPSKOJ View project," 2016. [Online]. Available: <https://www.researchgate.net/publication/311650844> (2/5/2023)
- [11] "What are the different types of solar panels?" [Online]. Available: <https://news.energysage.com/types-of-solar-panels/> (30/5/2023)
- [12] "WIND EXPLAINED TYPES OF WIND TURBINES." [Online]. Available: <https://www.eia.gov/energyexplained/wind/types-of-wind-turbines.php> (30/5/2023)
- [13] "We discover the founding precursors of wind power _ Siemens Gamesa _ International inventors' day". (30/5/2023)
- [14] "MPPT vs PWM _ What are the Different Types of Solar Charge Controllers_". (30/5/2023)
- [15] "Wind Resource_ Utilising Hydrogen Buffering". (30/5/2023)
- [16] "Types of battery energy storage _ Homes and housing _ Queensland Government". (30/5/2023)

- [17] "What is battery storage?" [Online]. Available: <https://www.nationalgrid.com/stories/energy-explained/what-is-battery-storage> (2/5/2023)
- [18] "Top 3 Main Types Of Solar Inverters_ Which Is The Best One For Homes_". (30/5/2023)
- [19] "Energy Systems Energy Systems Optimization Optimization." [Online]. Available: <https://hybrid-renewable.blogspot.com/2011/03/importance-of-hybrid-energy-systems.html> (31/5/2023)
- [20] B. Zohuri, "Hybrid Renewable Energy Systems," in *Hybrid Energy Systems*, Springer International Publishing, 2018, pp. 1–38. doi: 10.1007/978-3-319-70721-1_1.
- [21] "WINDGE~1". (31/5/2023)
- [22] "Smart BaseStation - off-grid communication masts". (31/5/2023)
- [23] Ūzhno-Ural'skiĭ gosudarstvennyiĭ universitet, IEEE Russia Siberia Section. PES/IES/IAS/CSS Joint Chapter, and Institute of Electrical and Electronics Engineers, *2018 International Ural Conference on Green Energy (UralCon) : proceedings : South Ural State University (national research university), Chelyabinsk, Russian Federation, October 4-6, 2018*.
- [24] L. Fraas, J. Avery, L. Minkin, H. X. Huang, and P. Uppal, "Portable concentrated sunlight power supply using 40% efficient solar cells," *IEEE J Photovolt*, vol. 1, no. 2, pp. 236–241, 2011, doi: 10.1109/JPHOTOV.2011.2172576.
- [25] "Output Power." [Online]. Available: <https://www.sciencedirect.com/topics/engineering/output-power#:~:text=Solar> (11/6/2023)
- [26] "What is a Solar Cell? Recent Posts." [Online]. Available: <https://www.electrical4u.com/solar-cell/1/8> (12/6/2023)
- [27] M. Bouzguenda, A. A. Al-Omair, and A. A. Al-Yamani, "Design and Performance Analysis of a Portable Solar PV Power Supply," in *2022 IEEE 21st International Conference on Sciences and Techniques of Automatic Control and Computer Engineering, STA 2022 - Proceedings*, Institute of Electrical and Electronics Engineers Inc., 2022, pp. 454–457. doi: 10.1109/STA56120.2022.10019225.
- [28] "Solar radiation - Understanding Global Change". (12/6/2023)
- [29] L. Q. Soh and C. C. D. Tiew, "Building of a portable solar AC & DC power supply," in *Proceedings - International Conference on Intelligent Systems, Modelling and Simulation, ISMS*, IEEE Computer Society, Sep. 2015, pp. 445–451. doi: 10.1109/ISMS.2014.82.
- [30] "6/12/23, 7:16 PM Stand Alone PV System for Off-grid PV Solar Power <https://www.alternative-energy-tutorials.com/solar-power/stand-alone-pv-system.html> 1/7 Home / Solar Power / Stand Alone PV System Stand Alone PV System A Stand Alone Solar System." [Online]. Available: <https://www.alternative-energy-tutorials.com/solar-power/stand-alone-pv-system.html> (2/5/2023)
- [31] "Ohm's Law - Statement, Formula, Solved Examples, Verification, FAQs". (12/6/2023)
- [32] Institute of Electrical and Electronics Engineers, *Proceeding of 14th International Conference on Telecommunication Systems, Services, and Applications (TSSA) : 4-5 November 2020, Bandung, Indonesia*.

- [33] "Off-Grid Solar Systems _ Advantages and Disadvantages _ Deege Solar". (12/6/2023)
- [34] H. Kim, "Magnet Dynamo - Princeton University EPICs," in *2020 9th IEEE Integrated STEM Education Conference, ISEC 2020*, Institute of Electrical and Electronics Engineers Inc., Aug. 2020. doi: 10.1109/ISEC49744.2020.9397842.
- [35] "Magnetism and electricity Content objective." [Online]. Available: <https://kaiserscience.wordpress.com/physics/electromagnetism/magnetism-and-electricity/> (12/6/2023)
- [36] "Links Electromagnetism Induced Current Revision Questions Physics Quiz Index Generator Quiz Home GCSE Chemistry GCSE Physics," 2015. [Online]. Available: <https://www.gcsescience.com/pme21.htm2/3> (12/6/2023)
- [37] S. Yathavan, G. Rameshkumar, and S. Gokulraj, "A Novel Design & Fabrication of Energy Generating Oscillatory Swing-A Play way Technique for Public Parks," 2017. [Online]. Available: www.sciencedirect.com/www.materialstoday.com/proceedings (2/5/2023)
- [38] M. Tang *et al.*, "A hybrid kinetic energy harvester for applications in electric driverless buses," *Int J Mech Sci*, vol. 223, Jun. 2022, doi: 10.1016/j.ijmecsci.2022.107317.
- [39] C. D. Sijoy and S. Chaturvedi, "Analysis of magnetic Rayleigh-Taylor instability in a direct energy conversion system which converts inertial fusion plasma kinetic energy into pulsed electrical energy," *Ann Nucl Energy*, vol. 62, pp. 81–85, 2013, doi: 10.1016/j.anucene.2013.05.024.
- [40] J. C. Liou and C. F. Yang, "Photovoltaics battery module power supply system with CIGS film applied in portable devices," *Microelectronics Reliability*, vol. 99, pp. 96–103, Aug. 2019, doi: 10.1016/j.microrel.2019.06.005.